NTNU

Norwegian University of
Science and Technology

Analysis of the novel solar heating wall installed as building envelop in the Green Energy Laboratory

Marte Wigen Nilsson

NTNU

Norwegian University
of Science and Technology

Department of Energy
and Process Engineering

EPT-M-2015-63

MASTER THESIS

for

Student Marte Wigen-Nilsson

Spring 2015

Analysis of the novel solar heating wall installed as building envelop in the Green Energy Laboratory

Analyse av den innovative solvameveggen installert som bygningsskallet i Green Energy Laboratory

Background and objective

Super-insulated envelopes of modern buildings put new demands on performances of heating and cooling installations. Solar heating wall used as building envelop is a promising technique that could contribute to enhanced efficiency of energy utilisation in modern buildings.

The goal for this collaborative activity is to analyse the novel solar heating wall installed as the building envelop at the Green Energy Laboratory (GEL) of the Jiao Tong University in Shanghai, China, by use of simulations and laboratory measurements. The necessary background for this work was partly developed through the project assignment accomplished at NTNU. The major part of the work on analysis and development of design methods will be performed during this Master thesis work that will be accomplished at the GEL of the Jiao Tong University in Shanghai. This collaborative assignment is realised as a part of the Joint Research Centre in Sustainable Energy of NTNU and SJTU.

The following tasks are to be considered:

1. Establish/Select an appropriate model for simulation of the novel solar heating wall installed as the building envelop at the GEL.
2. Verify the established model by use of measured data from the GEL novel solar heating wall.
3. Conduct analysis of the GEL novel solar heating wall focusing on their integration, design procedures, as well as the optimal use of renewable energy source and heat storage capacity.
4. Make a draft proposal (8-10 pages) for a scientific paper based on the main results of the work performed in the master thesis.
5. Make proposal for further work on the topic.

-- ” --

Within 14 days of receiving the written text on the master thesis, the candidate shall submit a research plan for his project to the department.

When the thesis is evaluated, emphasis is put on processing of the results, and that they are presented in tabular and/or graphic form in a clear manner, and that they are analyzed carefully.

The thesis should be formulated as a research report with summary both in English and Norwegian, conclusion, literature references, table of contents etc. During the preparation of the text, the candidate should make an effort to produce a well-structured and easily readable report. In order to ease the evaluation of the thesis, it is important that the cross-references are correct. In the making of the report, strong emphasis should be placed on both a thorough discussion of the results and an orderly presentation.

The candidate is requested to initiate and keep close contact with his/her academic supervisor(s) throughout the working period. The candidate must follow the rules and regulations of NTNU as well as passive directions given by the Department of Energy and Process Engineering.
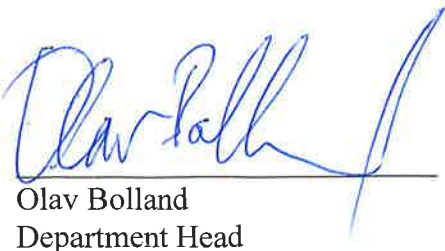
Risk assessment of the candidate's work shall be carried out according to the department's procedures. The risk assessment must be documented and included as part of the final report. Events related to the candidate's work adversely affecting the health, safety or security, must be documented and included as part of the final report. If the documentation on risk assessment represents a large number of pages, the full version is to be submitted electronically to the supervisor and an excerpt is included in the report.

Pursuant to "Regulations concerning the supplementary provisions to the technology study program/Master of Science" at NTNU §20, the Department reserves the permission to utilize all the results and data for teaching and research purposes as well as in future publications.

The final report is to be submitted digitally in DAIM. An executive summary of the thesis including title, student's name, supervisor's name, year, department name, and NTNU's logo and name, shall be submitted to the department as a separate pdf file. Based on an agreement with the supervisor, the final report and other material and documents may be given to the supervisor in digital format.

☒ Work to be done in lab (Green Energy Laboratory, Shanghai Jiao Tong University, China)
☒ Field work

Department of Energy and Process Engineering, 12. February 2015

Olav Bolland
Department Head

Vojislav Novakovic
Academic Supervisor

Research Advisor:
Prof. Yanjun DAI, Shanghai Jiao Tong University, e-mail: yjdai@sjtu.edu.cn
Prof. Tianshu GE, e-mail: baby_wo@sjtu.edu.cn
Prof. Laurent Georges, NTNU

Preface

This master thesis was completed the autumn of 2015 at the Norwegian University of Science and Technology and was realised a part of the Joint Research Centre in Sustainable Energy of the Norwegian University of Science and Technology and Shanghai Jiao Tong University. The thesis was conducted during the final part of the study program Energy and Environmental Engineering at the Department of Energy and Process Engineering. Four months of the research time was spent at the Green Energy Laboratory at Shanghai Jiao Tong University.

Marte Wigen Nilsson   Bergen 2015

Abstract

This study looks at the use of façade integrated solar collectors in Norwegian buildings. One wall consisting of 0.25 m of timber framed insulation, and one wall consisting of 0.2 m insulation and 0.2 m concrete were tested. The U-value of both walls were 0.17 W/m^{2}K. The solar collectors were mounted on these wall elements as a replacement of the external weather barrier. The investigations were conducted in TRNSYS and in a dynamic model describing the thermal performance of the façade integrated solar collectors, created at Shanghai Jiao Tong University. The complete solar collector system was designed according to recommended values from literature. A parametric study looking at the optimal design of the storage tank set point temperature, the ratio between the tank height and the diameter, the regulatory strategy, the flow rate, the water tank volume and the placement of the heat exchanger were conducted. Following was a heat pump installed in series with the solar collectors in the existing system. Different maximum evaporator inlet temperatures were tested to find the optimal system design.

The initial results showed that the heavy solar wall performed better than the lightweight solar wall. During the winter days, the heavy solar wall lead to a substantial reduction in the negative transmission compared to the conventional heavy wall. During the summer days, both of the solar walls introduced a positive transmission contribution, which may lead to overheating the building. The contribution was lowest for the heavy solar wall. When installing 6.68 m^2 collector area in the TEK-10 building with the heavy wall configuration, the annual negative transmission was reduced by 84 % through the wall area with the installed collectors. A positive transmission of 39 kWh annually was also introduced. The parametric study revealed that the best design for system performance was not necessarily the optimal design for transmission energy savings. Related to transmission, lowering the flow rate showed the highest energy saving, of 1.5 kWh/m^2 annually. In maximizing the collector performance, changing the regulatory strategy of the system led to an annual energy saving of 1.05 kWh/m^2 floor area. This was also the efficiency measure that led to the biggest energy saving when accounting for both transmission and collector performance. The use of a series connected heat pump further improved the system performance. A maximum evaporator inlet temperature of 15 °C led to the highest energy saving of 30 % compared to the system without the heat pump, when accounting for both transmission and collector performance.

Sammendrag

Denne studien ser på bruken av fasadeintegrerte solfangere i Norske bygg. To ulike vegger ble testet. En vegg bestående av 0.25 m isolasjon i bindingsverk, og en vegg bestående av 0.2 m isolasjon installert på 0.2 m betong. U-verdien til begge veggene var 0.17 W/m²K. Solfangerne ble montert på disse veggelementene som erstatning for ytterkledningen. Undersøkelsene ble gjort i simulerings-programmet TRNSYS i kombinasjon med en dynamisk modell som beskriver den termiske ytelsen til fasadeintegrerte solfangerne. Denne modellen er laget ved Shanghai Jiao Tong University. Det fullstendige solfangersystemet ble designet med bakgrunn i anbefalinger fra litteraturen. En parametrisk studie som så på det optimale designet av tank temperatur, forholdet mellom tank høyde og diameter, massestrøm, tank volum, regulerings strategi og plassering av varmeveksleren ble utført. Videre ble en varmepumpe installert i serie med solfangerne i det eksisterende systemet. Ulike maksimale fordampertemperaturer ble testet for finne den innstilningen som ga de høyeste energibesparelsene både med hensyn til transmisjon og solfangerytelse.

De innledende resultatene viste at den tyngre solveggen yter bedre enn den lette solveggen. Gjennom en vinterdag viste den tunge solveggen store reduksjoner i den negative transmisjonen sammenlignet med den konvensjonelle tunge veggen. Begge solveggene viste økt positiv transmisjon gjennom en sommerdag, noe som kan føre til overoppheting av bygget. Dette bidraget var minst gjennom den tunge solveggen. Ved å installere 6.68 m² solfangerareal på TEK-10 bygget med den tunge veggen, reduseres den årlige negative transmisjonen med 84 % gjennom vegg-arealet med de integrerte solfangerne. 39 kWh årlig ble også tilført gjennom positiv transmisjon. Den parametriske studien viste at det beste designet for å maksimere solfangerytelser ikke nødvendigvis var det beste designet for energibesparelser tilknyttet transmisjonen. I relasjon til transmisjon ville en reduksjon av massestrømmen gjennom solfangerne gi den høyeste energibesparelsen med 1.5 kWh/m² årlig. For å maksimere solfangerytelsen ville en endring i reguleringsstrategien gi en energibesparelse på 1.05 kWh/m²gulv areal årlig. Dette var også det tiltaket som ville gi den høyeste energibesparelsen totalt når både solfangerytelse og transmisjon ble evaluert. Bruk av en varmepumpe installert i serie med solfangerne viste en enda høyere systemytelse. En maksimal fordampertemperatur på 15 °C ga en energibesparelse på 30 % sammenlignet med systemet uten varmepumpen når både transmisjon og solfangerytelse ble evaluert.

Table of Content

x

List of figures

List of tables

1 Introduction

1.1 Objective and background

The topic of solar energy has become a matter of great concern all over the world due to the global energy shortage. The sun considered one of the most promising alternative energy sources, and even with the climatic situation in Norway, new regulations and building trends makes the use of solar energy in buildings highly applicable. In June 2012, 1000 residential passive houses were constructed or under construction in Norway [1]. The development is expected to continue with a strong increases in the number of passive houses and low energy buildings in both the residential and the commercial sector. By introducing passive houses, the energy budged of the building completely changes. The design power demand and the specific energy demand is reduced, while energy related to domestic hot water represents a relatively bigger part of the total energy consumption. This means that creating renewable energy systems for domestic hot water is increasingly important.

A wide variety of studies have been conducted, and a lot of knowledge exist on the thermal performance of solar collectors. Despite of this, the use of façade integrated solar collectors is a premature field where few studies have been conducted. The main focus in the implementation of façade integrated solar collectors has earlier been on the aesthetic integration with the building. This study will reveal performance advantages and disadvantages with the use of façade integrated solar collectors in the Norwegian climate with respect to aesthetics, thermal performance of the collectors and thermal performance of the building envelope. There exist several recommendations and rules of thumb for the optimal design of solar collector systems. Most of these rules describe the optimal system design for externally mounted solar collectors under optimal slope. When mounting the collectors vertically, the performance changes. This means that a different design will be optimal. As the use of façade integrated solar collectors leads to different transmission profiles compared to conventional walls, solar walls will influence the indoor environment as well. The transmission is sensitive to the system design, and parameters that in conventional collector panels only influence the collector performance will now also influence the transmission. The optimal design to maximize collector performance may lead to unfavourable transmission

profiles that can lead to increased energy consumption for heating and cooling. This means that finding the optimal system design for façade integrated solar collectors is a complex task.

A special focus point in this report is the refurbishment of existing TEK-10 walls with the integration of solar collectors for the production of domestic hot water. Constructing new energy efficient buildings is a relatively simple task, but refurbishing existing buildings to reduce energy consumption and increase the fraction of renewable energy is more complicated. The report looks at the use of façade integrated solar collectors in different configurations of conventional TEK-10 walls, and the possibility of reducing the insulation thickness in the solar walls to achieve the same thermal performance as in conventional walls with more insulation. The objective is further to look at the influence of different efficiency measures to improve the collector performance and the transmission profile. This includes a parametric study of different system parameters, and the optimal combination of façade integrated solar collectors and a series connected heat pump. The solar collector system investigated is installed in the Solar House in the Green Energy Laboratory (GEL) at Shanghai Jiao Tong University (SJTU).

1.2   Outline

The report is divided into two main parts, a literature study and a case study. The literature study starts in Chapter 2 with an introduction to solar thermal energy where different solar thermal systems are evaluated and explained. Chapter 3 consist of the characteristic of a façade integrated solar collector and its heat transfer mechanisms. Advantages and disadvantages with the integration of collectors are presented. The next chapter consist of a thorough evaluation of thermal energy system design, where every parameter important for the system performance is discussed. This also includes rules of thumb in the design of solar collector systems. Chapter 5 consist of an explanation of the simulation program and the model used in the case study. Here limitations and simplifications in the programs, which will influence the results are extensively evaluated. The case study starts in Chapter 6, with investigations on a physical solar collector system. The initial investigations in Chapter 6.3 focus on the performance of the façade integrated solar collectors during days with extreme weather conditions. This reveals the best solar wall configuration, which in the next part will be implemented into a complete concept building where the annual system performance is investigated. In Chapter 7.5, a parametric study of efficiency measures to improve the system

performance is included. Last but not least, a series connected heat pump is installed in the existing solar thermal system. Its influence on the system performance is extensively documented in Chapter 8.

1.3 Delimitations

The author spent four months at Shanghai Jiao Tong University to conduct measurements at the Solar House on the façade integrated solar collectors installed there. These measurements were supposed to verify the dynamic model describing the thermal performance of the curtain wall and work as support material to the investigations and simulations. Due to malfunctions on the laboratory, the solar wall was not operational when the author was in Shanghai. Consequently, no measurements were conducted. The author received measured data collected at the solar wall. These data was supposed to be sufficient to verify the model, but the obtained simulation results were not reliable. However, the model was verified through a study by R. Li et al.[2] and is thus assumed to be accurate. Delimitations in this model are cited in Chapter 5.2.2.

The dynamic model is created to investigate a limited segment of façade integrated solar collectors. This study has an expanded scope compared to previous studies where the model is used. This sets some limitations to which parameters that can be changed in the model, and how the model can be connected to other types in TRNSYS. Integration of façade integrated solar collectors into a complete building is not possible in TRNSYS, but separate simulations must be conducted for the building and the collector wall. This will be a simplification of the realistic situation. Chapter 7.3.2 explains how this is handled.

2 Solar thermal energy

The sun is a necessity for the life we live on earth, and almost everywhere on the planet, the sun can be utilized as a useful energy source. The earth receives annually 15 000 times more energy from the sun than the total consumption of humans [3]. Even though not all of this can be utilized, it still means that the sun represents an enormous energy source that with small means can reduce the quantities of fossil fuels used in buildings [4].

Figure 2-1 Solar radiation in Norway. January (blue) vs. July (green) [3]

Even though the sun is abundant, it is not available at all times. The distribution seen in Figure 2-1 shows that for solar energy to be a sustainable energy source in Norway, effective storage means must be installed. A wide variety of storage systems exist today. The most common storage systems in Norwegian buildings are hot water tanks for short time energy storage, while seasonal storages are used when heat is collected during the summer, and used during the winter. The most promising technology within seasonal storage is underground thermal energy storages (UTES) which are more commonly used in bigger solar thermal systems [5]. To further increase the solar thermal output, sub systems can be installed to utilize the sun also when the available radiation is low. Heat pumps installed in series or parallel with the collector panels are promising technologies [6-8]. There are several ways of utilizing the energy from the sun in buildings. Space heating with active or passive solar energy, daylight, heating of domestic hot water, cooling, production of process heat, solar boiling and production of electricity is some of them [3]. This report focuses on the use of

solar thermal energy for heating domestic hot water (DHW) using façade integrated solar collectors with and without a series connected heat pump.

2.1 Solar collector market today
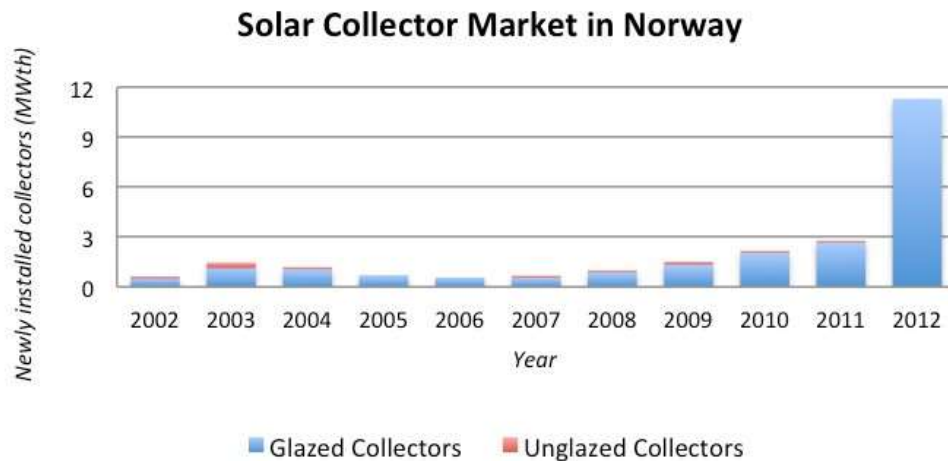
Figure 2-2 Annual installed solar collector area in Norway 2002-2012 [9]

Globally, the total installed area of solar thermal energy systems increased from 89 million m^2 in 2000 to 580 million m^2 in 2014 [10]. China is the main marked driver. The total sales of solar collectors in Norway have been slowly increasing the last ten years. In 2012 the district heating plant in Lillestrøm was commissioned as the first large scale solar thermal facility in Norway. This plant represents 13 000 m^2 of the total installed solar collector area in Norway in 2012. The remaining 3000 m^2 were small scale systems of flat plate collectors, evacuated tube collectors and air heaters [9]. Figure 2-2 shows how substantial this installation is, compared to the normal annual growth in solar collector area.

One of the reasons why the installation of new solar thermal systems have been almost constant the last years is the low electricity price in Norway. The investment and installation cost of a standard solar collector system in a Norwegian residential building is 50-60 000 NOK, and the energy cost is estimated to around 60 øre/kWh [11]. This means that the operational cost is only a little lower than for a conventional electrical energy system. Enova SF delivers economic support for the installation of solar collectors in residential buildings [12]. Despite of this, the increase in the installed area of solar collectors in Norway is still only slowly increasing.

2.2 Solar thermal energy systems in buildings

Passive solar heat is utilized intentionally or unintentionally in all buildings when the sun shines on the building envelope. The driving force is the second law of thermodynamics, where heat moves from cold to warm surfaces. The direct use of the solar energy without the use of auxiliary power is what defines passive solar energy systems. One do consequently not rely on mechanical components to collect and distribute the heat. By constructing buildings wisely regarding solar radiation, in addition to using materials designed for optimal thermal storage, one can make the passive solar gain an important part of the energy budget of the building. In an average Norwegian residential building, passive solar heat cover at least 10 % of the overall heating demand. In reality is this number even higher since the solar heat also contributes to the shortening of the heating season [3]. A good passive solar energy design is especially important in super insulated buildings. Here, the overall energy consumption is low, making it crucial that the passive system does not influence the energy balance of the building in a negative way. It should contribute to neither an increased cooling need nor an increased heating need, rather the opposite. This means that the utilization of passive solar energy must be an important aspect of the design process of any building from an early stage. Increasing the amount of useful passive energy is an important driving force for introducing façade integrated solar collectors in cold climates. When integrating solar collectors into the building façade, the collectors can potentially increase the amount of passive thermal energy through the facade. Former studies conducted on façade integrated solar collectors in Shanghai climate conducted by R. Li et al. [2] show that the transmission to the building is bigger through facades with integrated solar collectors, compared to a conventional, lightly insulated wall. This aspect is related to passive solar heat that in theory can be utilized in Norway as well. The magnitude of the transmission is highly dependent on the insulation thickness in the wall, but the potential of increasing the fraction of passive solar heat exists, also in heavily insulated Norwegian walls.

The definition of active solar energy systems are systems that require energy inputs [4]. The energy is used to run the typical process of the system, which are collecting the solar energy, storing this energy and distributing the energy to space heating and domestic hot water. In addition does active solar thermal energy systems introduce several sub-systems such as solar

collectors, storage systems, controlling systems, fluid distribution systems and heat exchangers. These systems exist to regulate the availability of the energy to a greater extent compared to passive systems, and to ensure an even more effective and applicable energy production. Solar collector systems are the most common active solar energy technology. By façade integrating the collector panels, the system has the potential of becoming a combined passive and active solar thermal system.

2.2.1 Solar collector components
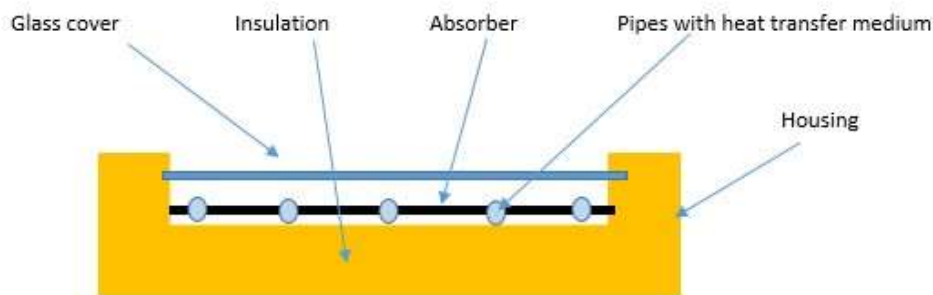
Figure 2-3 Flat plate solar collector

There are several different types of solar collectors, but the main principle is the same for all of them. The typical components in a solar collector are an absorber plate, pipes or tubes with fluid for heat distribution, a glass cover over or around the absorber and insulation, as seen in Figure 2-3. The glass cover minimizes heat losses form the absorber plate and works as a shield for damage. The cover transmits short wavelengths, but does not let the long wavelengths out - the same principle as in green houses. Radiative heat losses can be further reduced by the implementation of low emitting coatings on the cover. This will consequently also reduce the transmission to the absorber plate [4].

The absorber is a thin metal film painted black to absorb as much radiation as possible. Some absorbers have a selective coating that absorbs much of the visible light but reflect IR-radiation. This leads to a decreased heat loss from the absorber and an increased heat transfer to the working fluid. In cold climates in particular, one of the main challenges related to obtaining high collector performance is to reduce the heat loss through the top and the base of

the collector. It is important that the absorbed heat is effectively transferred to the working fluid. The pipes holding the working fluid are often made of aluminium or copper due to its heat conducting advantages.

The solar collectors should be oriented in the direction with the highest amount of solar radiation. In Norway, this means orienting the collector towards the south. The slope of the collector is defining for the collector performance, and the optimal slope varies with the location of the collector and the use of the collected heat. The type of solar collector investigated in report is the flat plate solar collector, as seen in Figure 2-3. Flat plate collectors can deliver temperatures up to about 100 °C above ambient temperature [4]. They do not require tracking of the sun to deliver relatively high temperatures, making them applicable for both walls and roofs of buildings. Despite of this, the orientation of the collectors should be wise with respect to the amount of available solar radiation when the demand is highest.
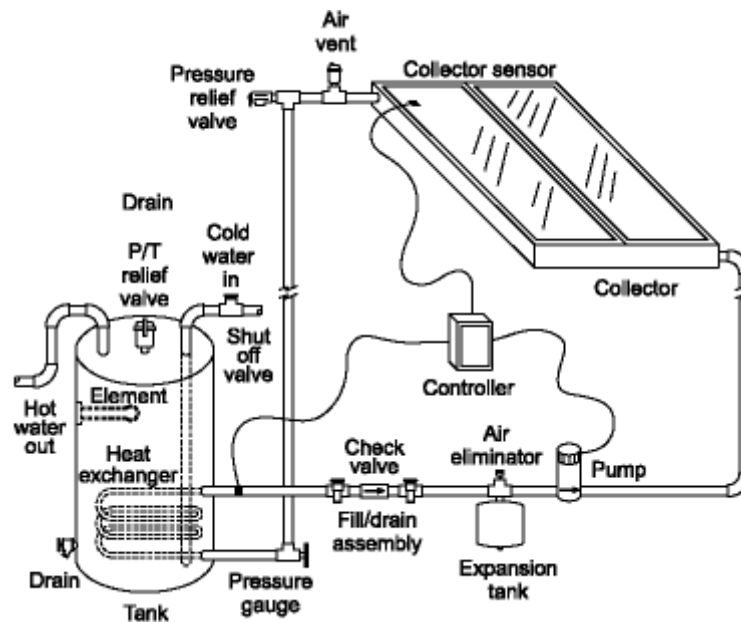
Figure 2-4 Indirect solar collector system [13]

A typical, complete flat plate solar collector system consist of the solar collectors, a water storage tank with an auxiliary heater, controllers that monitor temperature levels in the system, relief and checking valves, an expansion tank and a circulation pump, as seen Figure 2-4. The pump is turned on and off according to the temperature levels in the system. In systems where the liquid in the collector is pure water, a drainage tank is necessary to drain the collector when there is a risk of freezing. This device is not necessary in warm climates

8

and when the fluid is water mixed with anti-freeze liquid [4] . These systems are indirect with fluid circulating through the solar collectors in a separate circuit from the storage tank. The heat is transferred to the water tank through a heat exchanger. In direct systems, the water exiting the solar collectors goes straight to the water tank without the use of a heat exchanger.
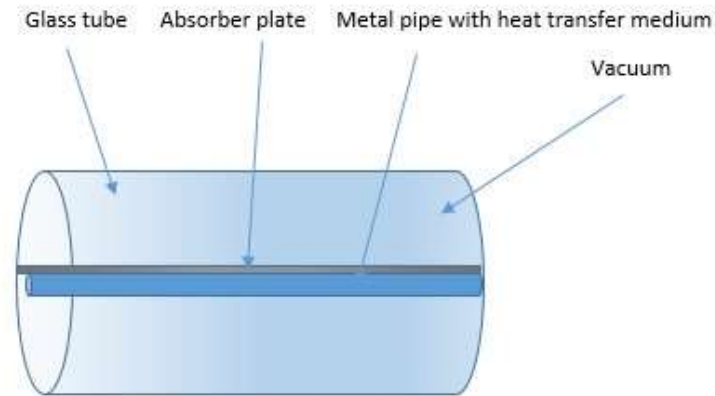
Figure 2-5 Evacuated tube solar collector

An alternative to flat plate collectors are evacuated tube collectors. Here the absorber and pipes are placed inside an evacuated tube, as seen in Figure 2-5. The vacuum decreases the convective heat loss from the tubes. This makes the evacuated tube collectors well suited for systems requiring high temperatures and for systems in cold climates [4]. This system cannot replace conventional materials in roofs and walls, but can be used in other innovative ways, for example as railing on balconies [14]. They are more efficient than the flat plate collectors, but are and are also more expensive.

When investigating which solar collector to choose, the deciding parameter should be the load the system is to cover and the use of space. Smaller collectors and collectors that can deliver high temperatures are often more expensive. When considering the use of façade integrated solar collectors, flat plate collectors are the most applicable of the different kinds of solar collectors. They can replace conventional building materials, and can work as the weather barrier of the façade.

2.3 Solar collector cost and lifetime

The lifetime of the collector is an important parameter when looking at the profitability of installing a solar collector system. Several Norwegian solar collector suppliers offer a warranty of the collector system of 10 years, and an estimated lifetime of 25 to 30 years [15, 16] . Even if the solar collector system is expected to run for 25 years, it does not mean that the collectors will perform satisfactory for its entire lifetime. Its useful life expectancy is assumed to be shorter. While plenty of studies have looked into the thermal performance of solar collector panels, few have looked at the performance as the panel ages. Reduction in efficiency can happen as a result of corroded copper pipes and broken seals between the glass cover and the insulation. Both can be a result of wear and tear on the collectors after several years in demanding weather conditions. D. Proctor et al. [17] conducted at study on the effect of aging on a 22 year old solar water heater. The result show that the most important factors leading to diminished collector efficiency is internal scale formation in the tubes and wet insulation because of broken glass-seals. These are consequences of diminished material traits, and are relatively hard to avoid even with proper maintenance. The reduction in the collector efficiency due to aging increases with the mean solar collector fluid temperature. Measurements done by J. Fan et al. [18] indicate that flat plate solar collectors show reduced thermal performance of between 1-4 % after 18 years of operation when the mean fluid temperature of the collector is 45 °C. The variation depend on the collector design. As the mean fluid temperature increases to 60 °C, the reduced thermal performance is 10-11 % for the same period.

3 Characteristics of façade integrated solar collectors

Solar collectors can be integrated in new walls or as a part of the refurbishment of existing walls. When adding solar collectors to an existing wall the thermal performance of the wall element completely changes. The magnitude of this change depends on the materials and the design of the original wall element. Knowing that the use of façade integrated solar collectors improves the performance of the wall during winter condition, but may contribute to overheating the building during the summer, it implies that extensive investigations should be followed through to ensure that the solar collectors contribute to lowering the annual use of energy in the building. For the system to be sustainable, the advantage during winter conditions must exceed the potential disadvantage during summer conditions.

3.1 Build-up of the façade integrated solar collectors
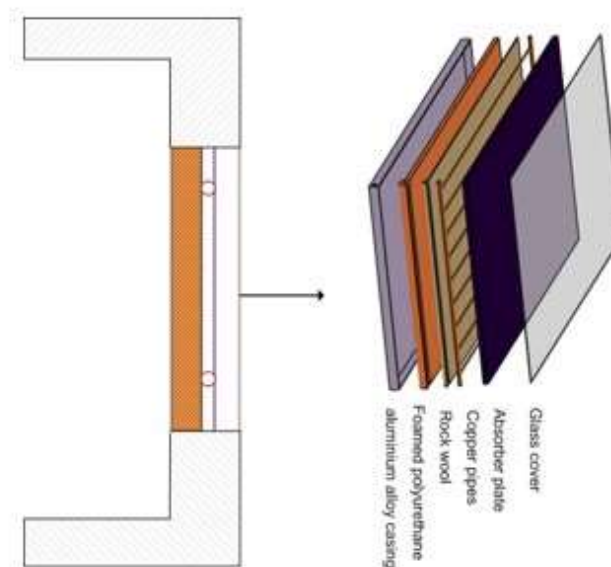
Figure 3-1 Facade integrated solar collector without thermal separation as seen in GEL [2]

There are two main ways of integrating the solar collectors in the wall. In the setup at The Green Energy Laboratory the collector panel is mounted directly in the façade without thermal separation between the collector and the insulation in the wall. This means that the insulation is a part of both the collector and the building as seen in Figure 3-1. The other option is to include a ventilated air gap between the collectors and the insulation in the wall. This will reduce the influence of the façade integrated solar collector on the transmission profile of the wall. The wall in Figure 3-1 does not consist of structural elements to ensure that the wall can withstand stress. This kind of curtain wall is most commonly mounted outside of a concrete frame, or other construction-elements that has the strength to support the rest of the building. This makes it possible to mount the solar collectors on existing buildings, on top of the construction material already there. The collector will then replace the weather barrier.

It is important to avoid thermal bridges between the collectors and moist penetration between the insulation and the collector. In Norway, there exist no standards or regulations on façade integration of solar collectors, so they must comply with standards for conventional building elements. To comply with Regulations on Technical Requirements for Building Works (TEK-10) [19], which is the Norwegian building regulation, the building materials should satisfy levels stipulated in the regulation, or the entire building should have a net energy consumption lower than a set value. This value varies for different building types. For the last option, there also exist minimum values for the building materials used. This makes it complicated to evaluate the thermal performance of solar walls in relation to the building regulations. The overall U-value of solar walls are not constant, but vary according to the fluid temperature in the collector panels.

3.2 Mechanisms of heat transfer in façade integrated solar collectors
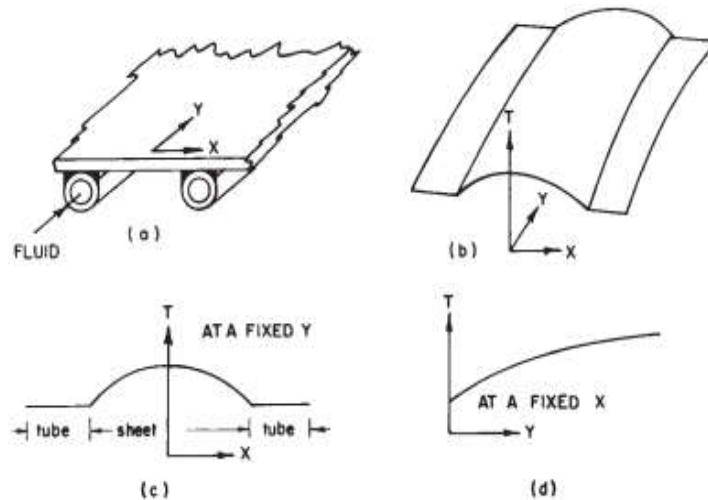
Figure 3-2 Temperature distribution in an absorber plate [4]

Analysing façade integrated solar collectors requires attention to several different means of heat transfer, and simplifications must be tolerated to make it possible to do calculations on such systems. It is important to realize that a detailed analysis of solar collectors is a complicated problem. Firstly, one must acknowledge that the temperature distribution in the collector is not uniform. When looking in the direction of the pipes, the temperature distribution in the water will vary between the inlet and the outlet. The temperature in the absorber is not constant, but will be higher at the centreline between two pipes, lower right above the pipe, and will vary according to the fluid temperature in the pipe as seen in Figure 3-2. Additionally will the fluid temperature depend on whether the forced circulation pump is running or not. Despite of this, has simplifications that lead to the problem being manageable shown to produce accurate results.

3.2.1 Conduction, convection and radiation in solar collectors

Heat transfer in façade integrated solar collectors happen through conduction, convection and radiation.

13

Heat is transferred through a solid by conduction. The parameters that decide the conduction rate for one dimensional, steady state situations are the temperature on each side of the solid, and the heat transfer coefficient of the material. Different solids have different heat transfer coefficients. Typically are the heat transfer coefficients of insulation materials low. In solar collectors, conduction will be the main heat transfer mechanism when heat is transferred through the absorber, from the absorber to the pipes and through the insulation. For one-dimensional steady state conduction, Fouriers law in Eq.1 describes the heat flow through the solid in the direction normal to the surface of the solid [20].

$$\frac{dQ}{dt} = -\lambda A \frac{dT}{dx} \qquad\qquad (\ 1 \ )$$

Q is the transferred heat, λ is the heat transfer coefficient, A is the area of the solid and dT is the temperature difference over the solid. This equation does not apply for transient heat transfer influenced by the heat capacity of the materials. To account for this, the equation for transient conduction must be applied, as seen in in Eq.2. There are several ways of solving the transient heat equation. The method chosen for this report is described in Chapter 5.2.1.

$$\rho C_p \frac{d\theta}{dt} = \frac{d}{dx} k \frac{d\theta}{dx} \qquad\qquad (\ 2 \ )$$

C_p is the heat capacity of the solid, ρ is the density, θ is the temperature and k is the heat transfer coefficient.

The heat transfer from the absorber to the pipes highly depend on the conductance of the bond, which is the connection mechanism between the pipe and the absorber plate. Whillier and Saluja [21] estimated that the conductance must be at least 30 W/m °C to achieve a sufficiently high metal-to-metal contact. Any values of conductance lower than this will lead to poor heat transfer between plate and pipes. This will affect the performance of the solar collector [4].

Convection is a heat transfer mechanism that occurs due to fluid movement. When air flows over a plate, heat is transferred by the flow by advection. Convection is a defining parameter for the performance of solar collector since it highly influences the heat loss from the

collector panel to the ambient. Newtons law of cooling describes convection and is defined in Eq. 3 [20]. The collector is influenced by convection between the glass cover and the ambient and between the insulation layer and the inside air. This factor increases with air velocity. Convection will also occur in the air gap between the glass cover and the absorber plate. This kind of convection is defined as natural convection, and occurs since hot air rises and creates a circular air movement within the gap. There is natural convection between the absorber plate and the insulation layer, and forced internal convection induced by the fluid flowing in the pipes. Heat transfer coefficients related to convection are a function of the air velocity-either directly, or through the Nusselt number.

$$\frac{dQ}{dt} = h * A * (T(t) - T_{env}) \qquad (3)$$

Radiation occurs when surfaces are exposed to other surfaces with different temperatures. Heat is radiated from warm surfaces to cold surfaces. Related to solar collectors, the radiative term is important to regard especially when inspecting the absorber plates. By constructing these low emitting, it ensures that the radiation from the absorber to the surroundings is small. This means that more heat will be transferred to the working fluid instead of being radiated back to the ambient.

When investigating radiation exchange between two surfaces the view factor F is an important parameter, which describes the fraction on the radiation that leaves the one surfaces and strikes another surface directly. The heat transfer also depends on the emissivity of both the surfaces. This means that the total thermal resistance of the situation consist of three terms, see Eq. 4 [20]. Q is the radiated heat transfer, σ is the Boltzmann constant and ε is the emissivity.

$$\dot{Q}_{1 \rightarrow 2} = \frac{\sigma(T_1^4 - T_2^4)}{\frac{1-\varepsilon_1}{\varepsilon_1} + \frac{1}{A_1 F_{1 \rightarrow 2}} + \frac{1-\varepsilon_2}{\varepsilon_2}} \qquad (4)$$

3.3   Advantages with façade integrated solar collectors

Submerging the solar collectors into the façade represents a transition where the building envelope goes from being an important element related to heat loss to being a source of heat and a mean of reducing the transmission during the winter. By varying the insulation

thickness in the base of the solar collector, the amount of heat transferred through the solar collector into the construction behind is affected. The question and the problem that will be investigated later in this report is if this heat transfer can contribute to a smaller annual energy use in the building.

3.3.1 DHW demand profile match

Façade integrating solar collectors sets restrictions to the orientation and tilt of the collector panel, but not being able to achieve the optimal orientation and tilt can actually be positive in some cases. Combined systems, which cover both DHW and SH require big solar collector areas to be able to cover a satisfactory part of the energy demand by the solar collectors during the winter. This may lead to long stagnation periods during the summer, when the available energy is far bigger than the demand, and the risk of overheating the system is big. The aspect of stagnation is evaluated in Chapter 4.2. Practical investigations show that it is normal to under-dimension roof mounted solar collector systems by 30-50 % of the solar fraction to avoid overproduction and overheating during the summer [22]. This problem is reduced when considering the use of façade integrated vertically mounded solar collectors. Matuska and Sourek [23] conducted an analysis in 2006 showing the advantage of façade integrated solar collectors compared to conventional roof placed solar collectors with a 45 degree slope used for DHW. The study shows that for a test reference year of Prague climate façade integrated solar collectors perform better than conventional externally placed collectors. This was because the amount of collected energy was almost equal to the DHW load throughout the year and large stagnation periods were thus avoided.

3.3.2 Heat transfer coefficients

Research done by Sparrow and Lau [24] show that the local heat transfer coefficient of a plate exposed to an airflow is bigger around the edges compared to the centre since the airflows is bigger at the edges. This means that the average heat loss coefficient of a plate exposed to an airflow is reduced if the plate is surrounded by another construction. This effect is achieved by integrating the collectors into the wall. Matuska and Sourek [23] conducted an analysis on the effect of different heat transfer resistances surrounding solar collectors, and realized that the solar energy conversion efficiency of the solar collector increases by increasing the

thermal resistance of the surroundings. The efficiency is always better than for external roof mounted collectors. The effect is especially evident for increasing collector and ambient air temperature differences, and may be a result of decreased heat loss though the edges of the collector. The study further shows that façade integrated solar collectors have reduced heat transfer coefficients for natural convection in the gap between the absorber and glazing. In addition was the wind related convection reduced. The same was the back and edge heat loss coefficients.

3.3.3 Other advantages

R. Li et al. [2] have conducted a study on the novel solar heating wall in the Green Energy Laboratory in Shanghai. The study was conducted for Shanghai climate, with small insulation thicknesses compared to the Norwegian building trend. The study revealed that the performance of a solar heating wall was better than the performance of a conventional wall during the winter season. This was because the solar collector wall led to lower transmission losses from the building. This indicated that the passive solar heat from the wall contributes to reducing the space heating demand in the building. This effect decreased as the insulation thickness increased, but the heat loss from the wall to the ambient was in every situation lowered when using façade integrated solar collectors.

The Norwegian building trend is moving towards zero emission buildings, and even plus-houses. In the emission balance here, one are also interested in the energy embodied in construction materials. At the same time is the demand for the energy-use so strict that the buildings have to be able to produce their own energy. This can be covered by solar collectors, and by façade integrating them, the total embodied energy is lower compared to using both conventional construction elements and externally mounted solar collectors.

In addition to the possible increased performance of the integrated collectors compared to roof mounted collectors, several other advantages arise from façade integration. Placing external collectors on roofs can be problematic due to space. The panels often have to compete for space with other technical equipment, and orienting the collectors optimally can therefore be difficult. The use of façade integrated solar collectors is especially interesting in high-rise buildings with high thermal demands. The roof areas are small compared to the wall areas, making it close to impossible to cover substantial thermal loads with solar collectors without

utilizing the building envelope. Additionally, In the Norwegian climate there is a problem that snow collects on roof mounted solar collector systems. One avoid this by integrating the collectors into the wall. At the same time will wall integrated collectors react to increased irradiation from snow on the ground. This effect enhances the performance of the collectors during the winter [25]. Complete façade integration of collectors makes it easier to make the collectors aesthetically acceptable compared to external collectors placed on roofs. Many suppliers of façade integrated solar collectors can deliver dummy elements that do not contribute energy wise, but look the same as the actual solar collectors. This is only to ensure aesthetic acceptability. It is also possible to get absorber plates in different colours. This makes the collectors even more applicable.

3.4   Barriers to façade integrating solar collectors

For summer days, the study of R. Li et al. [2] shows that the transmission to the building is higher with façade integrated solar collector walls compared to conventional walls. This effect is especially evident for small insulation thicknesses behind the solar collectors. This may lead to a higher cooling demand in the building, especially for office buildings with high internal heat loads.

Conventional solar collector systems are designed to maximize the annual solar gains. This is done by optimizing the slope of the collector with respect to the heat load and how the sun vary throughout the year, and facing it towards the orientation with the highest solar intensity. It is evident that optimization to this extent is not possible with integrated solar collectors. Matuska and Sourek. [23] investigated the solar fraction for a solar system in central Europe mounted with a 45-degree slope compared to the same façade mounted system installed with a 90-degree slope. The result show that the façade-integrated system should have a 30 % increased area to be able to deliver the same solar fraction as the optimally installed system. The solar fraction in further discussed in Chapter 4.9.1.

The use of façade integrated solar thermal systems is not as widely used as one would think when looking at the advantages. This is due to several reasons. For once, complete integration of collectors requires thorough planning. Many solar thermal systems are pre-produced, making it difficult to integrate the systems perfectly within the walls, especially for existing buildings. This may have aesthetic consequences that leads to the projects not being realized.

4 System design and operational considerations

4.1 Collector tilt angle

As earlier reviewed, the tilt angle of the solar collector is an important parameter for maximizing the collector performance. The collected energy is a result of both diffuse and direct radiation. This means that the optimal angle for energy collection changes according to the time of the day and the season. There are several reasons to aim for installing solar collectors with the optimal slope. One of them, and often the most important one is cost reduction. By having the right tilt, the collectors can deliver more energy, and the solar collector area can be reduced. The aim can be to maximise the available energy throughout an entire day, or maximise it for a specific time of the day. In some cases, especially for industrial solar thermal systems, it is profitable to ensure maximum radiation on the panels at all times with the use of a solar tracking system. The optimal tilt angle vary according to the season since the sun is higher on the sky during the summer. This allows for steeper collector slopes during the winter months, while this will not be optimal for summer times.

There are several studies and theories on the optimal tilt angle for collectors. Most of them relate the tilt angle to the latitude where the collector is installed. An angle of the latitude $\pm 10°/15°$ is the result of studies by Duffie & Beckmann, Heywood, Lunde, Chinnery, Löf & Tybout and Garg [4, 26-30]. Other approaches takes into consideration the monthly global and diffuse radiation on a horizontal surface. Statistics of the global radiation exist for most places in the word, but the diffuse radiation is harder to estimate. R. Tang et al. [31] developed a method for deciding the optimal tilt angle for collectors installed in China. This approach estimates the diffuse radiation from the global radiation and an air clearness index, and gives a relation between the total radiation, the albedo of the ground and the tilt angle of the collector.

The aspect of optimal tilt is important to acknowledge in the discussion around façade integrated solar collectors. With façade integration, the orientation and tilt cannot be adjusted according to solar availability, which will reduce the useful energy gain of the collector compared to externally mounted collectors installed with the optimal slope.

4.2 Area

There exist several rules of thumb on the optimal collector area. Zijdemans [32] recommends that single family dwellings using solar collectors for DHW production install 4-6 m^2 solar collector areas. Finding the optimal solar collector area is purely an economic consideration. One want the lowest possible investment cost for covering the load. This means that it is a choice between additional solar collector areas or investment in auxiliary energy systems and fuel [33]. Finding the optimal collector area is especially complicated for combined space heating and DHW solar thermal systems. To be able to cover a satisfactory amount of the energy during the winter months when the space heating need is biggest and the available radiation is smallest, big solar collector areas are necessary. With these high areas, the water tank easily reaches its maximum allowed temperature during the summer. The main circulation pump is then turned off and the stand-still water in the collector pipes rapidly reaches the stagnation temperature, which for a flat plate collector is 180°C - 210°C. Task 26 from IEA SHC [34] describes the process when the collectors reach stagnation temperature. Firstly, the liquid in the collectors starts to evaporate and expands. This causes the working fluid to be pushed out of the collector and into the expansion vessel as the system pressure increases. As the collector becomes increasingly dry, the remaining steam is superheated until the irradiations starts to decrease and the collector is refilled again. Stagnation periods are hard to avoid in any solar collector system, but the consequences of these periods do not have to be damaging to the system. Problems arise when the stagnation control schemes are not working satisfactory, for example in the drainage of the system. The high temperatures that then arises can seriously damage the system and even lead to used scalding [35].

The optimal area depend on the use of the collected heat. Zijdemans [32] further recommend that for a single-family dwelling using solar collectors for a combi-system with both DHW and space heating, a collector area of 8 m^2-12 m^2 is installed. Here the load is higher than for a separate DHW-system, and the higher collector area will therefore not cause stagnation in the system. It is important to realize that the optimal collector area depend on the available radiation, the load and the storage tank volume. It is likely that the collector area for façade integrated solar collectors should be bigger due to less collected heat compared to collectors under optimal slope.

4.3   Working fluid

The heat transfer fluid of the solar collector must be chosen with care to ensure good conditions for the system. When choosing the fluid, the deciding parameters are the coefficient of expansion, viscosity, thermal capacity, freezing point, boiling point and flash point [36]. Water is a common heat transfer media due to its outstanding thermo physical properties. The high specific heat and thermal conductivity and the low viscosity makes it possible to transfer big quantities of energy with the use of little auxiliary energy. However, water has some disadvantages. The temperature range is very limited due to its high freezing point and low boiling point compared to other options of heat transfer medias. It also corrodes some metals. The extent of corrosion depends on the oxygen content, the pH, the temperature and the presence of other chemical substances [37].

For the following investigations, a mixture of ethylene glycol is chosen. The volume percentage of glycol is set to 40 % [38]. Propylene glycol is chosen to avoid freezing. The specific heat capacity of a mixture of water and 40 % Propylene Glycol is 3747.2 J/kgK [39]. As the concentration of propylene glycol increases, the specific heat capacity decreases.

4.4   Storage tank stratification

Solar energy is a time dependent energy source. This means that the performance of the overall solar thermal system is highly dependent on the effectiveness and the capacity of the storage facilities. Properly designed storage will minimize life cycle costs and reduce auxiliary energy. SHC Task 44 [40] shows the great importance of proper stratification in solar energy storage systems to ensure high performance. In addition did the task reveal the lack of proper simulation tools to model the complex hydrothermal effects in water storages, especially with the mixing of hot and cold water, and the exergy losses in systems with high flow rates of the incoming flow. The degree of stratification in the storage tank heavily influences the collector system performance. In highly stratified tanks, there is a big temperature difference between the top and the bottom of the tank. This happens due to density differences of water with different temperature. A high degree of stratification is desired in solar heating systems. In indirect systems, low temperatures in the storage media surrounding the heat exchanger will ensure the maximum heat transfer from the collector circuit to the storage. This is achieved by placing the heat exchanger in the bottom of the stratified tank, adjacent to the inlet feeding the tank with fresh cold water. Warm water to the

21

load is drawn through an outlet positioned in the warmer section of the tank, which is at the top as seen in Figure 4-1.
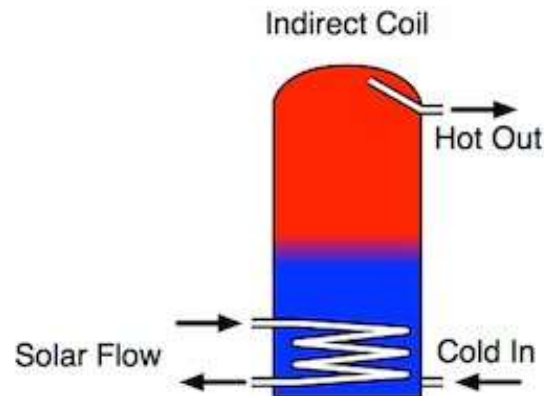
Figure 4-1 Stratification in indirect system water tank [41]

The extent of stratification depends on the design of the tank, where especially the mass flow rate and the location of the inlet and outlets are important. High degree of stratification is achieved through very low flow rates at the inlet and outlet. Even though relatively high mass flow rates in the collector leads to higher efficiencies, see Chapter 4.9.4, it also leads to higher fluid velocities in the piping, and subsequently higher inlet and outlet velocity to and from the tank for direct systems. This will lead to a lower degree of stratification. Also for indirect systems, lower mass flow rates through the heat exchanger leads to a higher degree of stratification due to decreased convection in the tank [42]. A high degree of stratification ensures a lower fluid temperature entering the solar collector, and this is desirable. In addition will the avoidance of lukewarm water due to the mixing of cold and warm water in the tank be desired for both direct and indirect systems.

The second important parameter influencing tank stratification is the ratio between the height and diameter of the tank. Taller tanks allows for a higher degree of stratification. Furbo et al.[43] show that a height to diameter ratio of 2:1 or higher is necessary to insure sufficient stratification.

The use of stratified tanks introduces challenges regarding the shielding against Legionella. The best conditions for the growth and formation of Legionella bacteria is between 20-60 degrees, with the optimum growth range around 40 degrees. The death rate of the bacteria is

high for temperatures above 60 degrees [44]. Byggforsk recommends that the thermostat for hot water solar heater tanks is set to minimum 60 degrees to minimize the risk of Legionella contamination [45]. Stratified water tanks is considered as high risk regarding the growth of Legionella bacteria, since they are likely to contain substantial volumes of water with a temperature between 20 and 50 degrees. The temperatures in the tanks are constantly changing according to solar availability and water draw, and the tank does not necessarily have a set temperature outside of the hazardous temperature interval. A common strategy to control the temperature in stratified tanks not connected to a solar heating system is to ensure that the whole tank is heated to at least 60 degrees once a day by the use of a pump that circulates water from the top to the bottom of the tank. This is done during low loads. If this is to be done in solar heaters, there is a risk that the water in the bottom of the tank is not cold enough to ensure satisfactory collector efficiency when the de-stratification is done. In addition is it not guaranteed that the water in the top of the tank is hot enough to create an overall temperature exceeding 60 degrees after mixing. If de-stratification is to be done, the best time to do it is when the power of the incident solar radiation is decreasing and the temperature of the water tank is at its highest. This corresponds to around 4 hours after solar noon [46]. With the stratification being essential to achieve a high solar water heater performance, overcoming the challenges with the Legionella bacteria is crucial to make the use of solar water heaters a safe and reliable solution,

4.5   Storage tank volume

The volume of the storage tank is an important parameter that influences the system performance. Studies by C. Comakli et al. [47] show that increased storage capacity leads to increased solar collector efficiency, but lower water tank temperatures and consequently higher auxiliary energy power. This means that thorough analyses should be carried through when designing solar collector systems with water tank storage. Finding the optimal tank volume is an optimization task with many parameters. Having a small tank compared to the available solar energy and the water draw leads to high tank temperatures and lower degrees of stratification. This will lead to shorter operational time for the collectors, lower collector efficiency and possible stagnation problems. Bigger tanks are more expensive, they impose a higher complexity to the system and leads to a bigger heat loss. Nevertheless will big tanks also ensure low inlet temperatures to the solar collector, higher temperature rises over the

collectors and consequently higher collector efficiencies. Research done by A.M Sharia et al.[48] on the correlation between storage volume and solar collector area for a thermophyson solar water heater system, shows that the solar fraction increases with an increase in water tank volume up to a certain value. Additional increases in the tank volume after this point leads to constant solar fractions. This happens when the additional useful energy gain is equal to the additional tank heat loss. As the volume reaches the point where all available heat is collected, the solar fraction will decrease as the heat loss from the tank further increases.

Research one by SSB [49] show that each person in a Norwegian residential building has a hot water consumption of around 70 l/day. For a four-person family this constitutes to around 300 l/day in total. Zijdemans [32] state that a storage tank with the capacity of 1-2 times the DHW consumption is sufficient for covering the demand in a proper way with the use of solar collectors. This leads to recommended tank volumes of 300 l-600 l for a single family dwelling.

4.6 Mass flow rate
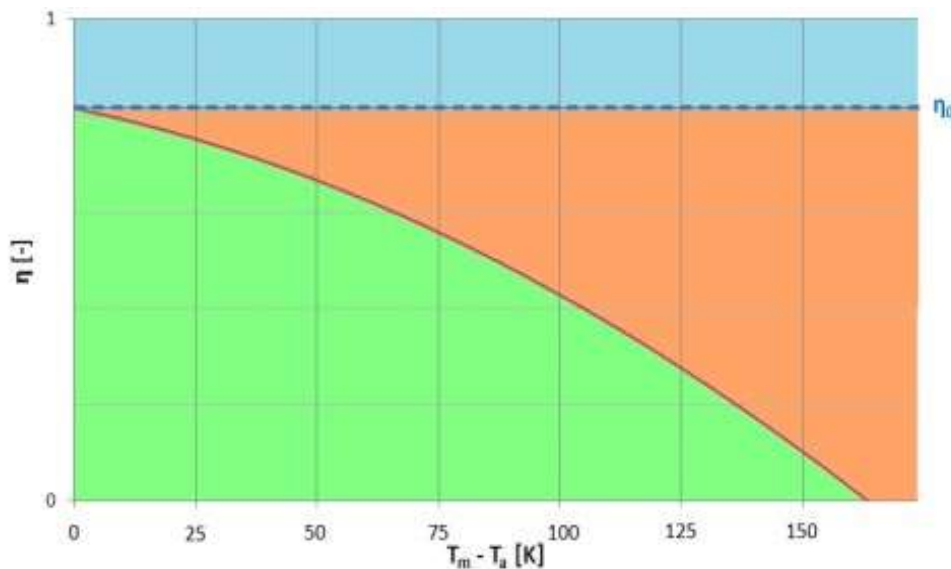
Figure 4-2 Example of losses in a solar collector. Green area: Useful energy, orange area: Heat losses, blue area: Optical losses. Tm = absorber mean temperature, Ta = Ambient temperature [50]

There are advantages and disadvantages with both high and low mass flow rates through the solar collector. High flow rates will lead to a smaller temperature differences between the inlet and outlet of the collector and therefore a lower mean plate temperature. As seen Figure 4-2 will this lead to a higher useful energy gain and a higher collector efficiency. Low flow rates will lead to a high absorber mean temperature. This increases heat losses from the absorber plate and the collector efficiency decreases. Z.Chen et al. [51] show this through experiments. The collector efficiency increases and the absorber heat loss decreases as the flow rate is increased to a certain point. If the flow rate is increased further, the collector efficiency decreases. This is basically because the flow rate is too high for the heat to be transferred from the absorber to the fluid in the pipes. This means that the optimal flow rate increases as the mean fluid temperatures increases.

High flow rates require bigger pumps and tube diameters, and a higher consumption of auxiliary energy. It will be the opposite for lower flow rates. In addition to the heat loss effects on the absorber plate, will the flow rate also affect the tank stratification as discussed in Chapter 4.4.

4.7 Circulation pumps

A technology that is gaining importance also within solar collector systems is the use of variable speed pumps. Compared to constant speed pumps, will these prevent the problem with short cycling. Short cycling is a situation where the pumps turn on and off rapidly since the climatic parameters make the system cycle between situations where the temperature requirement for the circulation pump is met and not. For solar collector systems, this requirement is commonly related to the temperature difference between the bottom of the storage tank and the outlet of the collector. Short cycling wears out the pumps, and reduces the useful energy gain. This is more likely to occur on days with low and moderate radiation, which are common in the Norwegian climate. With the use of variable speed pumps, the flow rate drops according to the temperatures in the system. If the radiation is high and a sufficient temperature rise over the collector is reached, the flow rate is increased. During times of lower radiation, the flow rate will be lower. This ensures smoother conditions for the pump, and increases the useful energy gain as seen by Z. Chen et al. [51] and as discussed in Chapter 4.6.

4.8 Solar assisted heat pump

There are two main ways of combining solar collectors and heat pumps. The heat pump can be installed in series or in parallel with the solar collector panels. The two configurations influence the system in different ways where the series configuration introduces the biggest impact. This installation affects the temperature levels in the solar collector loop.
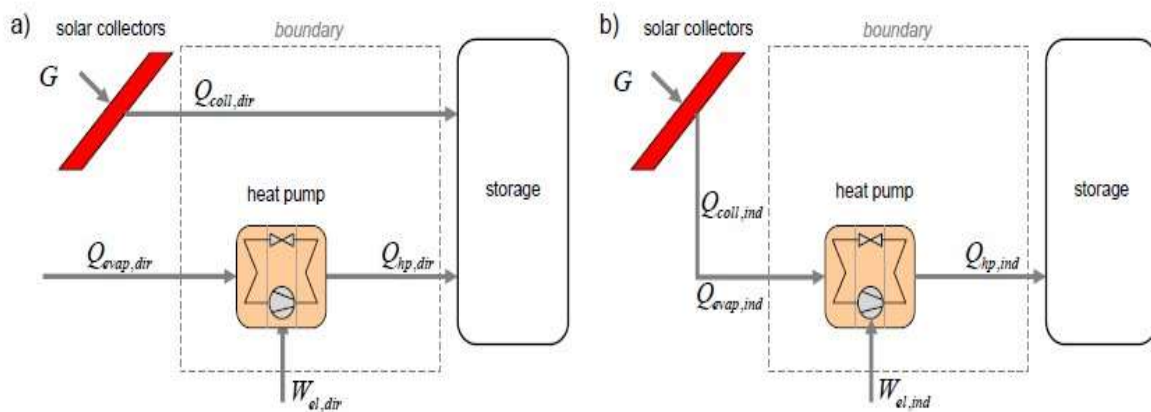
Figure 4-3 Combined solar collector and heat pump system a) Parallel configuration b) Series configuration [6]

4.8.1 Parallel configuration

Figure 4-3 a) shows a parallel solar collector and heat pump configuration. The heat pump operates independent of the solar collector panels, and only runs when the collector panels cannot deliver enough heat. The energy source of the heat pump is ambient air, or other low temperature heat sources such as brine water from a ground source or a seawater heat exchanger. A separate auxiliary heater should be installed to cover the peak loads when the solar radiation and the temperature of the heat pump energy source is low.

4.8.2 Series configuration

When installing the heat pump in series with the solar collector, the solar heat is used to enhance the performance of the heat pump evaporator as seen in Figure 4-3 b). By raising the evaporator inlet temperature one can increase the COP of the heat pump. When the water temperature exiting the solar collector is within a reasonable interval, using the heat pump

will be more energy efficient than running the working fluid directly through the tank heat exchanger and using the electric boiler. This is shown by the research of M. Haller et al. [8]. The acceptable evaporator inlet temperature depends on heat pump characteristics. If the water is too hot, the heat pump efficiency will be low and the heat pump may be damaged.
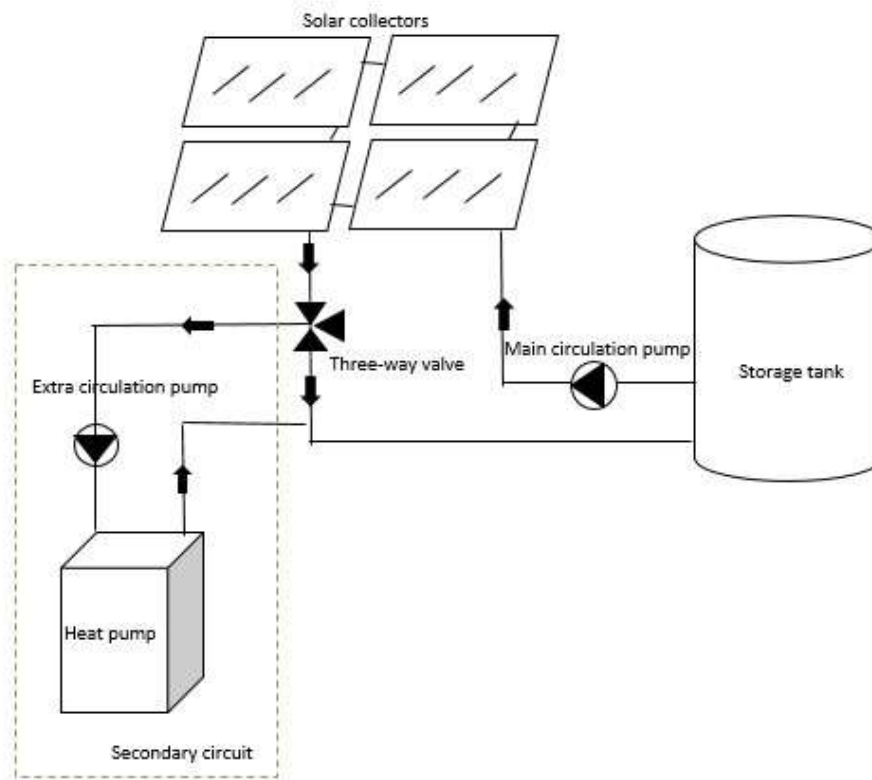
Figure 4-4 System sketch of parallel configuration solar assisted heat pump [52]

Solar assisted heat pump systems should have a bypass that makes it possible to run the water exiting the solar collector straight to the storage tank if the water temperature is high enough, as seen in Figure 4-4. This makes it possible to run the system in two different modes. This can be problematic, especially in systems with constant speed drive pumps. The heat pump represents an extra resistance to the water flow, especially small heat pumps that are usually installed with plate heat exchangers. In addition will the three-way valve that divides the system into the main circuit and the secondary circuit impose a resistance. This means that at times when the heat pump is running, the required shaft power for the circulation pump may be substantially increased. There are two ways of solving this problem. One can install a

single circulation pump to cover the entire system. This requires a variable speed pump where the pump power is increased when the heat pump is operational. Alternatively, two circulation pumps can be installed, as in the system in Figure 4-4. The second circulation pump only runs when the heat pump is operational and imposes the extra resistance. It is crucial that the regulatory strategy is well designed to ensure that the circulation pump is not operational before the three-way valve is completely open. For some valves, the opening time is relatively long. If the pumps starts running as the valve starts to open, there is a risk of pumping a pipe containing little or no liquid. This can impose heavy damages to the system [52].

This configuration requires a relatively complicated regulatory strategy to ensure that the heat pump is used instead of the electric auxiliary heater. In addition are through investigations necessary to reveal when it is profitable to run the heat pump and when it is profitable to send the working fluid directly to the tank heat exchanger. This depend on solar availability and the heat pump characteristics. M. Haller et al. [8] found that the series configuration introduces a higher energy saving compared to the parallel configuration for systems with high temperatures on the demand side and low temperature on the heat source side. This situation is common in the Norwegian climate when the solar thermal system is used for high temperature applications such as DHW.

4.9 System performance indicators

4.9.1 Solar fraction

The solar fraction describes the relationship between bought energy quantities in systems with and without solar thermal energy. It is defined in Eq 5. L_i is the purchased energy for a fuel based system in month i, and $L_{A,i}$ is the purchased energy in a system with solar energy the same month. The purchased energy is used to cover the load that the solar collectors cannot cover.

$$f_i = \frac{L_i - L_{A,i}}{L_i} \qquad\qquad (\ 5\ )$$

This equation does not include the energy consumption related to running fans and pumps in the system, so called parasitic electrical energy. If these effects are significant, it may be necessary to include them in the calculation of the solar fraction.

The solar fraction is typically an important parameter when evaluating the performance of the collectors and when deciding the optimal solar collector area. Reaching a solar fraction of 100 % is not practical. When looking at a solar collector system providing DHW, the increase in the solar fraction is not proportional to the increase in the solar collector area, even when the storage volume is increased accordingly to match the collector area. This is especially evident for collector panels installed in series. This means that there is an economic best point, which takes into consideration investment costs and collector performance [53].

4.9.2 Total heat loss coefficient

The total heat loss from the solar collector happens through the top, the bottom and the edges of the collector. The following relations are rendered from Duffie and Beckmann [4]. The heat transfer coefficients that are used in the following investigations are given in Table A-1 in Appendix A.

Calculating the top loss requires knowledge about the top loss coefficient of the collector. This is an iterative process since the temperatures and the heat transfer coefficients are all a function of each other. For a single cover solar collector the heat transfer coefficients influencing the system is radiative, $h_{r,p-c}$, and convective, $h_{c,p-c}$, heat transfer between the plate and the cover in addition to wind heat transfer h_w and radiative heat transfer, $h_{r,c-a}$ between the cover and the ambient. This gives the top loss coefficient in Eq. 6

$$U_t = (\frac{1}{h_{c,p-c}+h_{r,p-c}} + \frac{1}{h_w+h_{r,c-a}})^{-1} \qquad (\ 6\ )$$

For many applications, one assume no convection and radiation between the absorber plate and the back insulation. For these cases, the total heat transfer through the back of the collector is induced by convection through the insulation. The back loss coefficient is given in Eq. 7 where k is the insulation thermal conductivity and L is the insulation thickness.

$$U_b = \frac{k}{L} \qquad (\ 7\ )$$

Evaluation of edge losses is often complicated, but for most applications they are small and inaccuracies will not lead to great errors. By assuming one-dimensional heat loss through the edges of the collector, and relating the edge loss to the total collector area, the edge loss coefficient can be represented by Eq. 8. U and A is the U-value and the area of the edge of the collector and A_c is the total collector area.

$$U_e = \frac{(UA)_{edge}}{A_c} \qquad (8)$$

If all sides of the collector are exposed to the same boundary conditions, the overall heat loss coefficient will be the sum of the top, back and edge loss coefficient. This is not the case for façade integrated solar collectors. In the following investigation of façade integrated solar collectors, the total heat transfer coefficient is defined as the sum of the overall heat transfer coefficient from the plate to the cover and from the plate to the insulation. The edge losses are neglected.

4.9.3 Useful energy gain

In steady state, a balance between incident solar energy, thermal losses and optical losses describes the useful energy delivered by the collector, as seen in Eq 9.

$$Q_u = A_c\big(S(\tau\alpha) - U_L(T_{pm} - T_a)\big) = A_c \Delta T \dot{m} c_p \qquad (9)$$

A_C is collector area and S is solar radiation absorbed per unit area of absorber. The absorbed radiation depends on the absorbance of the absorber and the transmittance of the cover. The optical losses occur because the transmittance of the cover and the absorption of the absorber plate are not ideal. U_L is the overall heat transfer coefficient and T_{pm} and T_a is the mean absorber plate temperature and the ambient air temperature respectively. ΔT is the temperature rise over the collector, $\dot{m}$ is the fluid mass flow rate and c_p is the specific heat of the fluid. This equation is difficult to evaluate since the absorber mean temperature depends on the overall thermal performance of the solar collector. Physical systems are not steady state, which makes the situation even more complicated. This balance is not directly applicable for façade integrated solar collectors since the boundary conditions on the front and

the back of the collector are not equal. This means that the balance becomes more complicated, and is a function of the temperatures on the different layers in the collector. The equation must be revised to describe façade integrated collectors. Evaluation of this equation for façade integrated solar collectors under transient conditions is given in Appendix A.

4.9.4 Solar collector efficiency

The solar collector efficiency is a measure of collector performance. It is defined as the ratio between the useful energy gain of the collector over a specified time period and the incident solar radiation the same period, as defined in Eq. 10, where G_t is the incident radiation.

$$\eta = \frac{\int Q_u dt}{A_c \int G_t dt}$$

(10)

It may not always be beneficial to design the system for the maximum efficiency. Even though there is available solar radiation, this does not mean that it is beneficial to run the circulation pump. This could be because the load is too low to transport the already stored heat, or that the available energy than can be collected does not exceed the energy used for running the pumps. The best point is found through predictions of the performance of the collector seen with respect to the load variations.
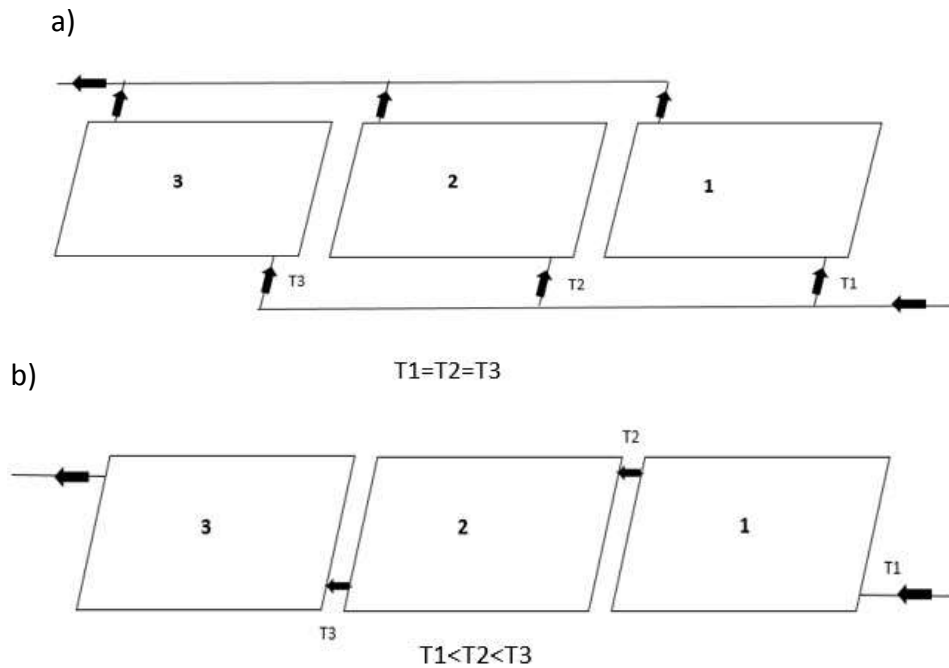
Figure 4-5 a) Collectors in parallel b) Collectors in series

The second part of Eq. 9 shows the importance of the mass flow rate for the system performance. This indicates that solar collector panels installed in parallel and in series may not behave equally. For series configurations, each panel will have the same flow-rate, but the collector inlet temperature will increase for each panel, as seen in Figure 4-5 b). The mean plate temperature and the heat loss from the collector plate will increase and the temperature rise over the collector will decrease as the fluid flows through each panel. This means that the efficiency of the first panel will exceed the remaining. For properly designed parallel installations the mass flow rate, the temperature rise over the collector and heat loss from the absorber will be equal for all panels, see Figure 4-5 a). The series configuration will require bigger pumps and pipes, which may lead to a lower solar fraction compared to the parallel configuration even if the efficiency is higher. Which configuration that will show the highest efficiency depend on the design [4].

5 TRNSYS and other simulation and design software

When simulating physical systems, an understanding of the assumptions and equations behind the models and simulation tools used is important to ensure accurate results. A mathematical model is always a simplification of the real situation, but the degree of simplification depends on the degree of detail in the model. Highly complex models require big computer power, and are time consuming, while too simplified models lead to inaccurate results. The best point is a trade-off between the two.

There exist several simulation programs to investigate the performance of solar collector systems, such as Polysun [54] and IDA ICE [55]. However, few software also include the possibility of investigating façade integrated solar collectors. This opportunity exist in TRNSYS [56] and the KOLEKTOR model created by T.Matuska [57]. Many former studies conducted on façade integrated solar collectors have used TRNSYS in combination with external models that describe the performance of the integrated collectors. These models are written in common programming languages such as FORTRAN or created in the MATLAB environment. The simulation tool chosen for this report is TRNSYS. In addition is the same model used in the study by R. Li et al [2] implemented into the TRNSYS interface to describe the performance of the façade integrated solar collectors.

5.1 TRNSYS

TRNSYS is an extensive simulation tool, which simulates transient and dynamic systems. TRNSYS simulates multi-zone buildings, an application that is highly needed by engineers all over the world. This aspect with the fact that TRNSYS has an open modular structure where the source code is available for the user has made TRNSYS a success over the past 35 years. TRNSYS is suited to validate new energy concepts and optimize these due to the programs ability to include control strategies, human behaviour and alternative energy systems such as solar technology, wind and hydrogen systems. TRNSYS was originally developed for solar energy applications and is therefore highly applicable for investigating solar collector systems. The program is complex and therefore mostly used for academic purposes [43].

33

The interface of TRNSYS is tidy and easy to use. The system is set up graphically in the Simulation Studio through a drag-and-drop approach. Components such as pumps, fans and heating and cooling equipment, known as types, are found in a big library of components. TRNSYS is created in the programming language FORTAN, and new custom-made types can be added to the library using all common programming languages. An explanation of the types relevant for this project is given in Chapter 5.3. TRNSYS solves the algebraic and differential equations that arises when types are linked through inputs and outputs. Outputs from one type is inputs in the next, and the types are visually connected in the simulation studio though links, which can be related to ducts, pipes and wires in a physical system. TRNSYS solves the dynamic equations related to each type for each time-step. If loops are detected, they are solved through iterations until convergence is reached.

The Simulation Studio is one of the programs that the TRNSYS package consist of. For this project the Simulation Studio and TRNBuild is used. TRNBuild is further explained in Chapter 5.3.1.

5.2   The dynamic model of the solar curtain wall at the GEL

The dynamic model of the façade integrated curtain wall created by R. Li et al. [2] describes the thermal performance of the façade integrated solar collectors installed at the Green Energy Laboratory at Shanghai Jiao Tong University. This model is used in the case study in this report. The configuration of the solar curtain wall that the model describes is shown in Figure 5-1.
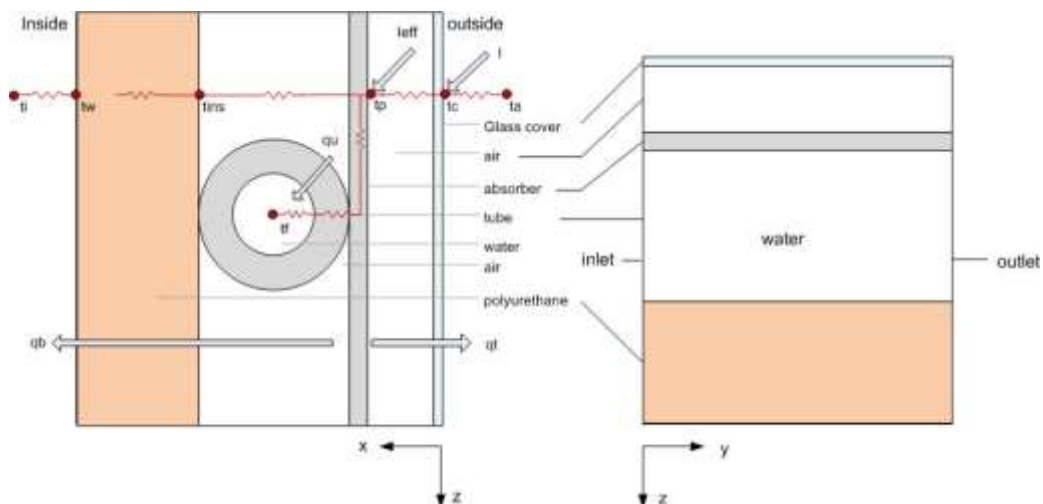
Figure 5-1 Description of the solar wall at the Green Energy Laboratory [2]

The model is created in FORTAN, and is programmed to fit the syntax of a TRNSYS Type. The type is called Type 701, and is used in the TRNSYS Simulation Studio along with the standard types from the TRNSYS library.

The differential equations of the dynamic model are derived and expressed systematically in Appendix A. They describe the overall energy balance of the collector. The main challenge with the system is that the temperatures of each layer in the collector are dependent on the heat transfer coefficient between the layer in question and its environment. On the other hand are the heat transfer coefficients again dependent on the temperature of the layers. In the FORTAN code, the energy balance of each layer in the solar collector is represented, and each temperature is found through iterations on these balances as described in Chapter 5.2.1

5.2.1 Numerical method used to solve the transient differential equations

To solve the differential equations that describe the thermal performance of the curtain wall, analytical methods are used. Certain physical effects, especially nonlinearities are ignored to make the problem simple enough to be solved through the finite difference method. The majority of these effects are the dependence of thermal properties and the temperature in the material. Both thermal conductivity and the radiation boundary conditions are temperature dependent, but these effects are ignored in the solving of the equations.

The finite difference method is based on replacing the differential equations with algebraic equation by replacing the derivatives with differences as seen in Eq. 11. The algebraic equation is then solved through iterations. When the situation investigated is transient, the finite difference solution requires discretization in both time and space to decide these differences [58]. A suitable time-step is chosen, and the equations are repeatedly solved for each time-step. For the situation with a several layer wall, such as the solar curtain wall, energy balances are created for every layer and each temperature node is treated as a volume element. The following explicit discretisation is used. $\dot{Q}$ is the heat flux to the volume element, $\rho, V_{element}$, and c_p is the density, volume and specific heat capacity of the material respectively.

$$\sum\nolimits_{All\ sides} \dot{Q} = \frac{\Delta E_{element}}{\Delta t} = \rho V_{element} c_p \frac{\Delta T}{\Delta t} = \rho V_{element} c_p \frac{T_m^{i+1} - T_m^i}{\Delta t} \qquad (\ 11\ )$$

5.2.2 Limitations and simplifications in the GEL model

There are some simplification in the GEL model that could lead to inaccurate results.

The calculation of the heat transfer coefficients influences the energy balances. The heat transfer coefficient for radiation between the cover and the ambient is dependent on the sky temperature and the ambient air temperature. The equivalent sky temperature must be estimated, and different researchers have found different approaches to this estimation such as Swinbank, Bliss, Berdahl and Brunt [57, 59, 60]. The approaches are accurate for a set of conditions, and each equation will therefore not be accurate for all situations. In the GEL model the Swinbank approach [59] has been chosen. This approach describes a situation with clear skies, and the model does not supply any alternative to this. To ensure as accurate results as possible, the model should allow the user to change the method of estimating the equivalent sky temperature according to the problem conditions. In addition, the GEL model simplifies the equation for the radiative heat transfer coefficient between the cover and the ambient. The equation originally depend on both the sky temperature and the ambient temperature, while the GEL approach assumes that these temperatures are equal, despite of the fact that the sky temperature are estimated as a function of the ambient temperature. The simplification is proposed by Duffie and Beckmann [4], but EN6946 [61] states that this approximation is valid only when the sky is cloudy. This simplification will lead to a different result compared to using the detailed equation, and the error increases as the ambient temperature increases.

For the heat transfer coefficient for convection between the cover and the ambient, the GEL model uses McAdams approach [20], but only for air velocities up to 5 m/s. McAdams has defined equations for estimating the coefficient also for velocities above 5 m/s, but this is not included in the GEL model. Additionally, the research of Sparrow [24], which describes the reduced convection heat transfer coefficient in the middle of a plate compared to the edges, is not included.

The GEL model completely neglect the heat loss through the edges of the solar collectors. Even though this heat loss is much smaller than for externally placed collectors, it could have an effect as seen in the research of T. Matuska [23].

In addition does the model set a few assumptions that are more commonly used, for example in evaluations by Duffie and Beckmann [4]. The heat transfer through the cover and the insulation layer is one- dimensional. All properties are independent of temperature, and the temperature gradients in direction of the flow in the tube and between the tubes can be treated independently. The last prerequisite simplifies the aspect discussed in Chapter 3.2.

5.3   TRNSYS components

5.3.1   The multi-zone building (Type 56)

The multi-zone building model of TRNSYS allows the user to implement a multi-zone building as a component like the conventional components in the simulation studio. The TRNBuild program is an external program that reads and processes the building description and generates files that are used by the type 56 component in the simulation studio. Through TRNBuild, all the structural details of the building are defined. The type 56 building model is an energy balance model where the energy balance of each air-node of the building is solved. Each zone in the multi-zone model may have more than one air node. In addition to the air nodes, each surface of the building is modelled as a surface-node. Consequently, the simulations are conducted with the temperature of each surface being homogeneous over its entire area.

In this report, the multi-zone building is used to calculate the transmission through conventional passive house walls. All the layers of the walls are defined in TRNBuild and the heat transfer is modelled through two nodes of the wall. One at the exterior surface and one at the interior. The model considers thermal mass, but it does not model the wall as a set of layers with different heat resistances. The wall is thus considered as a black box. Figure 5-2 shows the two-node model made by TRNBuild on an example wall. The subscripts s, o, and i stands for surface, outside and inside respectively. T represents the temperature and $\dot{q}$ represents heat flux. TRNSYS will model the thermal behaviour of the wall in one dimension only.
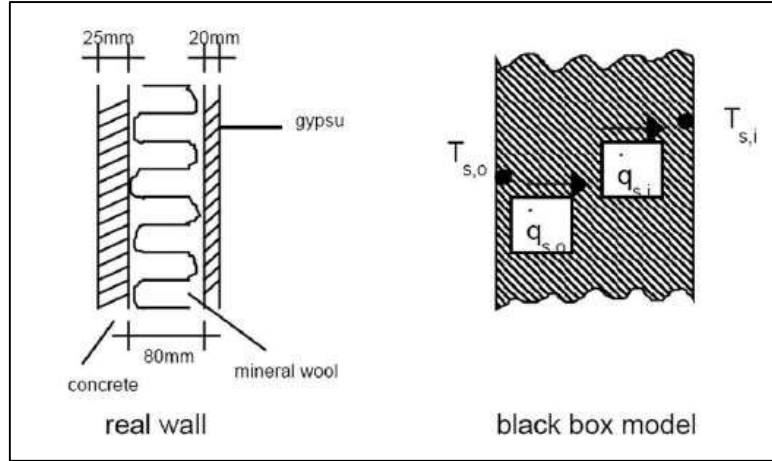
Figure 5-2 Real wall and the black box model of the wall created in TRNBuild [60]

The heat conduction through the wall is given in equation (12) and (13). k represents the term in the time series, where the number of k is influenced by the thermal mass of the wall. Heavy walls will have a high number of k. The coefficients a, b, c and d are coefficients of the time series and these are calculated as a matrix.

$$\dot{q}_{s,i} = \sum_{k=0}^{n_{b,s}} b_s^k T_{s,o}^k \sum_{k=0}^{n_{c,s}} c_s^k T_{s,i}^k - \sum_{k=1}^{n_{d,s}} d_s^k \dot{q}_{s,i}^k \qquad (12)$$

$$\dot{q}_{s,o} = \sum_{k=0}^{n_{a,s}} a_s^k T_{s,o}^k \sum_{k=0}^{n_{b,s}} b_s^k T_{s,i}^k - \sum_{k=1}^{n_{d,s}} d_s^k \dot{q}_{s,o}^k \qquad (13)$$

The multi zone model collects all constructional elements, and divides them from the rest of the simulation studio through the Type 56 component. TRNBuild does not have an open modular structure like the other types in the standard TRNSYS library. When a type 56 is defined, a building file (*.BUI file) is assigned, containing the required information for the type. This file has a rigorous syntax and should therefore not be edited [62]. This means that the dynamic model describing the curtain wall cannot be coupled directly with the Type 56 modelled building, but must be added as a separate type.

5.3.2 The storage tank (Type 60)

The water tank will in the following be modelled by the Type 60 storage tank from the standard TRNSYS library. The tank is stratified, and are divided into N (N<100) equally mixed volume segments, which decides the degree of stratification. This type allows the user

to decide the inlet heights, node sizes, auxiliary heater height, incremental loss coefficients and potential losses to gas flue if gas is used for the auxiliary heating [63].

5.3.3 The differential controller (Type 2b)

The differential controller generates a control function with a value of 0 or 1. The value is defined according to temperature differences and dead band values chosen by the user. For each iteration the temperature difference and the dead band values are tested, and the control function is changed according to these values and the former control function value. The equations deciding the control function are given in Eq. 14-17. γ_i and γ_o is the input control function and the output control function respectively. ΔT_L and ΔT_H is the lower and upper dead band temperatures respectively, while T_H and T_L are the upper and lower input temperature.

$$if\ \gamma_i = 1\ and\ \Delta T_L \leq (T_H - T_L), \gamma_o = 1 \qquad (\ 14\ )$$

$$if\ \gamma_i = 1\ and\ \Delta T_L > (T_H - T_L), \gamma_o = 0 \qquad (\ 15\ )$$

$$if\ \gamma_i = 0\ and\ \Delta T_H \leq (T_H - T_L), \gamma_o = 1 \qquad (\ 16\ )$$

$$if\ \gamma_i = 0\ and\ \Delta T_H > (T_H - T_L), \gamma_o = 0 \qquad (\ 17\ )$$

In the following investigations, the differential controller is used to control the main circulation pump according to the temperature difference between the bottom of the tank and the outlet of the collector. It also controls the auxiliary heater in the storage tank according to the DHW temperature. The control signal is automatically set to 0 if a monitoring temperature reaches its maximum allowed value [63]. This could be the boiling temperature in hydronic systems.

5.3.4 The circulation pump (Type 3d)

The pump receives the control function from the differential controller. The maximum power consumption and the maximum flow rate are input parameters to the component. The power consumption and the flow rate exiting the pump is the maximum input value multiplied by the control function. There is a temperature rise through the pump since some of the power is

converted into fluid thermal energy, see Eq. 18

$$T_0 = T_i + \frac{P f_{par}}{C_p m}$$ (18)

T_o is the outlet temperature of the pump, T_i is the inlet temperature to the pump, P is the pump power, f_{par} is the fraction of pump power converted into fluid thermal energy, C_p is the fluid heat capacity and m is the mass flow rate.

5.3.5 The heat pump (Type 41)

The heat pump used in the final investigations of this report does not exist in the standard TRNSYS library. It is characterized as a Nostandard Type that is developed by different authors than the standard types. The heat pump named Type 401 is modelled as a black box where the input values are the evaporator and condenser inlet temperatures and flow rates. In addition does the differential controller feed the heat pump with a control function. The heat pump component reads data from two input files containing the evaporator inlet and the condenser outlet temperature, in addition to the condenser and evaporator power. These data are obtained from manufacturer data sheets. The values are used to calculate coefficients of biquadratic polynomials, which are also included in the input file. These coefficients are used to increase the power of the heat pump in steady state situations by keeping the COP constant and linearly scaling the condenser and evaporator power with the constant factors. The heat pump includes non-steady state situations as well, through the evaluation of cycle, icing and defrosting losses [64].

6 Initial investigations

6.1 Method

Investigations are in the following divided into four parts. Firstly, the dynamic model describing the solar wall is verified trough real life measurements. Following, is the investigation of the thermal performance of different conventional walls and curtain walls for extreme weather conditions in the Norwegian climate. Four different days, two winter days and two summer days are evaluated to find the best wall configuration to further investigate. Then investigations on the influence of the chosen solar wall on the overall annual energy consumption of a concept building is the focus point. A parametric study is then conducted to reveal the potential of increasing the annual system performance by optimizing aspects of the system design. Aspects of interest are the optimal storage tank configuration, the regulatory strategy, the flow rate and the use of heat pumps.

For all investigations in the following chapters, the simulations are run with a time-step of 0.001 h. The dynamic model describing the thermal performance of the façade integrated solar collectors cannot be run with other time steps. Proceedings after the Solar World Congress in Jerusalem in 1999 [65] state that a time step of 0.5 hours is sufficient and commonly used in TRNSYS simulations of solar water heaters. This indicates that a time step of 0.001 h will be small enough to produce accurate results, but this assumption have not been tested through simulations since the source codes does not run with other time steps. The small time step causes the simulations to be time consuming. To save simulation time, some of the presented results reflect the situation over 24 hours instead of an entire year.

6.2 Model verification

Physical measurements done at the solar wall are in the following compared with simulated results obtained by the use of the dynamic model as an element in TRNSYS. The author did not get to make her own measurements due to malfunctions on the curtain wall when the author was at the Green Energy Laboratory. Ms. Rui Li. conducted the measurements some time ago, and granted the author access to these measurements to verify the model. The author

did not obtain reliable results in the verification of the model. The model is nevertheless verified in the study conducted by R. Li et al. [2].

The investigated solar wall configuration is shown in Figure 5-1. The insulation thickness behind the collector panels is 0.025 m and the properties of the collector module are given in Table 6-1. The height of the investigated collector panel is 0.89 m while the length is 1.9 m.

Material	Density (kg/m³)	Thermal capacity (J/kg·k)	Thermal Conductivity (W/m·K)	Absorptivity	Emissivity
Glass cover	2600	790	1.1	0.01	0.84
Absorber plate	2700	880	237	0.95	0.18
Tube	8900	390	401	—	—
Insulation	37	1670	0.025	—	0.9

Table 6-1 Properties of the solar collector module [2]
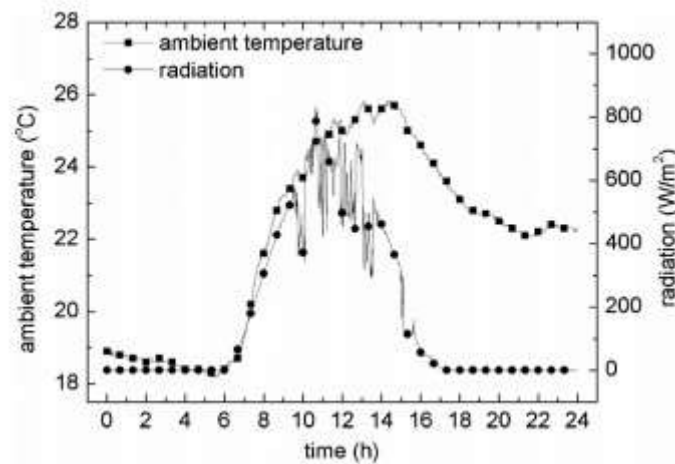
Figure 6-1 Daily temperature and radiation [2]
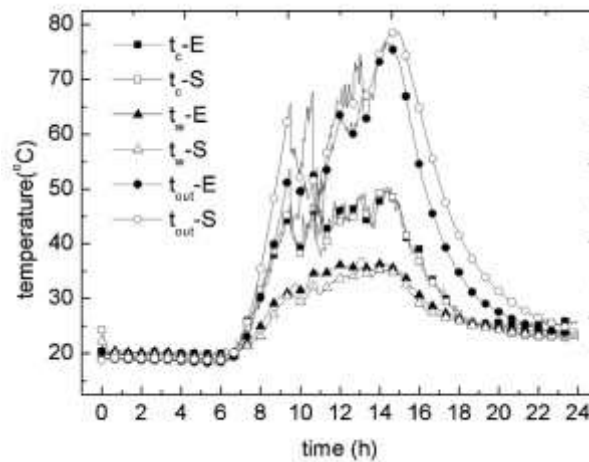
Figure 6-2 Experimental (E) and simulated (S) values of cover temperature, inner wall temperature and collector fluid outlet temperature of solar wall [2]

The measurements were conducted from 00:00 to 24:00 during one typical day in the Shanghai climate. The average temperature is 22.0 degrees, the maximum temperature is 25.6 degrees and the minimum temperature is 18.2 degrees. The maximum radiation is approximately 830 W/m^2 as seen in Figure 6-1. The results from Figure 6-2 show that the simulated values (S) matches the experimental values (E) well for the inner wall temperature, the cover temperature and the collector outlet fluid temperature. For the inner wall temperature the mean deviation is 1°C while the deviation for the fluid outlet temperature is 3°C [2]. The author has not received information on the deviation for the collector outlet temperature, but Figure 6-2 shows a good match between the experimental and simulated results also for this parameter.

The relatively small deviations between the experimental and the simulated results indicates that the model is accurate, and the author has therefore chosen to use this model in the following investigations.

6.3 Solar curtain wall as a refurbishment action in TEK 10 walls
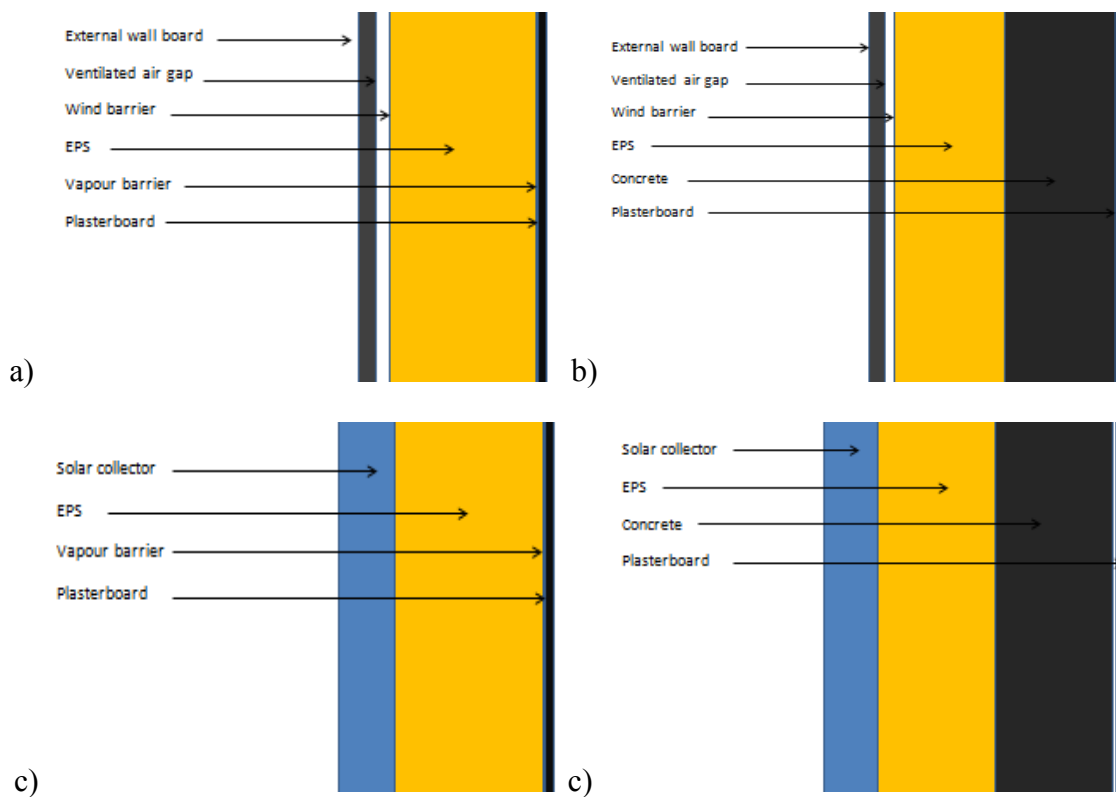
Figure 6-3 Conventional walls: a) Wall A b) Wall B, Solar walls: c) Wall C d) Wall D

The following investigations focus on the installation and integration of solar collectors into an existing wall following the TEK-10 regulations in Norway. Previous studies indicate that the wall is more sensitive to transmission fluctuations as the insulation thickness decreases. The following investigations will show if the installation of solar collectors in TEK-10 walls can reduce the energy consumption of the building. Two different walls are investigated. A lightweight wall consisting of timber framed insulation (Wall A in Figure 6-3) and a heavier wall consisting of timber framed insulation mounted on a concrete slab (Wall B). Wall A and Wall B has approximately the same U- value of 0.17 W/m²K. The lightweight wall (Wall A) consist of 0.25 m timber framed EPS insulation, a vapour barrier, external wall boards, a ventilated air gap, a wind barrier and internal 13 mm plaster boards. The U- value of the timber framed insulation accounting for thermal bridges in the timber frame is calculated from Byggforskblad 471.008 [51]. The wall consist of 36 mm timber studs installed 0.6 m apart. Each wall element will therefore consist of approximately 9 % wood and 91 % insulation. The heavy wall (Wall B) consist of 0.2 m concrete, 0.2 m EPS insulation, a ventilated air gap and the same wind barrier, plaster boards and exterior wall boards as Wall A [39]. Wall C is similar to Wall A, but has a façade integrated solar collector instead of the external wall boards. The same applies for Wall B and Wall D, as seen in Figure 6-3. In the thermal investigation, the wind and moist barriers are neglected due to the limited effect on the thermal performance of the wall. . The parameters of the walls are given in Table 6-2 and the properties of the collector module are given in Table 6-1.

	Conductivity (W/mK)	Heat capacity (kJ/KgK)	Density (kg/m³)
Plasterboard	0.16	0.84	950
Concrete	2.1	0.8	2400
EPS	0.038	1.45	30
Wall board	0.289	1	800

Table 6-2 Thermal and structural parameters of wall materials [52]

Due to limitations set in the source code describing the thermal performance of the curtain wall, each material layer of the wall cannot be defined separately. The structural and thermal parameters used in the simulation are describing one single alloy of all the respective layers in the walls. The materials behind the collector module are implemented into TRNSYS as one

homogeneous layer with properties equal to the average properties of the respective layers when neglecting all thermal bridges. This method is similar to the black box approach of the walls in the Type 56 building as described in Chapter 5.3.1. The properties of the alloys used in the simulation are given in Table 6-3. The conventional walls are modelled through the TRNBuild program. Here, each layer of the wall is defined separately. A complete building is implemented in TRNBuild, but in these initial investigations, only the south wall is under investigation. The properties of the rest of the building are explained more extensively in Chapter 7.1. The TRNSYS model schematics of the solar wall system and the conventional wall are given in Figure C-1 and Figure C-2 in Appendix C. An extensive explanation of the complete collector system is given in Chapter 7.1.3.

	Conductivity (W/mK)	Heat capacity (kJ/KgK)	Density (kg/m³)
Wall C alloy	0.046	1.38	148.04
Wall D alloy	0.074	0.81	1192.13

Table 6-3 Structural and thermal parameters according to the black-box method

In the comparison of the solar walls and the conventional walls, the indoor temperature is 23 degrees and 21 degrees during the summer days and winter days respectively. Since the model describing the solar wall is not created to deal with radiation affecting the inside of the wall, this radiation contribution is set to zero for the conventional walls as well. This is not realistic in a physical building, where the inside of the walls are struck with radiation from other windows in the room. The type 56 multi-zone TRNSYS building deals with this issue through the Geosurf function, but since this is not an option for the solar wall, all influence of the solar radiation on the inside of the wall is neglected.

Metrological data

a)

b)
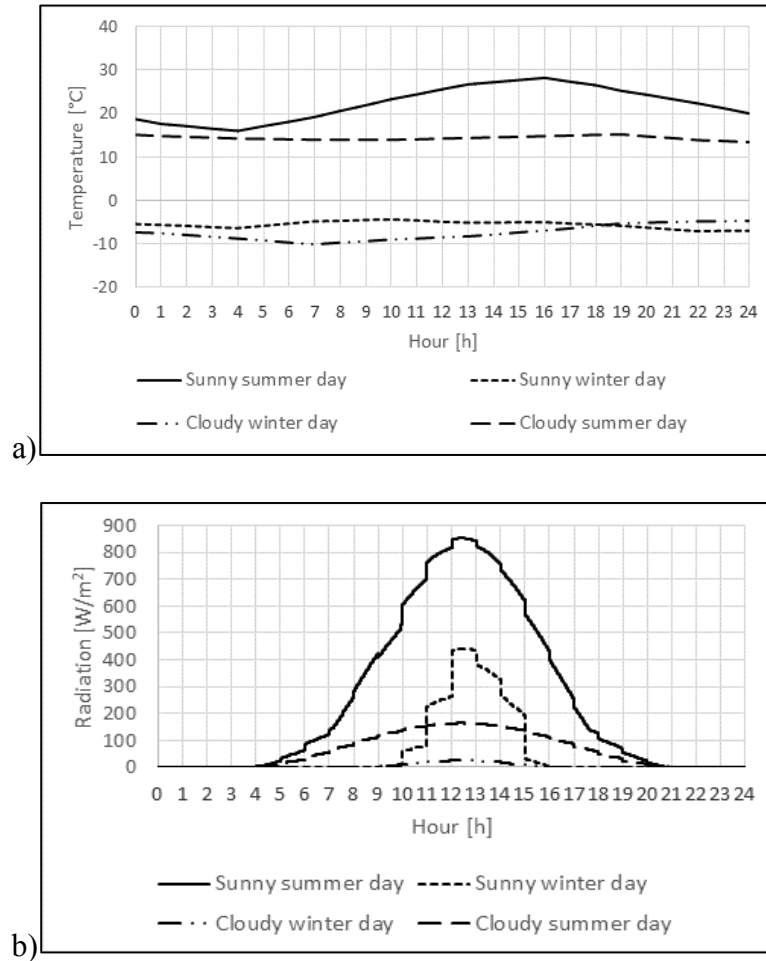
Figure 6-4 Metrological data for the four investigated days a) Temperature b) Radiation

The metrological data relevant for the simulation for the four investigated days are given in Figure 6-4. The chosen days are two days in January and two days in July in the Norwegian climate. One sunny and one cloudy day are chosen for both of the months. The average temperature for the summer days are 22 and 14 degrees for the sunny and cloudy day respectively. For the winter days, the average temperatures are -5 degrees and -7 degrees. The maximum radiation is 875 W/m^2 and 170 W/m^2 for the sunny and cloudy summer days respectively and 450 W/m^2 and 30 W/m^2 for the winter days.

Daily transmission winter days
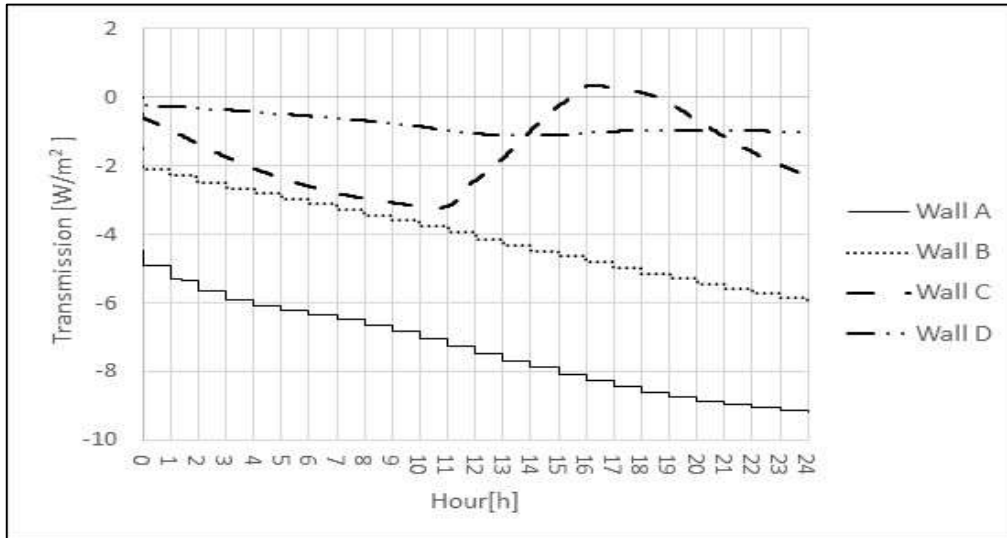
Figure 6-5 Transmission sunny winter day
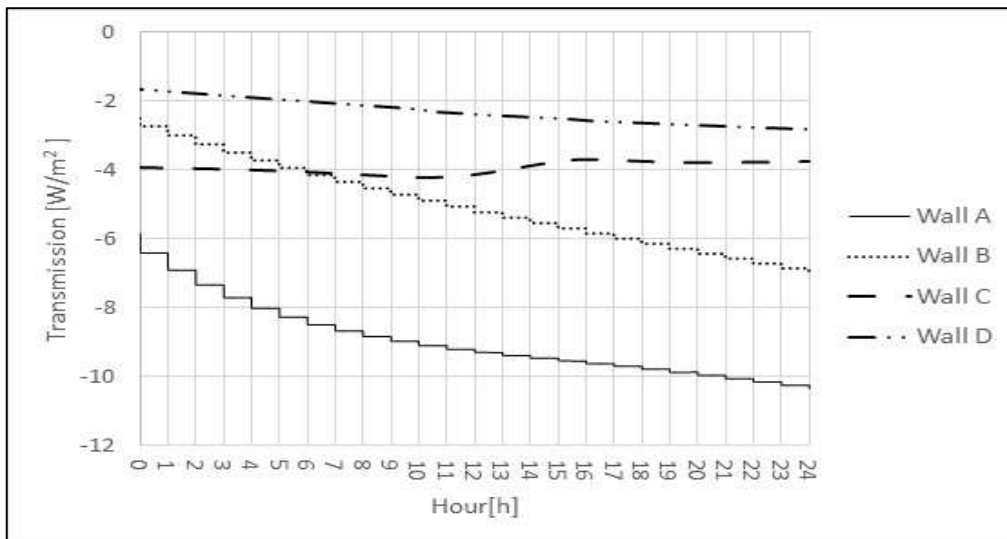
Figure 6-6 Transmission cloudy winter day

Figure 6-5 and Figure 6-6 show the daily transmission profile for the walls the two winter days. For both of the days the transmission profile through Wall A and Wall B, are similar but the lightweight wall has a higher negative transmission. This is because of the inertia in the heavy wall, which slows down the heat transfer through the wall. When the wall is

exposed to the cold outdoor environments the temperature decrease through the wall will be slower for the heavy wall, and the daily transmission will be lower.

During the winter, the aim for any wall is to minimize the negative transmission. In addition is it assumed that any positive transmission not will lead to a cooling need in Norwegian buildings, but will rather contribute to decreasing the heating demand. The sunny winter day, the lightweight solar wall (Wall C), shows a strong decrease in the negative transmission as the radiation increases around 11 am as seen in Figure 6-5. In addition is there a small positive transmission around 4 pm. The same development is not seen for the heavier solar wall due to inertia, but the negative transmission is overall smaller. For both the sunny and cloudy day, both of the solar walls will lead to a far lower negative transmission compared to the conventional walls. This means that the use of solar walls will reduce the heating need of the building during the winter.

	Wall A		Wall B		Wall C		Wall D	
Transmission (kWh/m^2) positive (+) negative (-)	+	-	+	-	+	-	+	-
Sunny winter day	0.000	-0.212	0.000	-0.139	0.006	-0.039	0.000	-0.019
Cloudy winter day	0.000	-0.244	0.000	-0.164	0.000	-0.094	0.000	-0.056

Table 6-4 Daily transmission winter days

By integrating a solar collector into an existing lightweight wall similar to Wall A, the daily negative transmission is reduced by 81 % and 61 % for the sunny and cloudy winter day respectively. For Wall B the decrease is 86 % and 66 % with the integration of a solar collector. These values represent the information in Table 6-4.

Daily transmission summer days

According to Figure 6-7 and Figure 6-8, both of the conventional walls will lead to a negative transmission also during the summer. It can be assumed that this contribution will not lead to an increased heating need, but rather a decreased cooling need, especially for buildings with large integral gains. This means that it may not be profitable to choose walls with the lowest negative transmission to reduce the energy consumption during the summer months. For the

cloudy summer day, the solar walls also have a negative transmission. Wall C reacts rapidly to small increases in temperature and radiation, making the negative transmission decrease rapidly around 6 am. This does not happen for the heavy solar wall, which will have the same transmission profile as the conventional wall but with a lower load. This means that when only a little heat is transferred from the solar collectors to the water tank, which is the situation the cloudy day, the collector works as extra insulation for the wall. For the sunny summer day, it is evident that both of the solar walls lead to increased positive transmission as seen in Figure 6-7. Wall C leads to the highest positive transmission.
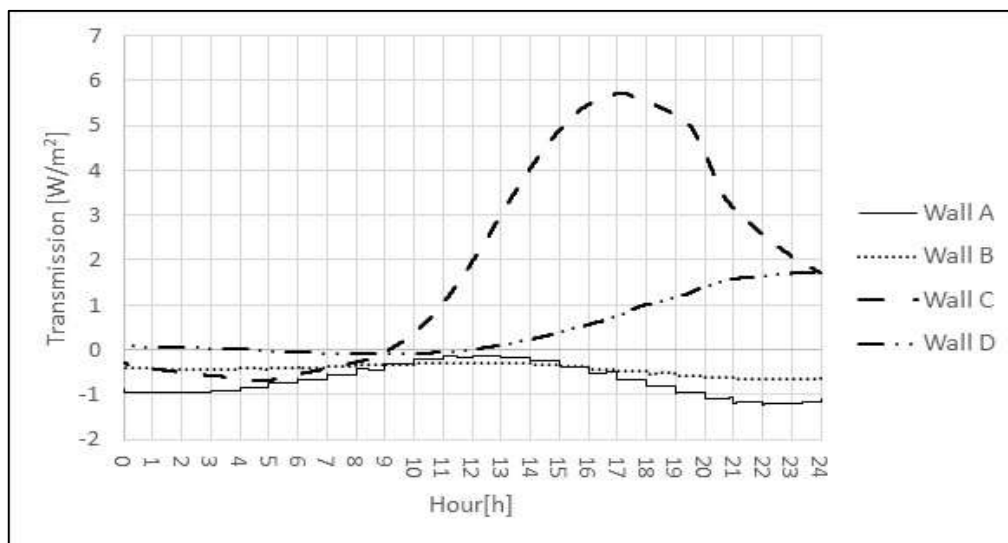
Figure 6-7 Transmission sunny summer day
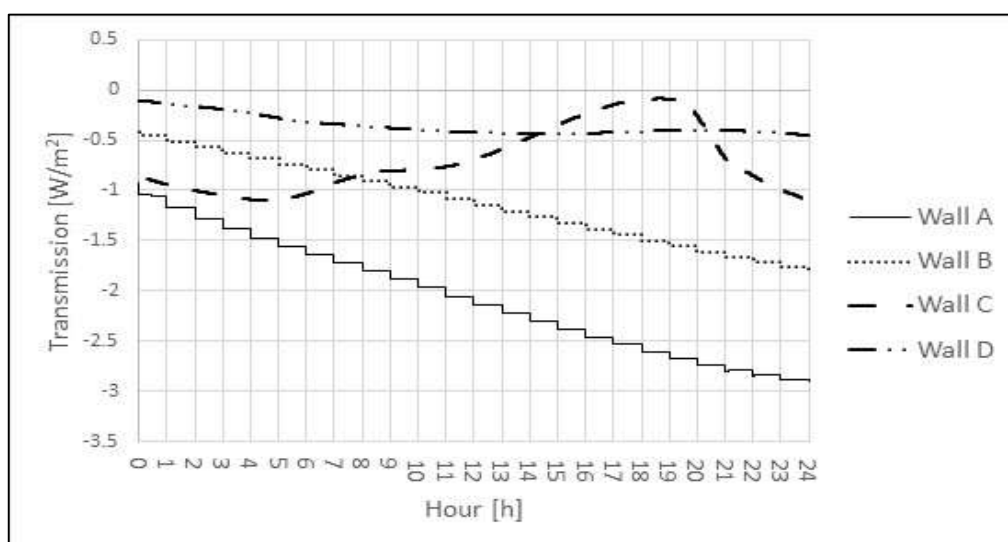
Figure 6-8 Transmission cloudy summer day

	Wall A		Wall B		Wall C		Wall D	
Transmission (kWh/m²) positive (+) negative (-)	+	-	+	-	+	-	+	-
Sunny summer day	0.007	-0.012	0.001	-0.008	0.050	-0.004	0.012	-0.001
Cloudy summer day	0.000	-0.065	0.000	-0.041	0.000	-0.017	0.000	-0.009

Table 6-5 Daily transmission summer days

The positive transmission is 86 % lower through wall A than through Wall C the sunny summer day, while Wall B has a positive transmission that is 91 % lower than Wall D the same day. The cloudy summer day the negative transmission decreases with 61 % when integrating Wall A with a solar collector, while in decreases with 79 % when integrating Wall B with a solar collector. This may increase, or lead to a cooling need in the building.

6.4　Potential of reducing the insulation thickness

As the thermal performance of the wall changes when the wall is integrated with a solar collector, the insulation thickness in the wall may be reduced and the wall will still perform equally as the conventional wall. This is an interesting aspect related to new walls since the investment in insulation influences the economy of the project.
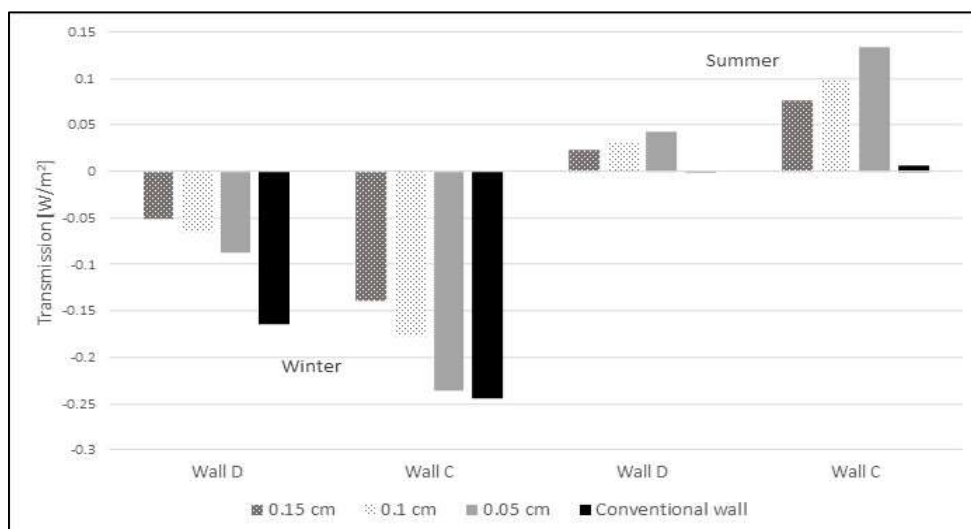
Figure 6-9 Negative transmission for cloudy winter day and positive transmission for sunny summer day for different insulation thicknesses in the solar walls compared to the corresponding conventional wall

Figure 6-9 shows the potential of reducing the insulation thickness behind the solar walls. The transmission for each insulation thickness is compared to the transmission through the corresponding lightweight and heavy conventional wall (Wall A and Wall B). The black poles in the figure represent these walls. For the insulated solar wall (Wall C), the insulation thickness can be reduced from 0.2 m to 0.05 m, and the negative transmission during the cloudy day in January will still be lower than through a conventional wall insulated with 0.20 m insulation as seen in Figure 6-9. For the heavy solar wall (Wall D), an insulation thickness of 0.05 m leads to a negative transmission of less than half of the negative transmission through Wall B the same winter day. None of the conventional walls will have a mentionable positive transmission during the sunny summer day. This means that all of the insulation thicknesses tested in the solar walls will contribute to a higher positive transmission to the building. By reducing the insulation thickness in Wall D to 0.05 m there will still be an overall energy saving since the saved energy during the winter still exceeds the extra energy gain during the summer. Compared to the conventional wall, the energy saving during the winter day will be approximately 0.07 kWh/m^2 with the use of the solar wall with 0.2 m concrete and 0.05 m insulation, while the increased positive transmission is less than 0.05 kWh/m^2. For Wall C, the insulation thickness can only be reduced to 0.15 m if it is assumed that the increased positive transmission during the summer day leads to a cooling need in the building. For smaller insulation thicknesses, the increased cooling need the summer day exceed the reduced heating need the winter day.

Despite of clear tendencies, the optimal situation depend on the building in question. Directly translating every increase in positive transmission into increased mechanical cooling need is not always viable, since the problem with overheating may be solved by opening a window.

6.5 Influence of the circulation pump operating time

The following results show the transmission through the south façade for the days presented in Chapter 6.3, but the circulation pump is passive the entire day. This reflects a situation where there might be a potential of collecting heat from the collectors, but the hot water tank is fully charged. This could be during holiday periods.

Daily transmission winter days
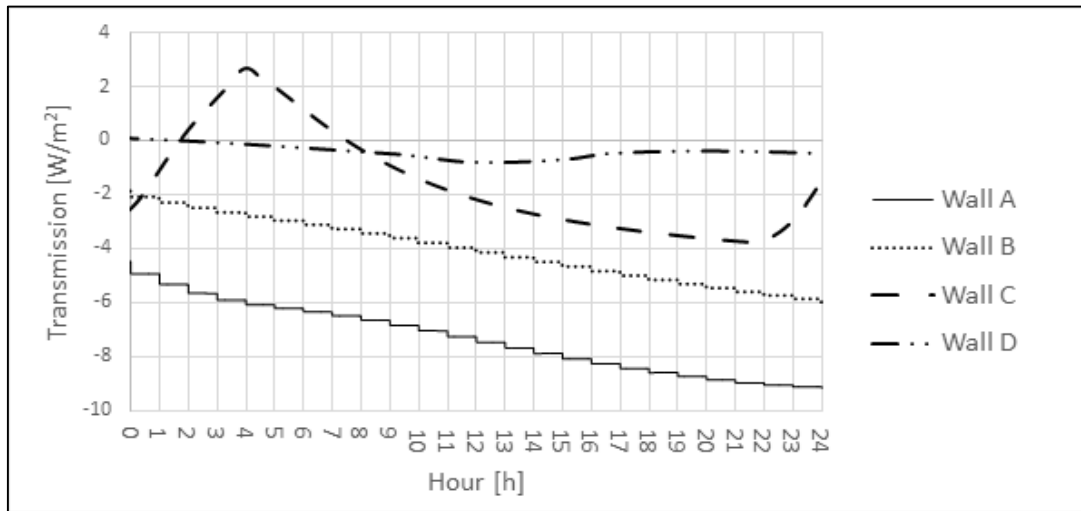
Figure 6-10 Transmission sunny winter day, circulation pump passive
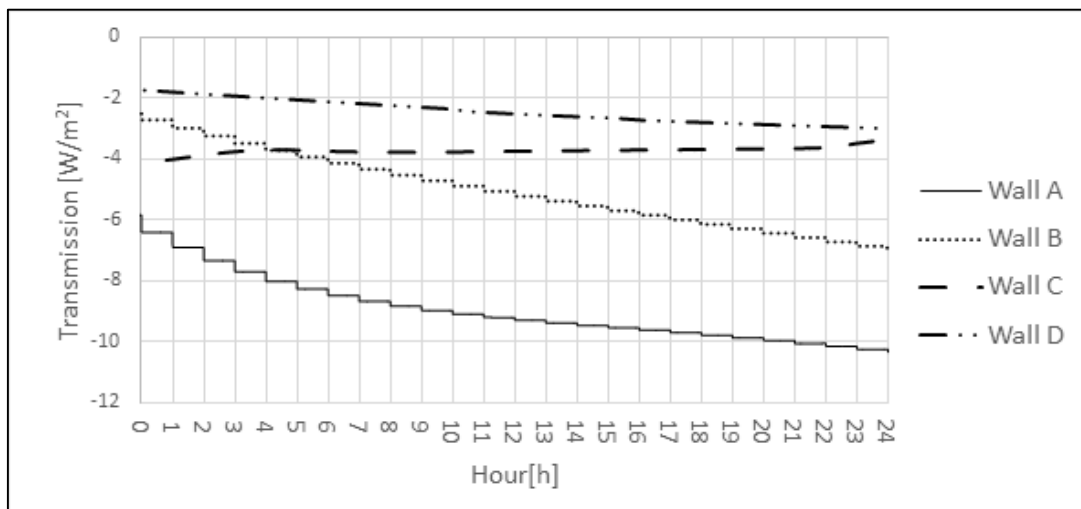
Figure 6-11 Transmission cloudy winter day, circulation pump passive

During both of the winter days, the transmission profiles with the passive pump are quite similar to the situation with the normal regulatory strategy as seen in Figure 6-10 and Figure 6-11. This is because the pump operating time with the normal regulatory strategy is short during the winter days, giving a situation similar to keeping the pump turned off. The sunny winter day, the transmission through both of the solar walls are sensitive to temperature and radiation changes. This can be seen by the strong decrease in the negative transmission and

the development of the positive transmission around 4 am for Wall C, and the decrease in the negative transmission for Wall D around 3 pm, see Figure 6-10.

	Wall A		Wall B		Wall C		Wall D	
Transmission (kWh/m²) positive (+) negative (-)	+	-	+	-	+	-	+	-
Sunny winter day	0.000	-0.212	0.000	- 0.139	0.008	-0.043	0.000	-0.011
Cloudy winter day	0.000	-0.244	0.000	-0.164	0.000	-0.094	0.000	-0.056

Table 6-6 Daily transmission winter days, circulation pump passive

For Wall C, the overall negative transmission increases by 9 % the sunny winter day compared to the situation with the normal regulatory strategy seen in Table 6-4. For Wall D, the negative transmission decreases with 37 % the same day. The transmission the cloudy winter day is affected only marginally by the operating time of the circulation pump. This applies for both of the solar walls. As with the normal regulatory strategy, there is no mentionable positive transmission for neither of the solar walls as seen in Table 6-6.

Daily transmission summer days
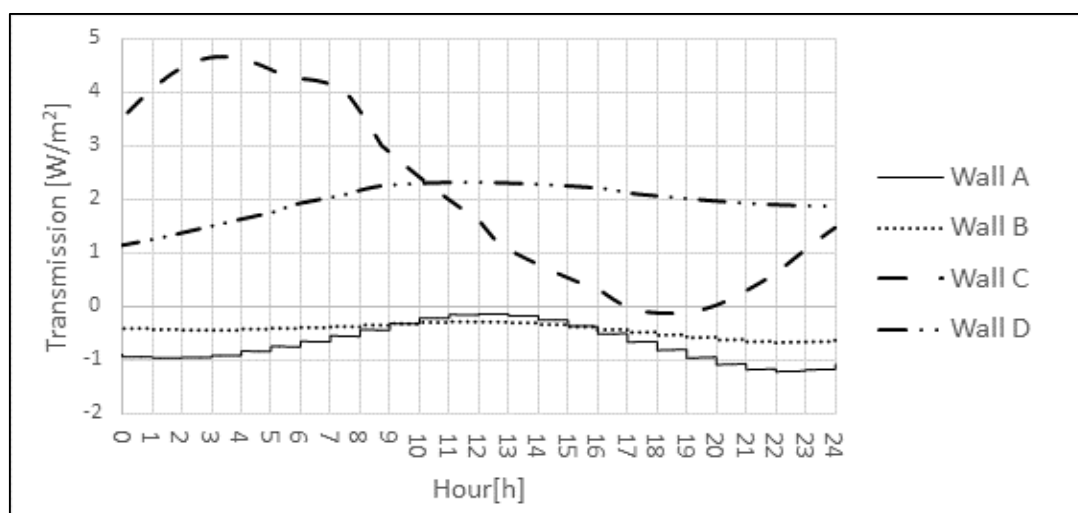
Figure 6-12 Transmission sunny summer day, circulation pump passive
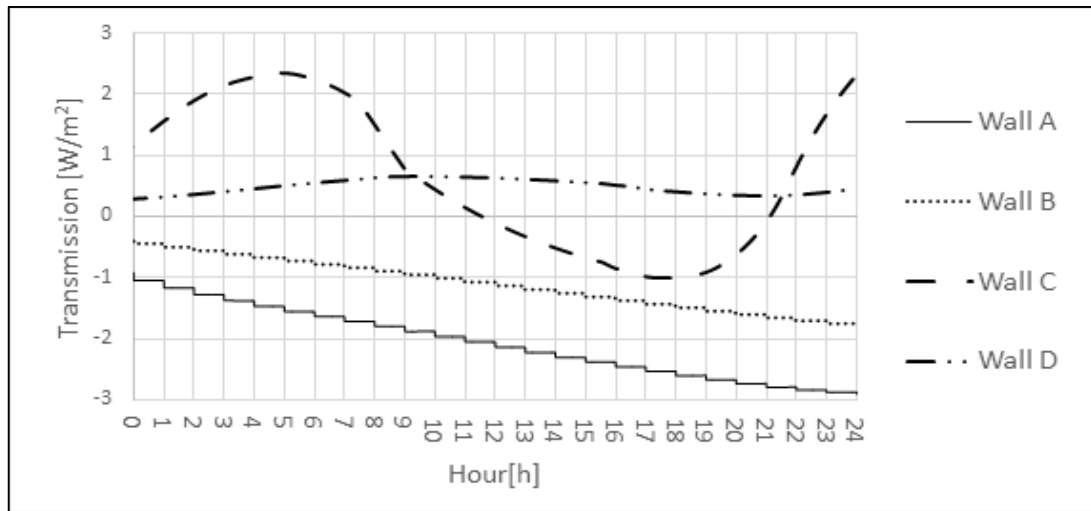
Figure 6-13 Transmission cloudy summer day, circulation pump passive

Figure 6-12 and Figure 6-13 show that the difference between the transmission profiles of the conventional walls and the solar walls increases when the pump is passive the summer days. Both of the days, the solar walls contribute to increased positive transmission loads. Also here, Wall C is sensitive to temperature and radiation changes, even more than with the normal regulatory strategy. Despite of this, the big changes in the transmission does not happen as the temperature and radiation changes, but there is a delay. The decrease in the transmission in the middle of the day is a reaction to the temperature and radiation drop during the night.

	Wall A		Wall B		Wall C		Wall D	
Transmission (kWh/m^2) positive (+) negative (-)	+	-	+	-	+	-	+	-
Sunny summer day	0.007	-0.012	0.001	-0.008	0.058	0.000	0.034	0.000
Cloudy summer day	0.000	-0.065	0.000	-0.041	0.020	-0.005	0.010	0.000

Table 6-6 Daily transmission summer days, circulation pump passive

For Wall C the sunny summer day, the positive transmission increases with 16 % while the negative transmission decreases from 0.004 kWh/m^2 to 0.000 kWh/m^2 compared to the normal regulatory strategy. The cloudy summer day the negative transmission decreases by 70 %, while there is introduced a positive transmission contribution of 0.02 kWh/m^2. For Wall D, the positive transmission increases by 64 % the sunny summer day. The negative transmission

the sunny day and both the positive and negative transmission the cloudy day is approximately the same as with the normal regulatory strategy.

7 Analysis of a concept building

The Research Centre on Zero Emission Buildings have in the report A Zero Emission Concept Analysis of a Single Family House [66] defined a shoebox building for the analysis of the energy use, the embodied energy and total CO_2 emission for a typical residential Norwegian building fulfilling the Zero Emission Building Concept. For the further investigations on the thermal performance of façade integrated solar collectors, the same shoebox building have been investigated but with construction materials and systems complying with TEK 10.

7.1 Building model

The building is modelled in TRNBuild and implemented into the TRSNYS simulation studio through the type 56 multi-zone building. The building is modelled as one thermal zone.

7.1.1 Building envelope
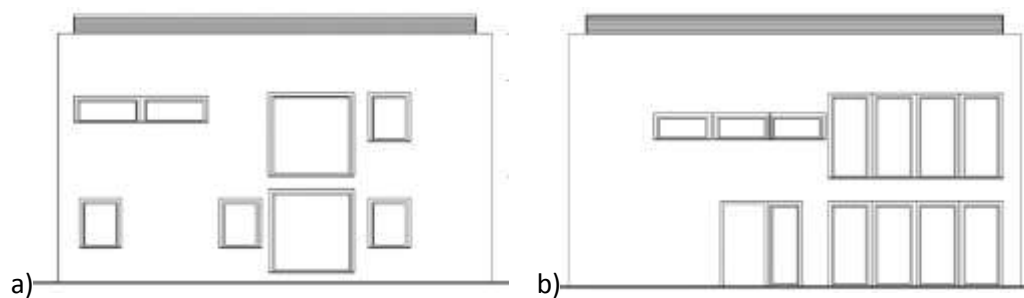
Figure 7-1 Concept building a) North façade b) South facade

Figure 7-2 Concept building floor plan a) first floor b) Second floor

The building has a total heated floor area of 160 m² with two floors of 80 m² each. The building has a rectangular footprint measuring 10 m x 8 m with its long sides towards north and south. The facades has windows on the north and south wall, adding up to 36 m² in total, see Figure 7-1 This corresponds to 22.5 % of the total heated floor area. The properties of the building envelope are chosen according to NS3031 and are given in Table 7-1 [67].

	Demand	Chosen value	Solution 1	Solution 2
External walls (W/m²K)	< 0.18	0.17	25 cm timber framed insulation (Wall A)	20 cm concrete slab insulated with 20 cm timber framed insulation (Wall B)
Roof (W/m²K)	< 0.13	0.13	Compact roof with 15 cm concrete and 0.28 m insulation	Compact roof with 15 cm concrete and 0.28 m insulation
Slab on ground (W/m²K)	< 0.15	0.15	Concrete and 0.25 m insulation (not accounting for thermal resistance of the ground)	Concrete and 0.25 m insulation (not accounting for thermal resistance of the ground)
Infiltration (1/h)	< 2.5	1	Few air leakages	Few air leakages
Thermal bridges (W/mK)	<0.03	0.03	Attention to joints in the construction to keep the value low	Attention to joints in the construction to keep the value low
Windows and doors (W/m²K)	< 1.2	1.1	Saint Gobain PLANISOL Neutral 6242 6/16/6 from TRNSYS library	Saint Gobain PLANISOL Neutral 6242 6/16/6 from TRNSYS library

Table 7-1 Thermal parameters of the modelled building

7.1.2 Ventilation system

The building has a mechanical ventilation system with supply air ducts in the bedrooms, living rooms and kitchen and extracts air from the bathrooms and the kitchen. As stated in NS 3031, residential buildings needs ventilation that secures an average air supply of minimum 1.2 m^3/hm^2 when the rooms are occupied, and minimum 0.7 m^3/hm^2 when the rooms are not being used. In addition must bedrooms be supplied with 26 m^3/h per bed when the room is being used. For this situation, the extract air in bathrooms and kitchen is related to air amounts exceeding the demanded 1.2 m^3/hm^2. However, it is assumed that this effect seen with the decreased air amounts during unoccupied times allows the building to be modelled with a constant air supply of 1.2 m^3/hm^2. Table 7-2 shows the air flow rates during occupied times. The AHU is equipped with a rotary wheel heat exchanger with a high heat recovery factor of 87 %. For the majority of days, this high heat recovery factor makes it possible to run the system without using a secondary heating coil to heat the supply air. The building is not equipped with cooling equipment other than the opportunity of free cooling and night cooling through the ventilation system.

	Supply air (m^3/h)	Extract air (m^3/h)	Comment
Bedroom 1	26	0	1 person
Bedroom 2+3	52	0	2 persons
Bedroom 4	52	0	2 persons
Bathroom 1	0	60	Overflow from other rooms
Bathroom 2	0	60	Overflow from other rooms
Living room/kitchen 2nd floor	32	72	Overflow from bedrooms
Living room 1st floor	30	0	Overflow from other rooms

Table 7-2 Air flow rates

7.1.3 Domestic hot water system
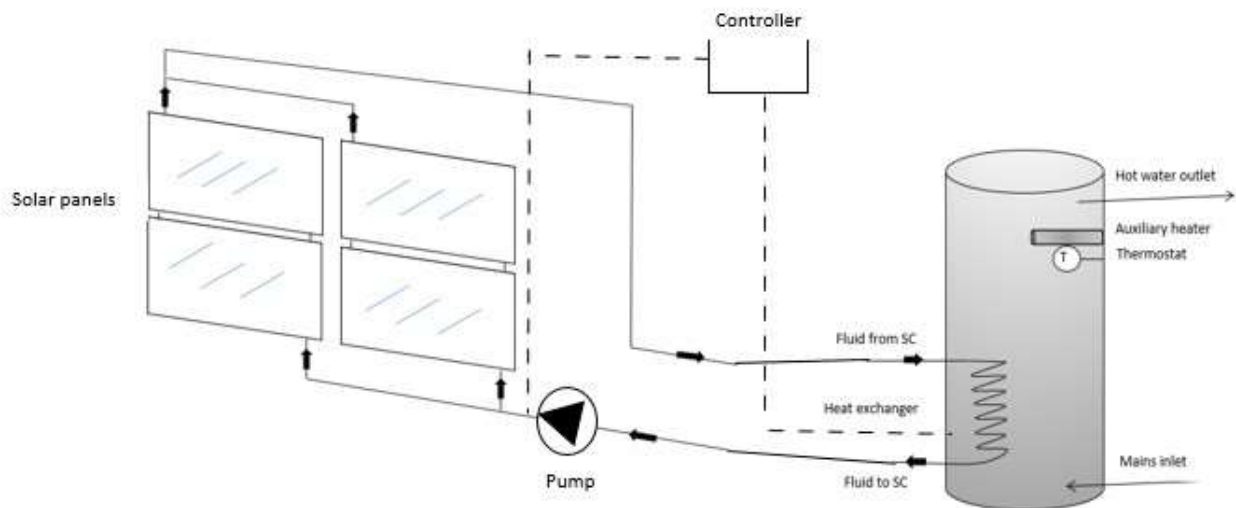
Figure 7-3 Solar collector system design

The domestic hot water system in the building consist of façade integrated solar collectors connected to a hot water tank with a spiral heat exchanger as seen in Figure 7-3. The tank has an immersed electric auxiliary heater to supply heat when the solar collectors are not sufficient to cover the load. Research one by SSB [49] show that each person in a Norwegian residential building has a hot water consumption of around 70 l/day. For a four-person family this constitutes around 300 l/day in total. Figure 7-4 shows the chosen daily DHW profile. It reflects the expected DHW draw from a Norwegian family with the highest peaks of DHW in the morning, and the afternoon. The data behind this profile is found in IEA-ECBCS Annex 42 [68], which illustrates DHW water profiles for every 15 minutes for an entire year. The profiles are generated from probability functions. The profile in Figure 7-4 represents one of the days in Annex 42, and are chosen according to the expected water draw of a Norwegian family. The load profile is important for the performance of the system. If the bulk of the load is used in the morning, solar water system can only cover a small part of the load. If the main hot water use occurs in the afternoon or night, the solar heating system has the potential of covering a substantial part of the load.
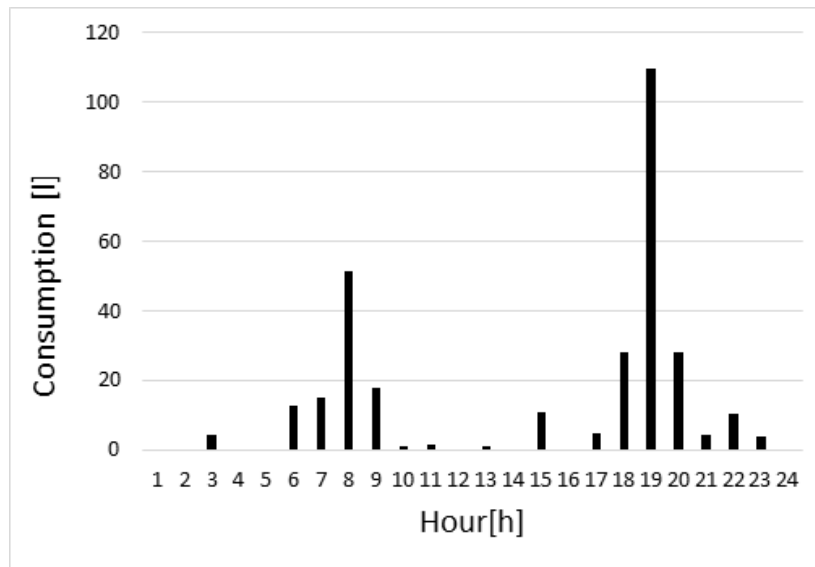
Figure 7-4 Daily domestic hot water draw

The hot water tank volume is 450 l and is chosen according to the rule of thumb set by Furbo et al.[43], of installing a tank volume of 1.5 times the hot water load. Four solar panels each with an area of 1.67 m² are connected in parallel, constituting to a total solar collector area of 6.68 m². This is a bit higher than recommendations set by Zijdemans [32] who recommends that single family dwellings using conventional solar collectors for DHW production install 4-6 m² solar collector areas. This decision is made because it is assumed that the collector output for the façade integrated solar collectors are smaller than for collector panels installed under optimal slope, allowing for larger areas without big stagnation problems. The specific flow rate through the collectors are set to 72 kg/hm² based on the capacity of the pump installed in the Green Energy Laboratory. The pumps will be turned on when the temperature difference between the bottom of the tank and the fluid exiting the heat exchanger exceeds 8°C and turned off when the difference is less than 5 °C. This also reflects the initial regulatory strategy used in the Green Energy Laboratory, but includes lower allowable temperature differences to suit the Norwegian situation.

The water tank is modelled as a stratified storage tank with 15 nodes. The height of the hot water tank is 1.4 m and the radius of the tank is 0.64 m. This equals a height to diameter ratio of 2.2, which is in the same range as the recommended ratio from Furbo et al. [43] of 2:1 to ensure a high degree of stratification. In reality will the tank be bigger when counting in the

insulation. However, this will not influence the stratification effects. The hot water outlet is set in the top of the tank, while the cold water outlet is in the bottom. The auxiliary heater is installed 30 cm below the top of the tank and the thermostat is set just below the auxiliary heater, as seen in GEL. The heater will be switched on when the thermostat detects temperatures below 50 degrees, and will be switched off when the temperature exceeds 55 degrees. The thermostat is placed below the electric heater to ensure that the water volume above the electric heater is at a satisfactory temperature at all times. The temperature of the water surrounding the thermostat will be colder than the water above the electric heater due to stratification. The heat exchanger connecting the tank to the solar collector system has its inlet and outlet at 0.55 m and 0.16 m respectively. The heat exchanger surface area is 0.9 m^2 and the pipe internal and external diameter is 0.01 m and 0.012 m respectively. This is the heat exchanger installed in the Solar House in the Green Energy Laboratory.

A mixture of propylene glycol and water is the working fluid in the solar collector loop. The volume percentage of glycol is set to 40 % [39]. Propylene glycol is chosen to avoid freezing.

7.2 Climate

Figure 7-5 shows the ambient temperature and radiation profiles used in the following investigations. The weather data reflect a typical meteorological year in Fornebu in Oslo. The minimum annual temperature is - 17°C and the maximum is 29 °C. The maximum radiation is approximately 800 W/m^2.

a)

b)
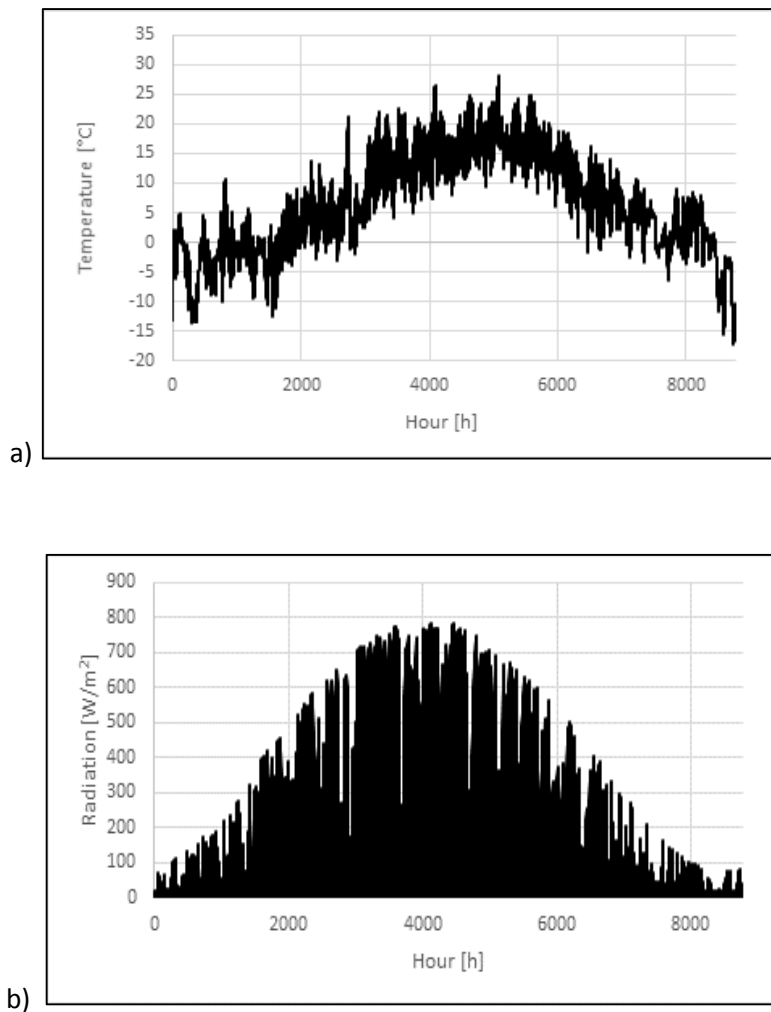
Figure 7-5 Annual meteorological data a) temperature b) radiation

7.3   Performance of the building envelope

	Wall A	Wall B
Annual space heating need (kWh/m^2)	65.55	65.27

Table 7-3 Annual space heating need of the concept building

The annual heating demand related to the floor area of the building is given in Table 7-3. The annual heating demand is approximately 65 kWh/m^2 floor area for both of the wall configurations when the set point indoor temperature is 21 °C. To comply with the demand from TEK-10 regarding the total net energy consumption of the building, the total energy demand to space heating, domestic hot water, lighting and appliances, cooling and fans and pumps must not exceed 130 kWh/m^2 floor area annually. As a comparison, the concept building modelled as a Zero Emission Building has a net energy consumption of 70 kWh/m^2

floor area annually, and a space heating need of 21 kWh/m² floor area annually [66]. This means that the net energy consumption demand from TEK-10 can be met if the same technical equipment is installed in this building.
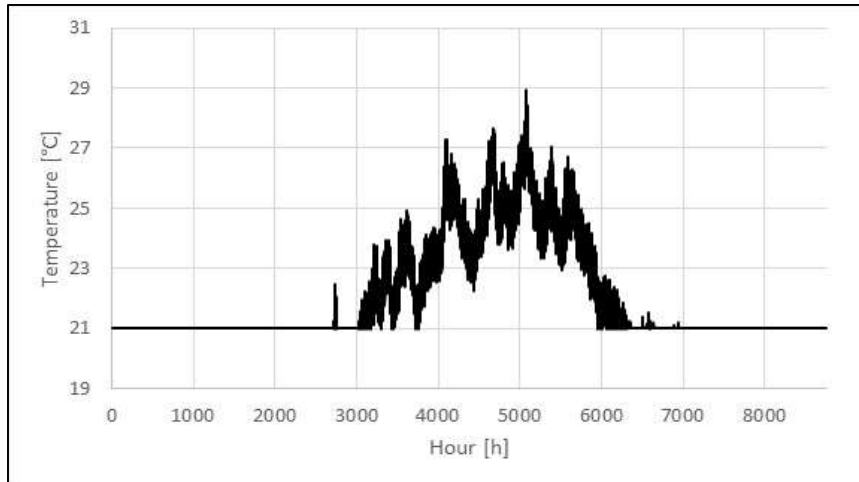
Figure 7-6 Annual indoor temperature of the concept building with lightweight external walls (Wall A)
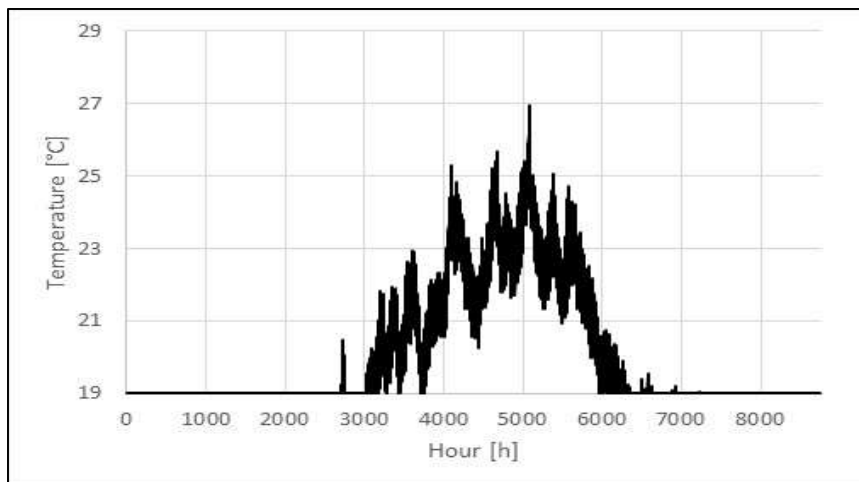
Figure 7-7 Annual indoor temperature of the concept building with heavy external walls (Wall B)

Figure 7-6 and Figure 7-7 show that there is a problem with overheating the building during the summer season for both of the wall configurations. A few days in July and August, the indoor temperature exceeds 26 degrees during the early afternoon, and this effect is especially evident for the lighter wall. For the heavy wall, the problem is not as big, and it can be fixed by the use of free-cooling or additional solar shading. By comparing the indoor temperature profiles with the ambient temperature and radiation profiles it is evident that the highest indoor temperatures are induced by radiation loads through the windows. The current solar shading scheme is dominated by the windows being submerged 0.01 m into the wall. In

addition is there installed an external shading system with a total shading factor of 0.4 that is activated when the total radiation exceeds 540 W/m^2 and is deactivated when the radiation drops below 432 W/m^2. These limits are default values from TRNSYS, and are assumed to be reasonable regarding comfort and temperature considerations to ensure a good indoor environment and a low energy consumption to heating and cooling. For the heavy wall, it is assumed that these actions will lead to satisfactory summer temperatures without any mechanical cooling. Potentially can the shading factor be increased. This will effectively bring down the summer indoor temperatures.

In the following investigations, the concept building is modelled with the heavy wall (Wall B) because this wall shows the smallest potential of overheating the building. In addition do investigations from Chapter 6.3 show that Wall D introduces the lowest increase in the positive transmission and at the same time shows relatively high energy savings related to negative transmission.

7.3.1 Transmission through the conventional wall
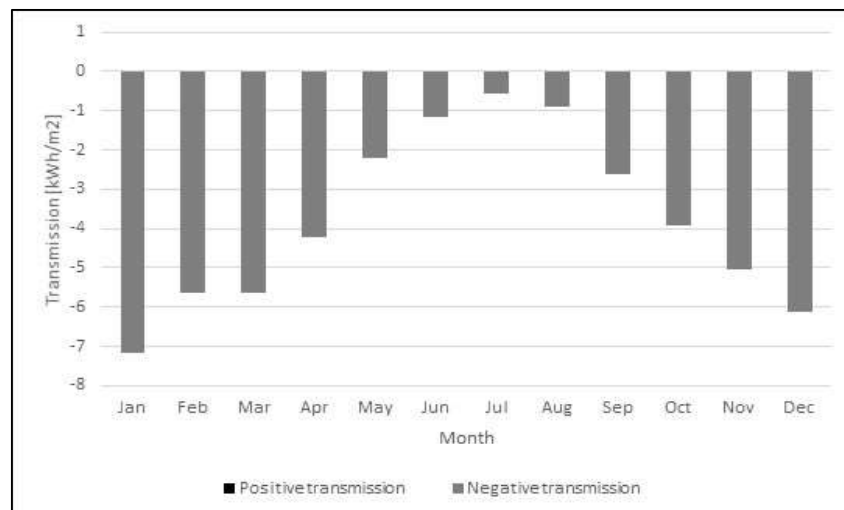
Figure 7-8 Annual transmission through south façade of conventional insulated concrete wall (Wall B)

Figure 7-8 shows the monthly transmission through the conventional heavy wall (Wall B) installed in the south façade of the concept building. The profile is dominated by negative transmission with a very small positive transmission contribution in July and August. This contribution will be neglected. The annual negative transmission 45.22 kWh/m^2.

7.3.2 Transmission through integrated solar collector wall

The model created by SJTU describing the thermal performance of the solar curtain wall cannot be coupled with a Type 56 building in TRNSYS. This means that the curtain wall and the building must be simulated separately. The indoor temperature is a constant input in the model for the curtain wall. Since the use of solar walls increases transmission, it may actually influence the indoor temperature, especially since no cooling is installed in the building. In the following simulations of the integrated solar wall, the indoor temperature is set to 21 degrees during the heating season and 23 degrees during the summer months to get a realistic view of the transmission compared to the conventional wall. This is the best way to match the indoor temperatures in Figure 7-7. It is evident that if the annual positive transmission with the use of collectors strongly exceeds the transmission through the conventional walls, there will be a problem with overheating the building.
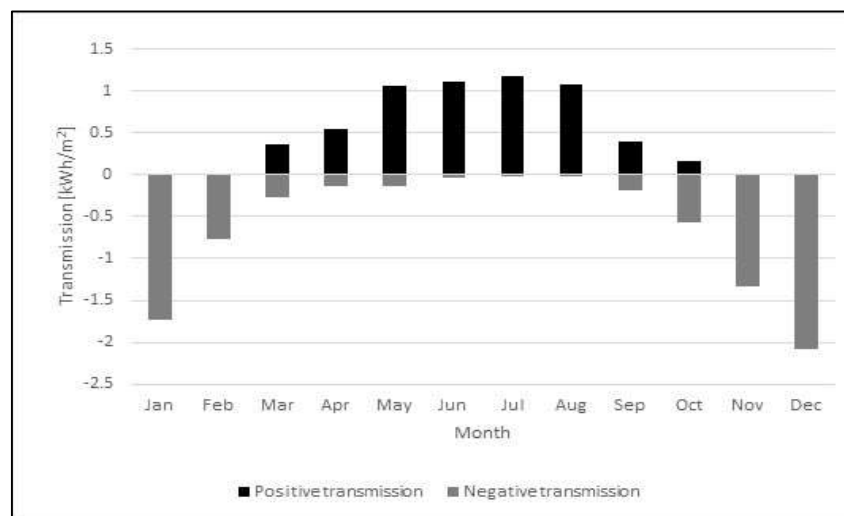
Figure 7-9 Transmission through south façade with insulated concrete curtain wall (Wall D)

Figure 7-9 shows the monthly transmission through the south façade of the concept building with the heavy solar wall (Wall D). The total positive transmission is 5.9 kWh/m^2 and the negative transmission is 7.2 kWh/m^2 annually. This is far lower than the negative transmission related to the conventional insulated concrete wall of 45.22 kWh/m^2 annually. Assumed that the increased positive transmission can be dealt with by opening windows or using free cooling, the façade integrated solar collectors leads to an energy saving of 38.02 kWh/m^2

annually. In the concept building with 6.68 m^2 solar collectors, this translates to a reduction in the total annual space heating demand of 2.4 %.

7.4   DHW system performance

Annual energy consumption for DHW (kWh/m^2)
42.5

Table 7-4 Annual energy consumption for DHW

The overall annual energy consumption for DHW is approximately 43 kWh/m^2 floor area for a daily consumption of 300 l/day with the use of the electric auxiliary heater. NS 3031 sets a normalized annual energy demand for DHW to 30 kWh/m^2 floor area a for a single family dwelling. This reflects a lower daily DHW consumption pr. person and not the newer numbers from SSB [49].

7.4.1   Monthly useful energy gain and auxiliary energy
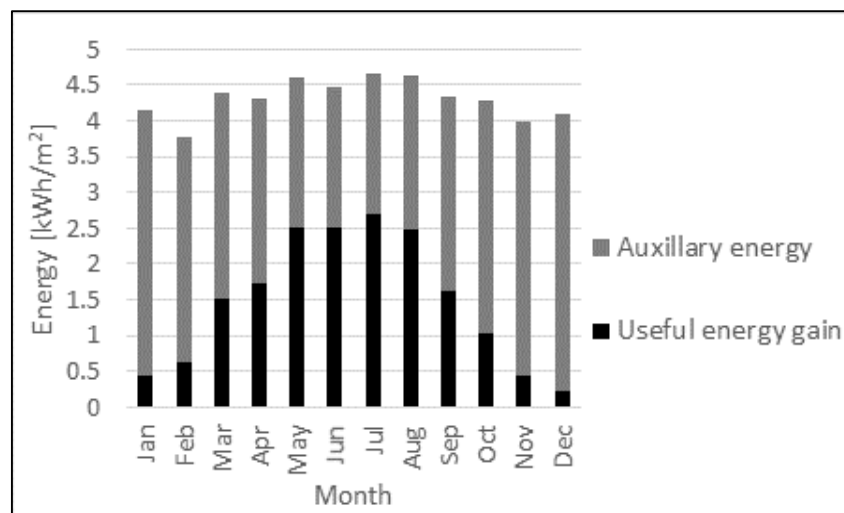
Figure 7-10 Monthly contribution from solar collectors integrated in insulated concrete wall (Wall D)

Figure 7-10 shows the monthly distribution of solar energy and auxiliary energy delivered to the storage tank with the use of Wall D. The collectors deliver approximately 18.2 kWh/m^2

floor area annually. This constitutes to approximately 36 % of the overall DHW energy demand with an auxiliary energy need of around 33 kWh/m² floor area. This means the total delivered energy to the water tank is higher with the use of solar collectors compared to electric heating alone. This is because the auxiliary heater delivers 8 kW every time it is turned on. With the use of the collectors, the actual heating demand may be lower, but the 8 kW is still delivered. The DHW load is equal for each day. The differences in the total column heights in Figure 7-10 are a result of the uneven number of days in each month in addition to increased auxiliary energy to account for heat losses in the tank. This is dependent on the average water temperature in the tank, which again depends on the solar availability.

7.4.2 Tank stratification
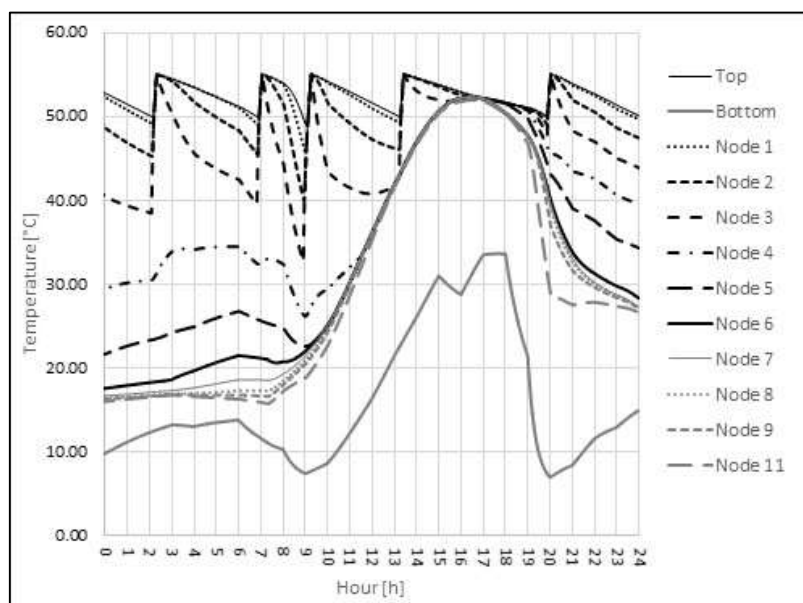
Figure 7-11 Stratification in storage tank, circulation pump active
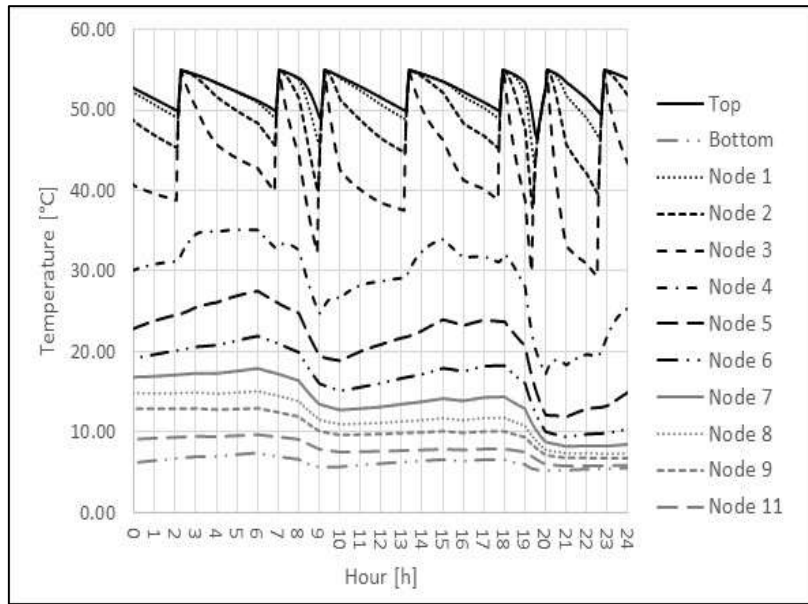
Figure 7-12 Stratification in storage tank, circulation pump passive

Figure 7-11 shows the temperature layers in the storage tank the sunny day in July with a normal regulatory strategy. The distance between each temperature node is 0.09 m and node 1 is placed 0.09 m below the top of the tank. The figure shows that there are clear stratification effect in the water tank, with far higher temperatures in the top of the tank compared to the lower part. When the collectors are operational, they generate enough heat to heat up all layers of the tank parts of the day. This makes the auxiliary heater turn off between around 1 pm and 8 pm. Some layers in the figure have not been included in the figures to ensure a clear presentation. Figure 7-12 illustrates the temperature levels in the tank the same summer day but the circulation pump is passive all day. No heat is transferred from the solar panels to the water tank and the auxiliary heater is operational throughout the day. The use of the auxiliary heater only influences the temperature in the top layers of the tanks. These temperatures vary between 50 and 55 degrees, controlled by the thermostat. This ensures that the bottom temperature and the fluid temperature in the heat exchanger is as low as possible at all times, so that the solar collector efficiency is as high as possible when the pump starts running again.

7.4.3 Water tank bottom temperature
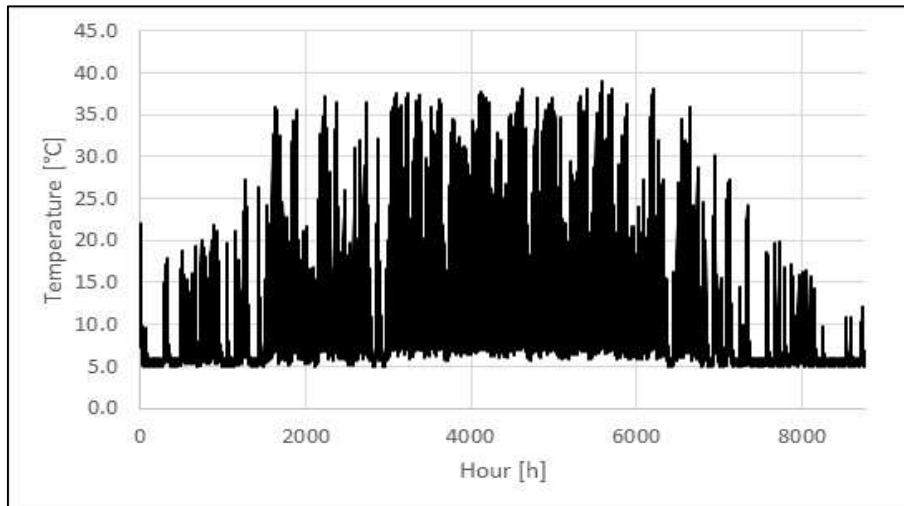
Figure 7-13 Bottom temperature in water tank

Figure 7-13 shows the annual tank bottom temperature. The temperature varies between 5 °C, which is the temperature of the water that enters the water tank through the bottom inlet and approximately 40 °C. The temperature is highest during the summer when the amount of available radiation is the highest and the stratification effects are reduced as seen in Figure 7-11.

7.4.4 Solar collector outlet temperature

Figure 7-14 shows the outlet temperature of the collectors throughout the year. The temperature exceeds 40 degrees even during colder months, but it hardly exceeds 60 degrees during the summer. The maximum outlet temperature heavily depend on the water tank temperatures, and the meteorological conditions, but it is possible to achieve temperatures far above 100 degrees also for Norwegian climate. During the summer, a tilted solar collector would collect more heat, and would be able to produce higher temperatures compared to a vertical collector. This explains the relatively low summer temperatures. In addition is the water tank in this system big enough to ensure relatively low bottom water temperatures also at times with high radiation. This limits the outlet temperature peaks of the collector. In the winter, a vertical collector will produce higher temperatures than a tilted collector, since the

sun is lower on the sky. This explains the relatively high winter temperatures. During the summer months, the collectors cover approximately 60% of the DHW load as seen in Figure 7-10. According to Figure 7-14, there are never extremely high collector outlet temperatures. This means that there is a potential of profitably investing in additional solar collector areas to cover more of the load without risking stagnation periods. This further indicates that common recommendations regarding the design of solar collector systems should be revised when dealing with vertically installed solar collectors since the useful energy gain is smaller compared to solar collectors installed at an optimal slope.
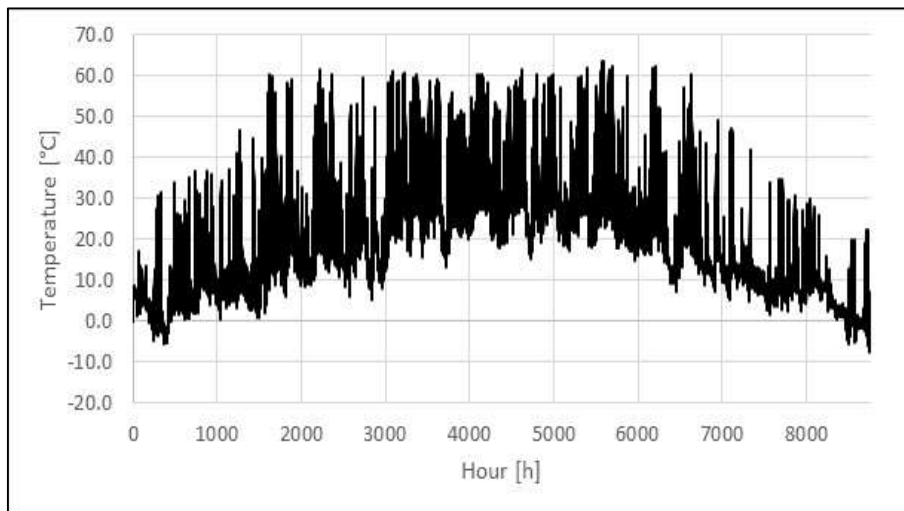
Figure 7-14 Outlet temperature of solar collector

7.4.5 Flow rate
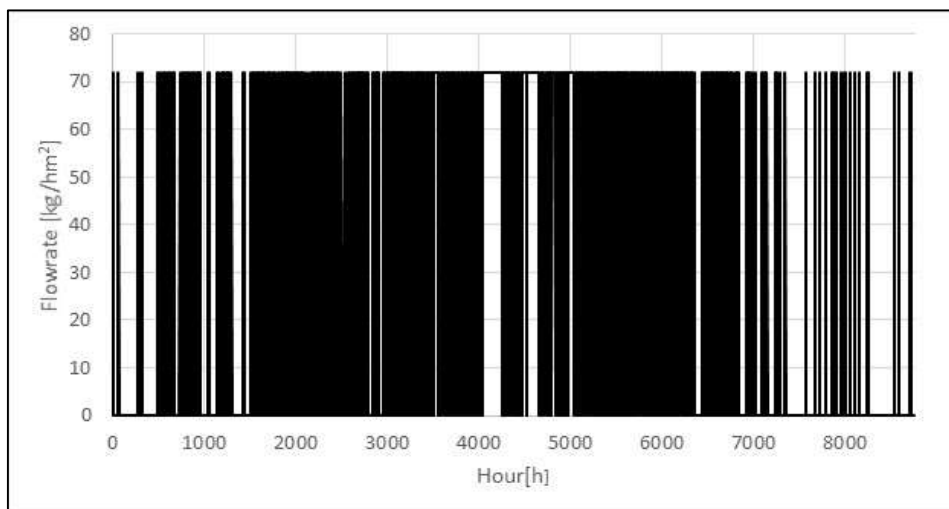
Figure 7-15 Specific flow rate through the solar collector circuit

Figure 7-15 shows that the main circulation pump is running most of the year. Fluctuations in the flow rate between 0 and 72 kg/hm^2 creates the coherent black areas in the figure. Between April and September the pumps are running almost every day at times when the sun is up. This is yet another indication that the storage tank is sufficiently large to store all available heat at all times of the year, and that there may be profitable to install a bigger solar collector area. When the pump is not running, it is because the required temperature difference between the outlet of the collector and the bottom of the tank is not met. This happens more frequently between January and April and between September and December.

7.4.6 Auxiliary heat input

The auxiliary heater installed in the water tank is a 8 kW electric heater. Figure 7-16 shows that the auxiliary heater is operational throughout the year. The operating time of the auxiliary heater is approximately 2660 hours annually. The heater is turned off when the water in the top of the tank exceeds 55 degrees as seen in Figure 7-11. The operational time of the auxiliary heater will decrease as the collectors cover more of the load.
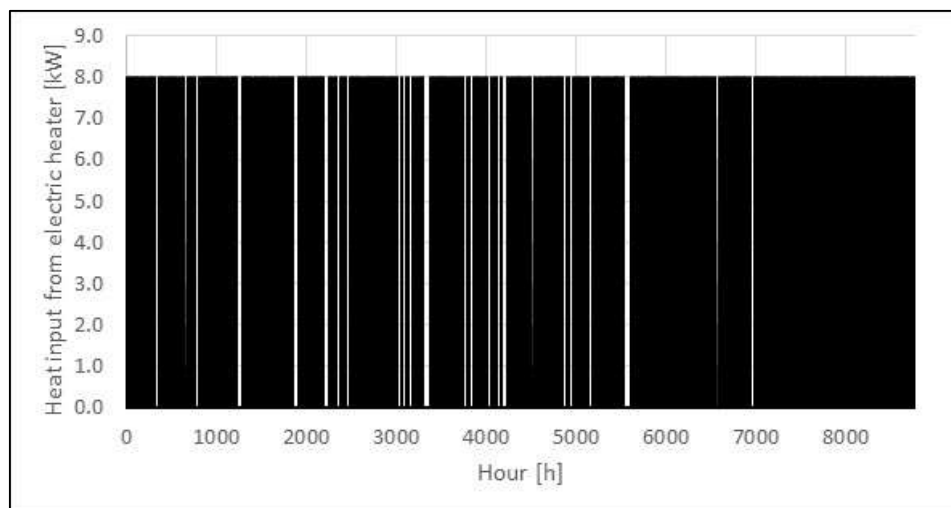
Figure 7-16 Heat input from electric heater in water tank

7.4.7 Heat transferred from heat exchanger to the water tank
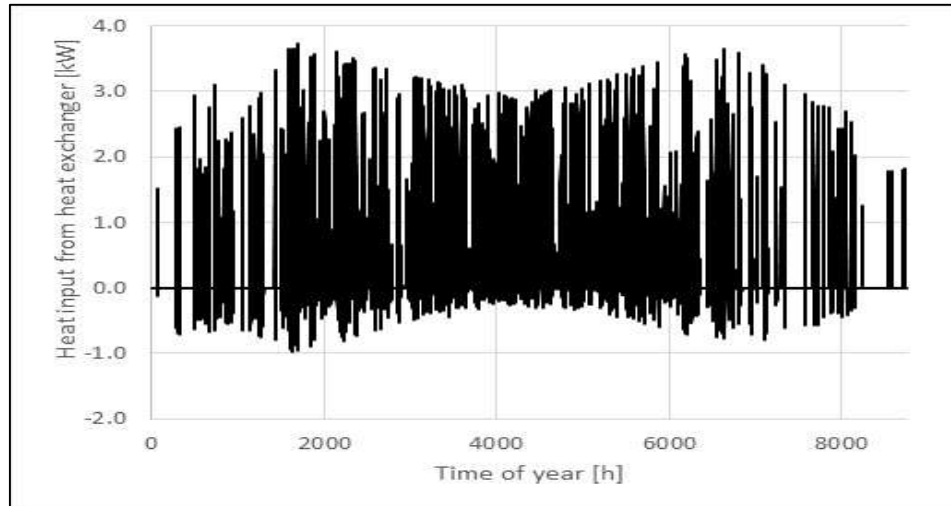
Figure 7-17 Heat transferred from heat exchanger to water

Figure 7-17 shows the heat transferred from the heat exchanger in the water tank to the water. The highest heat transfer load happen when the amount of radiation that strikes the vertical south surface is at its maximum. This happens during the spring and the autumn. The heat loads are lower during the summer months when the sun is high on the sky and a tilted collector would receive more of the radiation. The vertical installation is the most optimal during the winter, but here the heat loss from the absorber plate is big, and the heat transfer to the tank will decrease. Even though the radiative loads to the collectors are higher during the spring and the autumn compared to the summer months, the total collected energy is higher during the summer as seen in Figure 7-10. This is a result of lower ambient temperatures and less total radiative energy during the spring and autumn. When the heat input is negative, the water temperature of the water surrounding the heat exchanger in the tank exceeds the temperature of the water in the heat exchanger. When this occurs, the circulation pump is not running, so in reality, no heat will be transferred from the tank to the working fluid in the solar collector loop.

7.5 Parametric study of efficiency measures

The following chapter looks at the effect of changing different system parameters to optimize the DHW system design, and compares the result with the system introduced in Chapter 7.1.3. The initial system is designed according to recommendations from literature regarding the design of solar thermal systems for DHW, as evaluated in Chapter 4. Most of these recommendations are related to tilted collectors installed with optimal slope. Vertically installed façade integrated collectors will not only perform differently, they will also influence the transmission of the wall, as seen in Chapter 6.3. The following parametric study will reveal how each of a number of parameters can be regulated to increase the overall system performance with regard to both collector performance and transmission.

Parasitic effects such as energy for running the pump is neglected in the following investigation unless the opposite is specified. This approach is chosen because the investigated system is small, with small height differences for the pump to overcome. This is further explained in Chapter 7.5.3. In addition will this lead to results that are applicable for other solar thermal systems as well, not only this system in particular because the influence of the collectors on the system performance will have a greater impact. However, it is important to acknowledge the influence that big parasitic effects can have on the system performance. This is somewhat illustrated in Chapter 7.5.6 where energy for pumps is indeed included in one of the investigations for illustration purposes.

An important aspect of any solar collector system is finding the optimal solar collector area. A parametric study of this is not included in the following chapters, since the dynamic model is not suited for investigating this. Economic considerations regarding energy savings in relation to investment cost should be included in any evaluation of optimal solar collector area. The economy aspect is not included in the following parametric study.

7.5.1 Base case

Total solar collector area (m²)	6.68
Daily load (l/day)	300
Mass flow rate (kg/hm²)	72
Regulatory strategy (dT on- dT off)	8-5
Tank volume vs collector area (m³/m²)	0.07
Tank set point temperature (°C)	50
Tank height (m)	1.4
Tank height vs. diameter ratio (-)	2.14
Heat exchanger outlet height (m)	0.16

Table 7-5 Summarized base case parameters

Table 7-5 summarizes the parameters of the initial DHW system presented in Chapter 7.1.3. This system is referred to as the base case. The following parametric study will be compared to the base case. For every investigation, only one system parameter will be modified, while the others will be set equal to the base case.

7.5.2 Optimizing the tank volume

There may be a potential of modifying the tank volume to cover a larger fraction of the DHW energy consumption with the solar collectors. Tank sizes between 200 l-600 l have been tested. For each tank size, the heights of all the components in the tank have been modified, so that every tank looks proportionally the same as the tank in the base case. All other parameters are as stated in Table 7-5.

Solar fraction
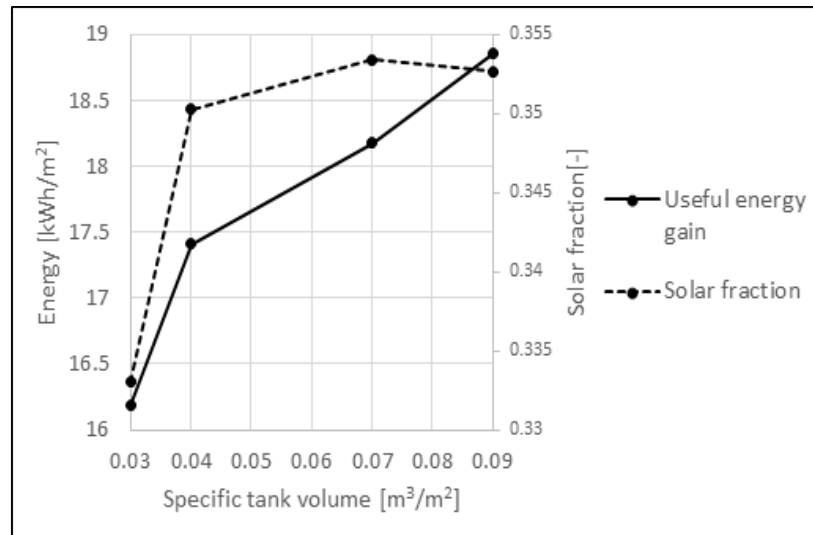
Figure 7-18 Annual solar fraction and useful energy gain for different specific tank volumes

Figure 7-18 shows the solar fraction and the useful energy gain of the system with different specific tank volumes. The useful energy gain keeps increasing as the tank volume increases. This means that the smaller volumes are too small to collect all the available heat throughout the year. This leads to stagnation periods and lower annual collector efficiencies. In addition, will the higher bottom temperatures for the lower tank volumes also lead to lowering the collector efficiency. Even though the useful energy gain keeps increasing for bigger tank volumes, the solar fraction decreases for the highest volumes. This reflects a situation where the marginal auxiliary energy increases more than the marginal useful energy gain. The tank heat losses increase with the tank surfaces area. When the tanks are large enough to store close to all available heat the useful energy gain will remain constant or only increase marginally as the tank size increases while the tank heat loss will increase. This leads to decreased solar fractions.
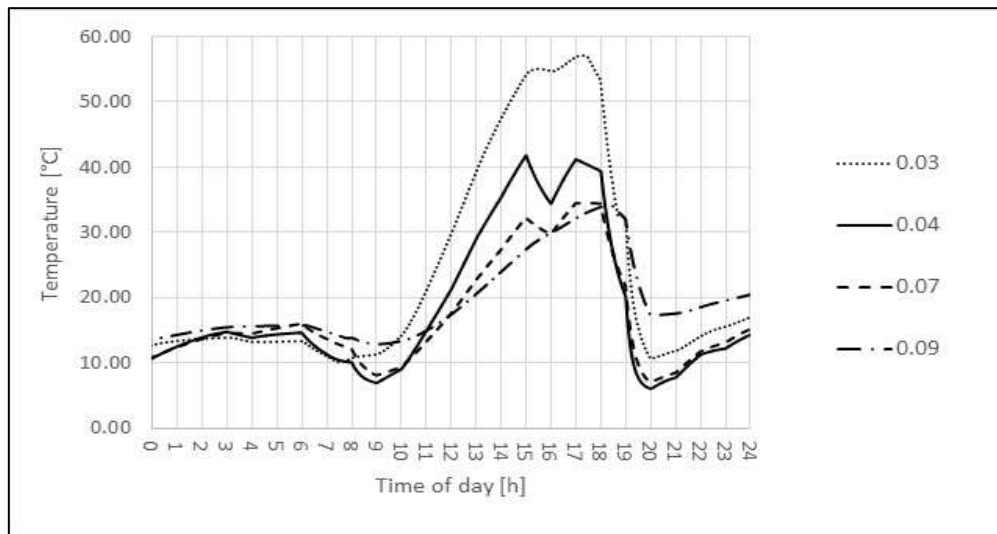
Figure 7-19 Temperature in the bottom of the tank for different specific tank volumes

As seen from Figure 7-19will the temperature in the bottom of the tank vary according to the tank volume. The graph shows the bottom tank temperature for a sunny summer day where the circulation pump is running most of the day. As expected will the lowest tank volume have the highest bottom temperature at solar peak hours. This will lead to the lowest collector efficiency and accordingly the lowest useful energy gain for the collectors. What is interesting to notice is the tank temperatures after 7 pm. Here the highest tank volume will have the highest bottom temperature. This diverts from intuition, and occur due to the higher inertia in the bigger tank. The bottom temperature follows the temperature rise and fall off the water exiting the solar collector. When the outlet temperature decreases due to lower radiation, the bottom tank temperature will decrease. For the bigger tank, this takes longer than for the smaller tank.

Operational time

Figure 7-20 illustrates the problem with stagnation periods for the smaller tank volumes. As the tank volume increases the annual operational time increases accordingly, until it decreases again for the highest tank volumes. The useful energy gain increases during this decrease in the operational time, while the solar fraction decreases. The operational time does not influence the solar fraction directly since the parasitic effects are not included in the solar

fraction. The reason for the decrease in the operational time is the aspect of inertia in the bigger tanks as illustrated in Figure 7-19.After times of peak solar radiation, the bigger tanks will have high temperatures in the bottom of the tank leading to stagnation periods. The operational time is the longest for a specific tank volume of 0.07 m^3/m^2. This is the base case volume. This is also the point where the solar fraction is the highest.
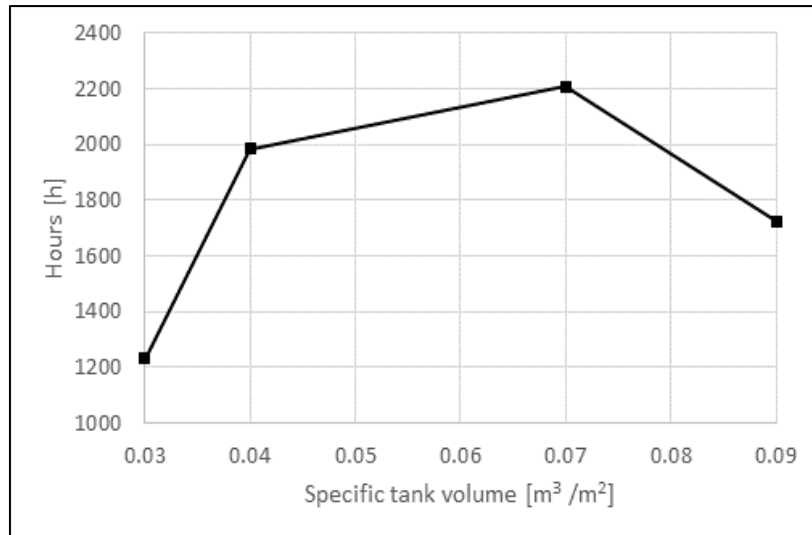
Figure 7-20 Annual operational time for different specific tank volumes

Transmission
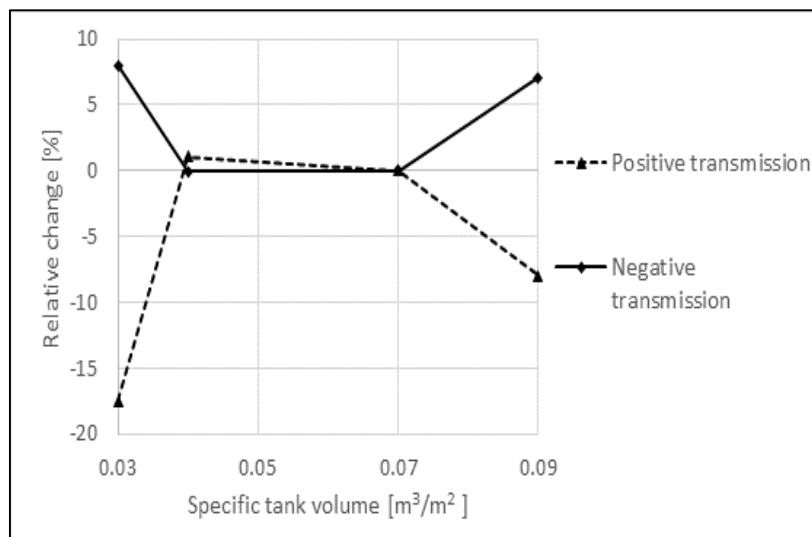
Figure 7-21 Annual relative change in transmission for different specific tank volumes compared to base case

Figure 7-21 shows the relative change in transmission between the tank volume in question and the base case. It shows that the tank volume influences the transmission through the wall,

and changing the tank volume can reduce the positive transmission and increase the negative transmission. None of the tank sizes will reduce both. For the 200 l tank (0.03 m^3/m^2), the positive transmission is approximately 17 % lower than for the base case, while the negative transmission is 7 % higher. The transmissions for a specific tank volume of 0.04 m^3/m^2 and 0.07 m^3/m^2 are approximately equal, while the biggest tank leads to an 8 % decrease in the positive transmission and a 7 % increase in the negative transmission

7.5.3 Optimizing the flow rate

An important aspect with increasing the system mass flow rate is the need to use bigger pumps. This will increase the parasitic effects, and decrease the solar fraction that takes these into account. In the discussion about pump power, the flow rate in the tubes and the diameters of the tubes are highly important. Narrow tubes and high flow rates lead to big friction pressure losses in the tubes that can be directly translated into is increased pump power. In the evaluation of these pressure losses, a few simplifications have been made. Firstly, the pressure loss through the collector panel itself have been neglected. The solar panels are header-riser collectors with eight separate tubes on the absorber plate. The flow rate through each tube will be the system mass flow rate divided by eight. The friction pressure loss increases proportionally with the flow rate, and will therefore be small.

Table 7-6 shows the friction pressure drop and head loss for different flow rates for the solar collector system when the collector panels have been neglected and when the supply-and return pipe diameter is 3 cm. The length of the pipes are set to 8 m and the vertical height difference is neglected since it is not affected by the flow rate. The Reynolds number is calculated from Eq. 19.
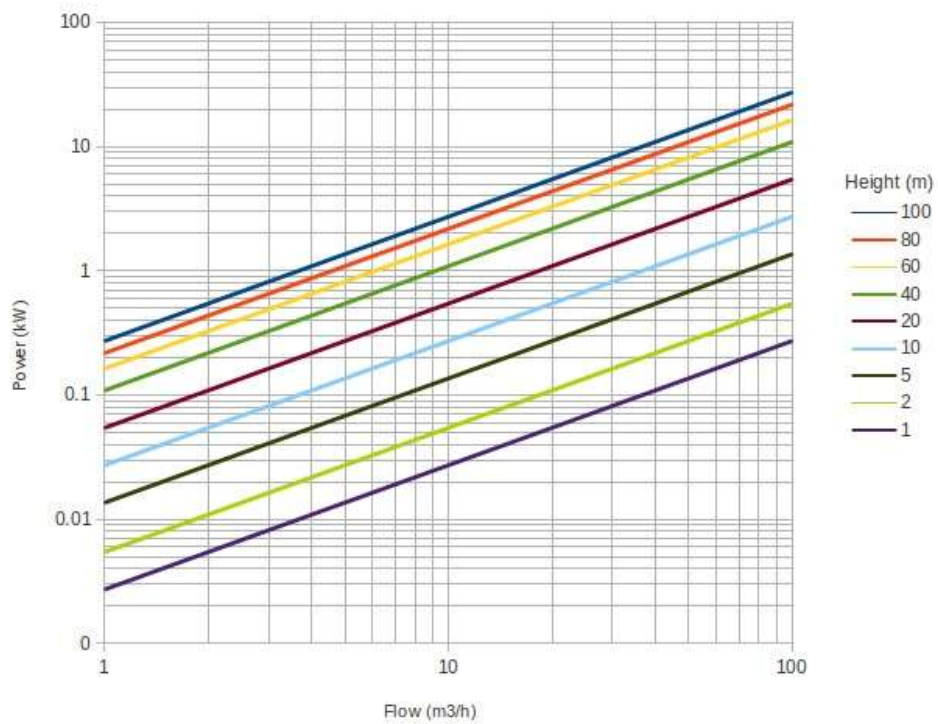
Figure 7-22 Shaft power required for pumping [69]

Specific mass flow rate, $\dot{m}$ (Kg/hm²)	18	36	43	54	66	72	78
Mass flow rate, $\dot{m}$ (Kg/s)	0.033	0.067	0.078	0.100	0.122	0.134	0.153
Velocity, v (m/s)	0.040	0.094	0.113	0.142	0.173	0.189	0.205
Reynolds number, Re (-)	1404	2821	3368	4234	5154	5644	6125
Friction pressure coefficient, λ (-)	0.056	0.044	0.042	0.039	0.037	0.036	0.035
Friction pressure loss, ΔP (pa)	16.38	52.76	71.13	105.21	147.19	172.23	197.79
Heat loss, H (m)	1.67E-3	5.38E-3	7.25E-3	0.010	0.015	0.017	0.020

Table 7-6 Pressure losses for different flow rates

78

$$Re = \frac{uL}{v} \qquad\qquad\qquad (\ 19 \ )$$

u is the velocity of the water based on the actual cross section area of the pipe. L is the length of the pipe, while v is the kinematic viscosity of the fluid. The friction pressure loss and head loss is calculated from the Darcy- Weisbach equation seen in Eq. 20. [70]

$$\Delta p = \lambda \frac{L}{d_h} \frac{\rho v^2}{2} \qquad\qquad\qquad (\ 20 \ )$$

ρ is the density, L is the length of the pipe, d_h is the hydraulic diameter of the pipe and λ is the Darcy-Weisbach friction coefficient calculated from the Colebrook equation in Eq. 21. [71].

$$\frac{1}{\lambda^{\frac{1}{2}}} = -2log\left[\frac{2.51}{Re\lambda^{\frac{1}{2}}} + \frac{k/d_h}{3.72}\right] \qquad\qquad (\ 21 \ )$$

 k is the roughness of the duct, and is set to 0.001E-3 for a copper pipe [72].

From Table 7-6 it is it evident that the friction head losses are very small for all of the flow rates. The head loss for the highest flow rate is only 0.02 m. From Figure 7-22 it can be seen that the pump power necessary to counteract the friction pressure loss in the pipe is less than 0.01 kW even for the highest flow rate. This happens since the flow rate is still relatively small, and the pipes are thoroughly large for the pressure losses not to get too high. This is not the total power of the pump since it also has to work against the static height of the water column. This will not change when the flow rate is increased like the friction will, and will therefore be neglected in the comparison between the different flow rates.

Solar fraction
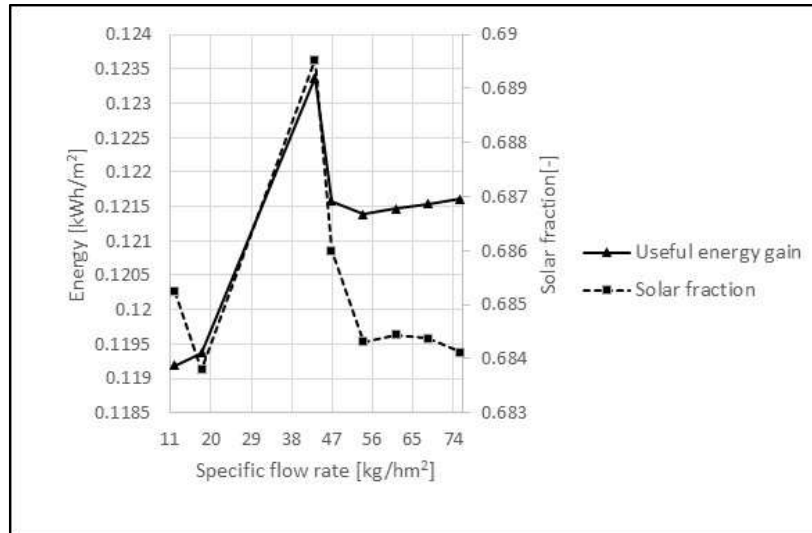
Figure 7-23 Daily solar fraction and useful energy gain for different specific flow rates, high radiation day
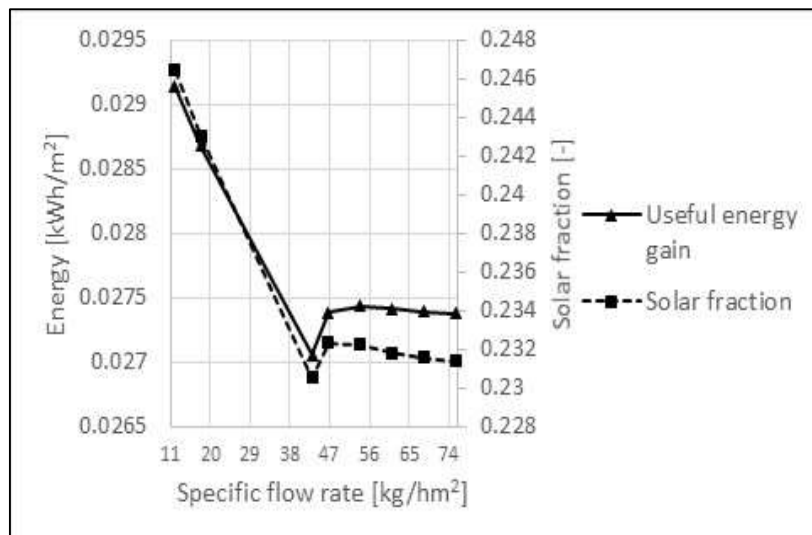
Figure 7-24 Daily solar fraction and useful energy gain for different specific flow rates, low radiation day

Figure 7-23 and Figure 7-24 show the solar fraction and useful energy gain of the collectors for two different days in July. One sunny and one cloudy day. The results show that the

optimum flow rate depend on the solar availability. For sunny times, high flow rates lead to high solar fractions. The sunny day, the optimal specific flow rate is around 43 kg/hm^2, while the lowest tested flow rate gives the highest solar fraction the cloudy day. Here the available heat is low and the flow rate must be accordingly low to ensure satisfactory heat transfer to the water tank. The heat losses from the absorber plate are small as well. For the high radiation day, the flow rate is increased to remove the energy and to avoid big heat losses from the absorber plate. This corresponds to research done by Furbo et al. [43] showing that high temperatures across the pump will lead to higher optimal flow rates through the solar collector.
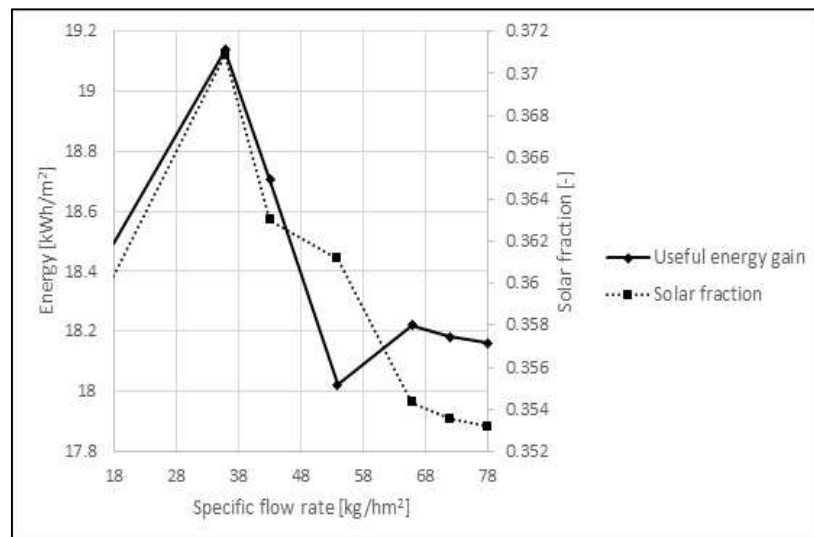
Figure 7-25 Annual useful energy gain and solar fraction for different specific flow rates

Figure 7-25 shows that a specific flow rate of 36 kg/hm^2 gives the highest annual solar fraction. The development of the useful energy gain and the solar fraction correlates for lower flow rates, but between the flow rates of 54 kg/hm^2 and 66 kg/hm^2 the useful energy gain increases, while the solar fraction decreases. This means that the auxiliary energy increases more than the useful energy gain. The effect is not related to increased power for running the pumps, so the reason must be unfavourable thermal effects in the system. The results did not indicate exactly what these effects were. The solar fraction keeps decreasing further as the flow rate is further increased. Between 36 kg/hm^2 and 54 kg/hm^2, the solar fraction and the

useful energy gain both decreases. The two values follow each other, meaning that the auxiliary energy increases at about the same rate as the useful energy gain decreases.

Operational time
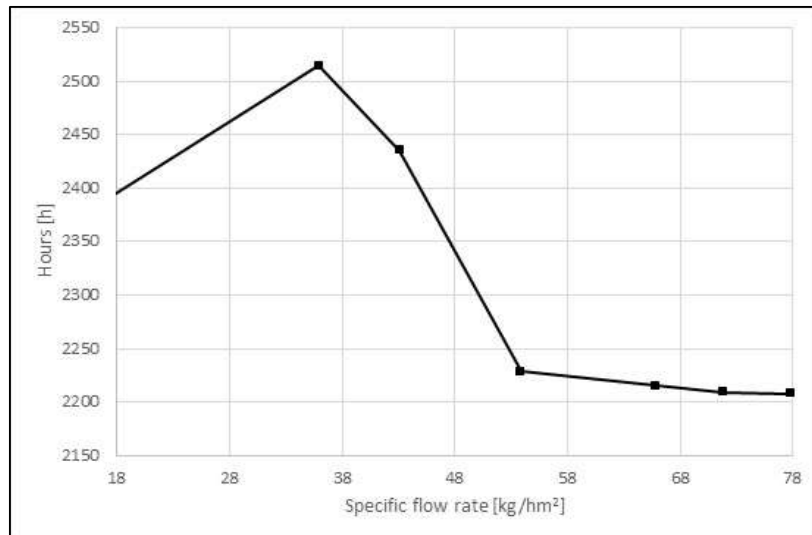
Figure 7-26 Annual operating time of solar collectors for different specific flow rates

Figure 7-26 shows that the annual system operating time is sensitive to changes in the flow rate. For the smaller flow rates the operational time increases as the flow rate increases. This illustrates that the heat loss from the absorber plate decreases as the flow rate increases, and the required temperature rise over the collector panel for the circulation pump to run is more easily met. This increases the annual operational time. For the highest flow rates, the operational time is decreasing. Here the flow rate is too high to absorb enough energy from the absorber plate for the circulation pump to run. The highest operational time occurs for a specific flow rate 36 kg/hm^2 where the solar fraction is the highest. The shape of this curve follows the shape of the curve describing the solar fraction.

Transmission

50
40
30
20
10
0
-10
-20
-30
Relative chenge [%]
18
28
38
48
58
68
78
Specific flow rate [kg/hm²]
Positive transmission
Negative transmission
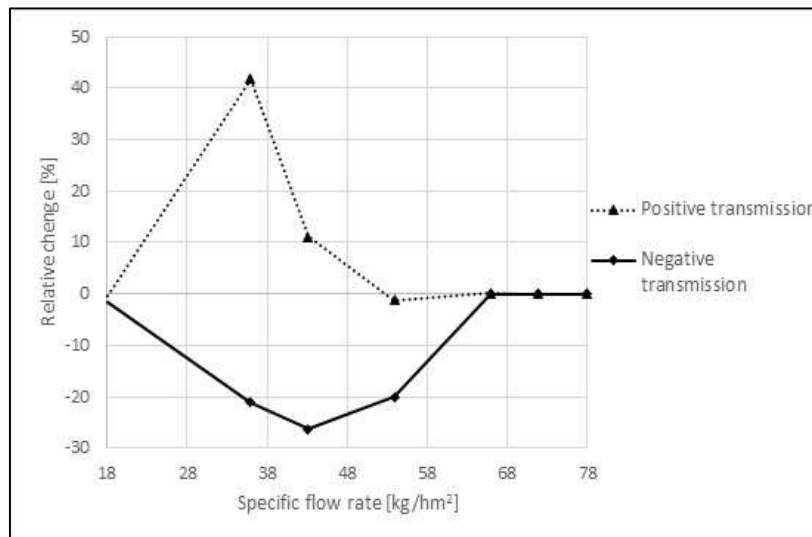
Figure 7-27 Relative change in transmission for different specific flow rates compared to the base case

Figure 7-27 shows the relative change in the transmission through the south façade when the flow rate through the solar collector changes compared to the base case. Both the positive and negative transmission is more or less equal to the base case for the lowest and the highest specific flow rates. The solar fraction is highest when the positive transmission is 40 % higher than for the base case and the negative transmission is 35% lower. A specific flow rate of 54 kg/hm^2 will lead to a reduction of both the positive and negative transmission, and will reduce the total energy used to cover transmission losses and gains with 20 %. A flow rate of 43 kg/hm^2 will reduce the energy used for transmission losses and gains by 25 % when reduced negative transmission is seen as the equivalent of reduced heating loads and increased positive transmission is increased cooling loads. The shape of the curve of the positive transmission follows the shape of the solar fraction curve and the curve describing the operating time. Increased positive transmission is the equivalent of increased heat loss from the absorber plate and will in this situation be highest when the solar collector output is highest.

7.5.4 Optimizing ratio between tank height and diameter

In the following investigations, the ratio between the tank height and diameter is modified. For every situation, the ratios between the tank height and the auxiliary heater, the thermostat and all inlets and outlets heights are equal to the base case. All other parameters are held constant and equal to the base case.
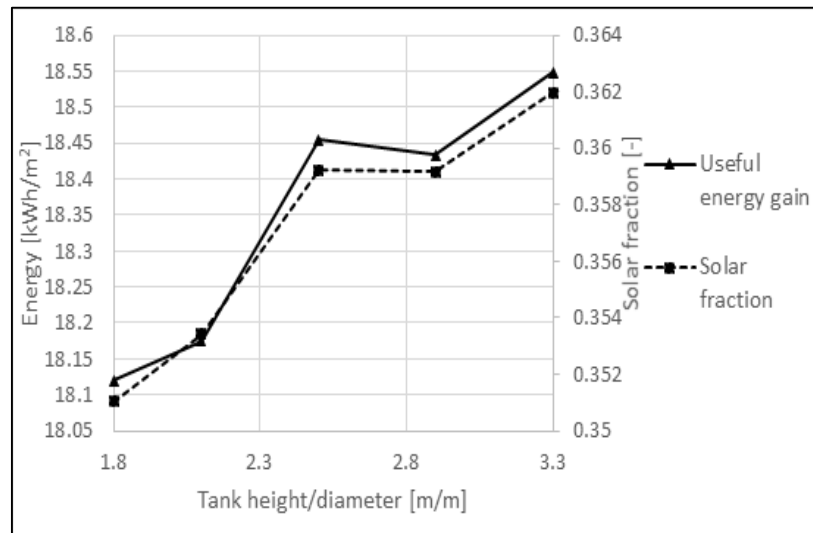
Solar fraction

Figure 7-28 Useful energy gain and solar fraction for different ratios between tank height and diameter

As the tank height increases, the stratification and the useful energy gain increases accordingly. This can be seen in Figure 7-28. As the ratio between the tank height and the diameter increases from 2.5 to 2.9 the useful energy gain decreases marginally, while it keeps increasing again as the ratio approaches 3.3. For the tested tank heights, there is no upper limit where the solar fraction starts to decrease permanently. This indicates that the only aspect limiting the tank height is practical considerations regarding space, which is most commonly the height between the floor and the ceiling in the room where the tank is installed.
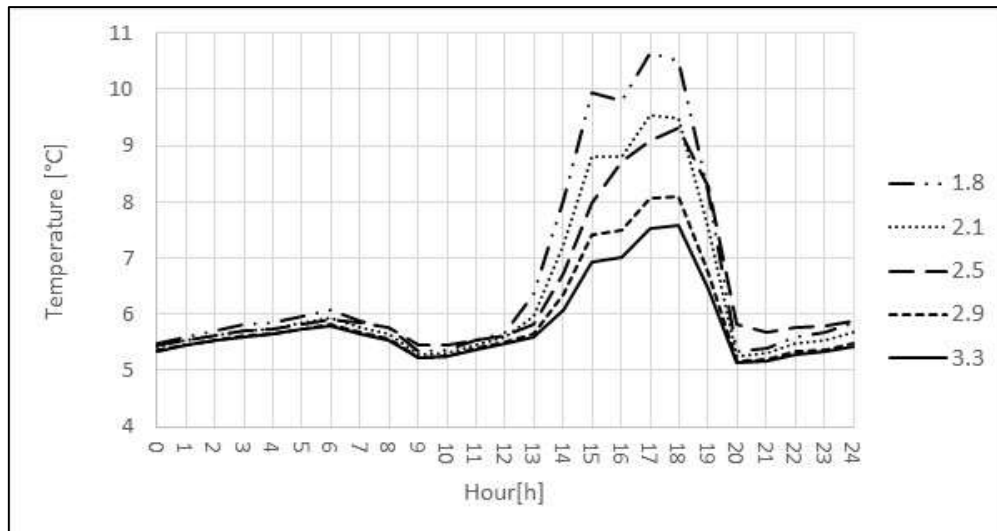
Figure 7-29 Daily tank bottom temperature for different ratios between tank height and diameter

Figure 7-29 shows that the tank bottom temperature decreases as the ratio increases throughout the day, except for after 20 pm. Here the bottom temperature for the tank with a ratio of 2.5 is the highest. Intuitively, this should lead to lower collector efficiencies for this system in particular, but the annual solar fraction for his ratio is high. This must mean that this ratio causes some favourable thermal effects in the system that lead to the high solar fraction. The curve of the solar fraction has the same shape as the curve for the useful energy gain. This means that the useful energy gain alone, and no other aspects such as increased heat loss from the tank influences the change in the auxiliary energy and consequently the solar fraction. Exactly what causes these favourable thermal effects have not been detected from the simulation results.

Operational time
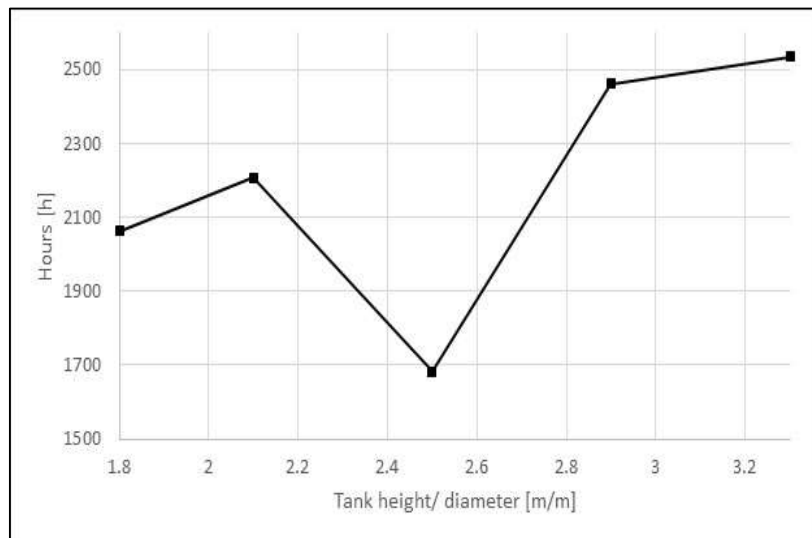
Figure 7-30 Annual operational time for different ratios between tank height and diameter

As the ratio changes from 2.1 to 2.5, the annual system operating time decreases with about 500 hours. This can only be explained by the phenomenon in Figure 7-29, where the bottom temperature for the 2.5 ratio is higher than for the lower ratios. This leads to a smaller temperature rise over the collectors, and consequently shorter annual operating times. Apart from this, the useful energy gain increases as the operational time increases. High ratios lead to low bottom temperatures, meaning that the required temperature rise over the collectors are more easily met, and the operational time will therefore be longer.

Transmission

Figure 7-37 shows that the positive transmission is more sensitive to changes in ratio between the height and the diameter than the negative transmission. For all the tested ratios, the negative transmission will be higher or equal to the transmission in the base case. For the lowest ratio, the positive transmission will be higher than for the base case, while it will be lower for all the other ratios tested. The highest solar fraction occurs for a negative transmission equal to the base case, while the positive transmission is approximately 6 % lower. By translating the decrease in positive transmission into a decrease in a mechanical

cooling load, the highest ratio leads to a total energy saving related to transmission of 6 %, which would be the best configuration of the tested tanks. In the concept building, no cooling is installed, but it is still achievable to reduce the positive transmission to improve the indoor environment during the summer. Also with this view, a height-diameter ratio of 3.3 is the best, even though this will not lead to any energy savings. Here the positive transmission is reduced, while the negative transmission is equal to the base case. The ratio of 2.5 will lead to a lower positive transmission, but the negative transmission will be higher. This leads to a higher annual energy consumption.
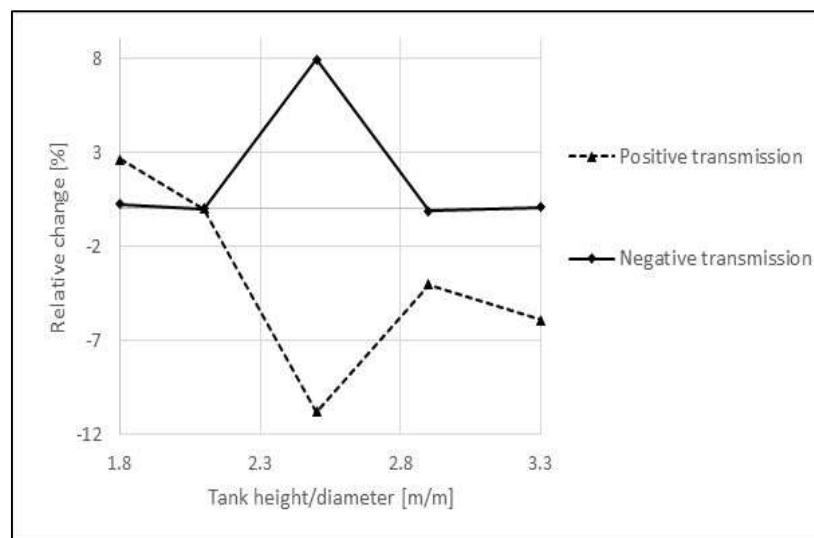
Figure 7-31 Relative change in annual transmission for different ratios between tank height and diameter compared to base case

7.5.5 Optimizing inlet and outlet positions

The heat exchanger from the base case is used in all of the following investigations, but its placement in the tank is modified. All other parameters are according to Table 7-5.

Solar fraction
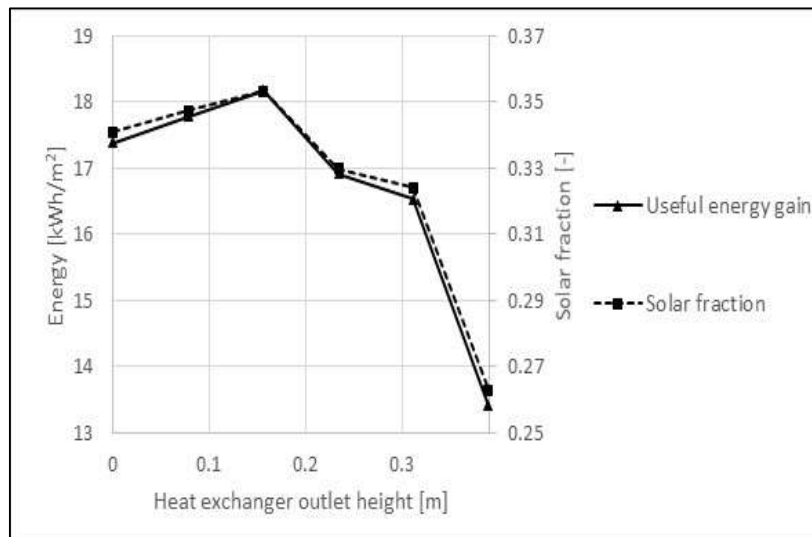
Figure 7-32 Useful energy gain and solar fraction for different heat exchanger outlet heights

The system performance heavily depends on the inlet temperature of the collectors. The heat exchanger placement influences this temperature. Figure 7-32 shows that the lowest heat exchanger outlet heights leads to the highest solar fractions. The solar fraction vary between 0.26 and 0.35 for the best and worst case. The water surrounding the heat exchanger has a higher temperature the higher the heat exchanger is installed in the tank. This means that the collector inlet temperature increases as the heat exchanger height increases. Of the investigated heat exchanger heights, the base case configuration shows best system performance. This is surprising since one would believe that the lower heat exchanger placements would lead to higher collector efficiencies.
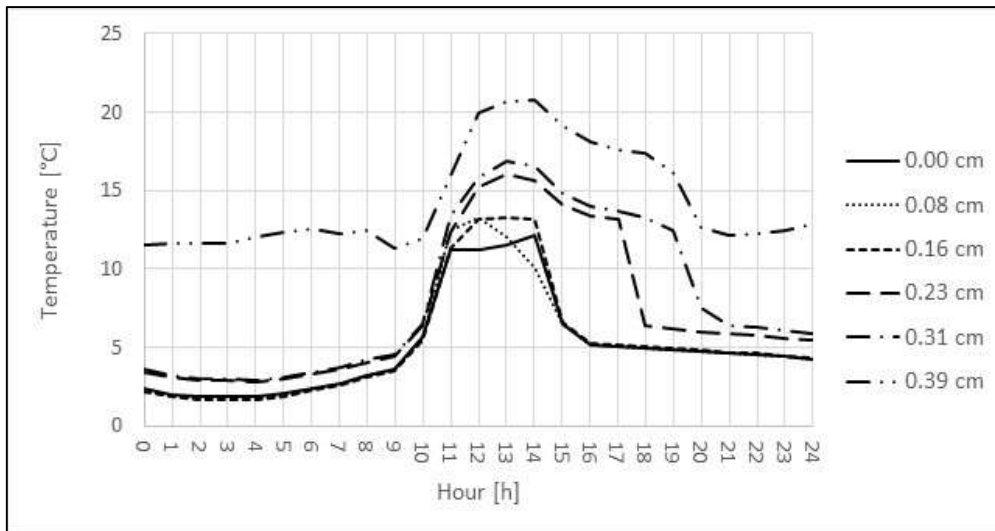
Figure 7-33 Collector outlet temperature for different heat exchanger outlet heights

Figure 7-33 shows the collector outlet temperature for different heat exchanger heights. The outlet temperature increases as the height increases. A higher outlet temperature out of the collector is directly connected to a higher collector inlet temperature, higher heat loss from the absorber plate and a lower temperature difference over the collector panel.

As seen in Figure 7-32 will the absolute lowest heat exchanger height not give the highest solar fraction. The reason is somewhat illustrated in Figure 7-33 where the heat exchanger outlet height of 0.16 m has the lowest outlet temperature until 10 am. Between 10 am and 3 pm the three lowest exchanger heights have outlet temperatures related to each other that are different than expected. These abnormalities throughout the year makes the solar fraction increase as the exchanger height approaches 0.16 m.

Operational time
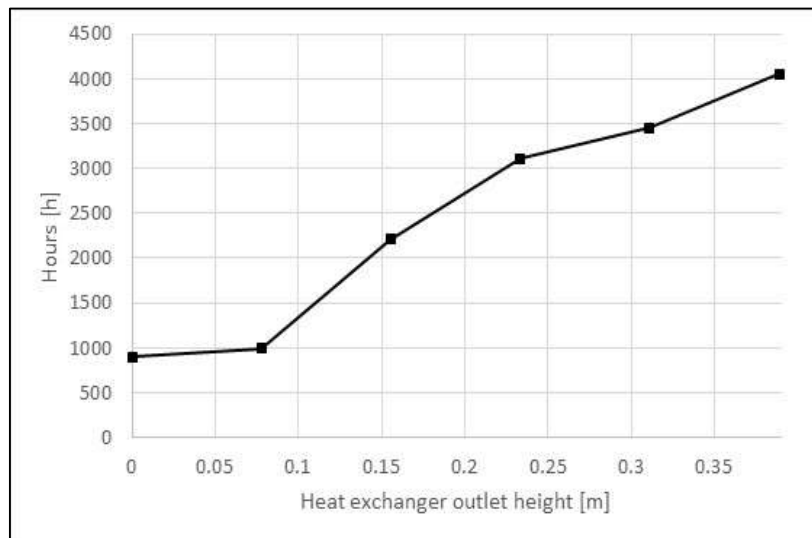
Figure 7-34 Pump operational time for different heat exchanger outlet height

Figure 7-34 shows that the highest heat exchanger outlet height leads to the longest annual operational time. This is when the solar fraction and the useful energy gain is the lowest. In earlier investigations, the tank bottom temperature influenced the collector inlet temperature directly since the heat exchanger was placed in the bottom of the tank. As the heat exchanger is installed higher up, the water bottom temperature will be lower, since the heat exchanger will not influence this temperature to the same extent as before. Since the regulatory strategy of the system is controlled by the temperature difference between the water bottom temperature and the collector outlet temperature, the operational time will be heavily influenced by any changes in the heat exchanger height. When the heat exchanger height increases, the water bottom temperature will decrease, and the required temperature rise through the panels for the circulation pump to run will be more easily met. This can explain why the lowest heat exchanger placement did not achieve the highest solar fraction

To ensure that the system is regulated optimally, the thermostat controlling the circulation pump should be placed adjacent to the heat exchanger and not in the bottom of the tank. This to ensure that the pump only runs when the fluid in the heat exchanger is hotter than the water in the storage tank.

Transmission
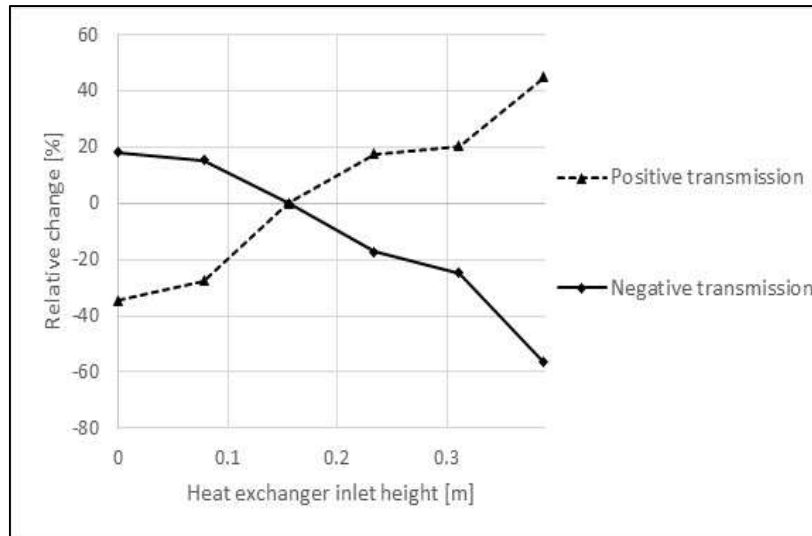
Figure 7-35 Relative change in annual transmission for different heat exchanger outlet heights compared to the base case

Figure 7-35 shows that for heat exchanger outlet heights lower than 0.16 m the negative transmission is higher and the positive transmission is lower than for the base case. This happens since the lower heights leads colder water through the solar panels. As the heat exchanger height increases, the negative transmission decreases, while the positive transmission increases. None of the heights will lead to a decrease in both the positive and the negative transmission compared to the base case. The transmission is very sensitive to the changes in the heat exchanger height, and the negative transmission can be decreased by as much as 60 % with an inlet height of 0.39 m. This will consequently also increase the positive transmission.

7.5.6 Optimizing the regulatory strategy

Investigations in this report focuses on the use of a constant speed pump controlled according to the temperature difference between the outlet of the solar collectors, and the bottom of the storage tank. If this difference exceeds 8 K the pumps will turn on, and the collectors will collect energy. If the temperature difference drops to below 5 K, the pumps will turn off. This is in the following written as the 8-5 strategy.

Finding the optimal regulatory strategy translates to finding the temperature interval where the marginal useful energy gain exceeds the marginal pump power. Increasing the operational time of the pump will increase the useful energy gain of the collector and the collector efficiency, but the parasitic energy increases as well. Especially for the single speed pump, a poor regulatory strategy will cause the system to run with big parasitic effects to collect only a small amount of heat.

Table 7-7 shows the regulatory strategies tested. Each strategy will be referred to by its number.

Strategy	1	2	3	4	5	6	7
	6-5	7-5	8-4	8-5	8-6	8-8	10-5
Strategy	8	9	10	11	12	13	14
	11-5	11-7	11-8	11-9	12-8	12-9	12-11

Table 7-7 Regulatory strategies

Solar fraction
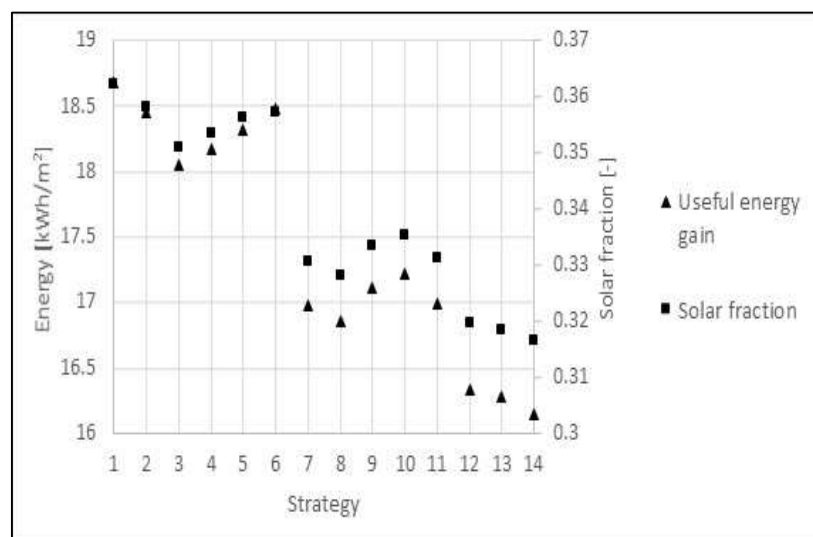
Figure 7-36 Useful energy gain and solar fraction for different regulatory strategies

Figure 7-36 shows that the highest solar fractions are obtained for the lowest pump start up temperature differences. This is intuitive, since this will give the pump the longest operating

time. The fact that the profiles of the useful energy gain and the solar fraction are so similar indicates that there are no other effects in the systems that increases the auxiliary energy for any of the strategies. The total supplied energy are approximately the same for every strategy. When the useful energy gain decreases, the auxiliary energy has to increase and the solar fraction decreases.
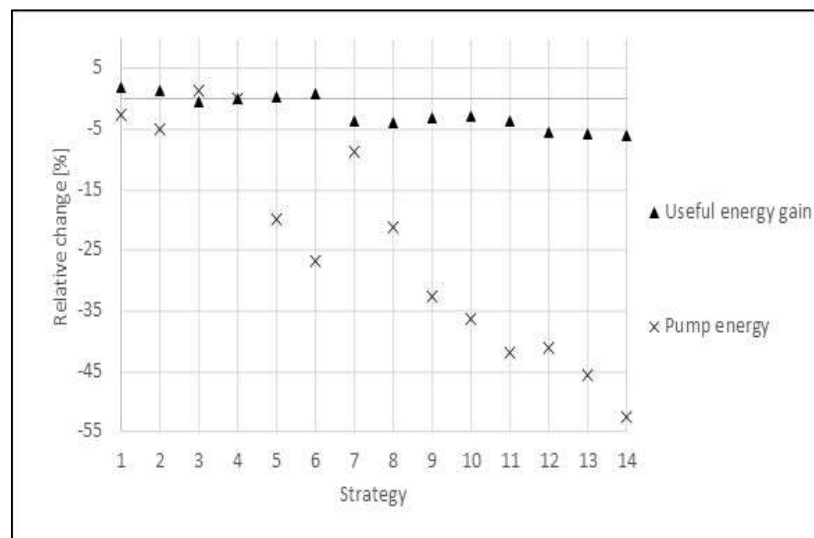
Figure 7-37 Relative change in useful energy gain and pump energy for different regulatory strategies compared to the base case

The solar fraction in Figure 7-36 will not be the best performance indicator when investigating the optimal regulatory strategy. The increased operating times will increase the parasitic effects, but these are not included in the solar fraction. The pumping power is very small, but in this investigation, so is the change in the useful energy gain. At the same time are the operating times varying substantially as seen in Figure 7-37. The relative change in the annual pump energy in Figure 7-37 is equal to the relative change in the pump operating time since this is a constant speed pump. The useful energy gain is only reduced by approximately 10 % when the operational time for the pump is reduced by 52 %. This is when the operating strategy changes from Strategy 4 (the base case) to Strategy 14. The economy of this change depend on the design of the system, where poorly designed systems with high pump loads will benefit from having higher temperature intervals (Strategy 8 to Strategy 14).
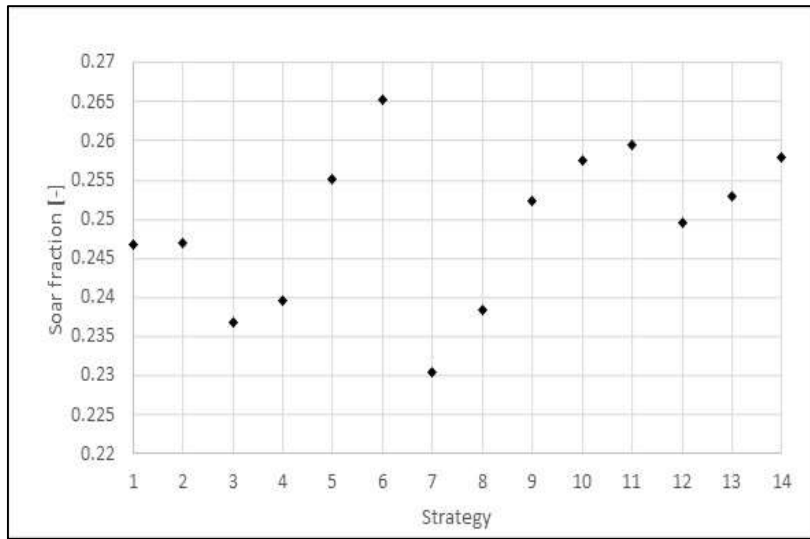
Figure 7-38 Solar fraction for different regulatory strategies with a pump power of 0.01 kW

Figure 7-38 shows the solar fractions for the different regulatory strategies when the pump power is set to 0.01 kW and this contribution is included in the solar fraction. As seen in Chapter 7.5.3 is this pump power sufficient for covering the friction pressure losses and a vertical height difference of as much as 5 m.

The annual solar fraction for all of the strategies decreases when the pump power is included, as seen in Figure 7-38. In addition is the optimal configuration now different compared to the system where the pump power was neglected. Strategy number 6 will now give the highest solar fraction. This is not the strategy with the smallest annual operating time, which was strategy number 14. This means that the useful energy gain collected during the extra operating hours under strategy 6 exceeds the additional pumping energy. There is an overall tendency of the shortest operating times giving the highest solar fractions with this pump power. This tendency will change if the pump power changes.

Transmission
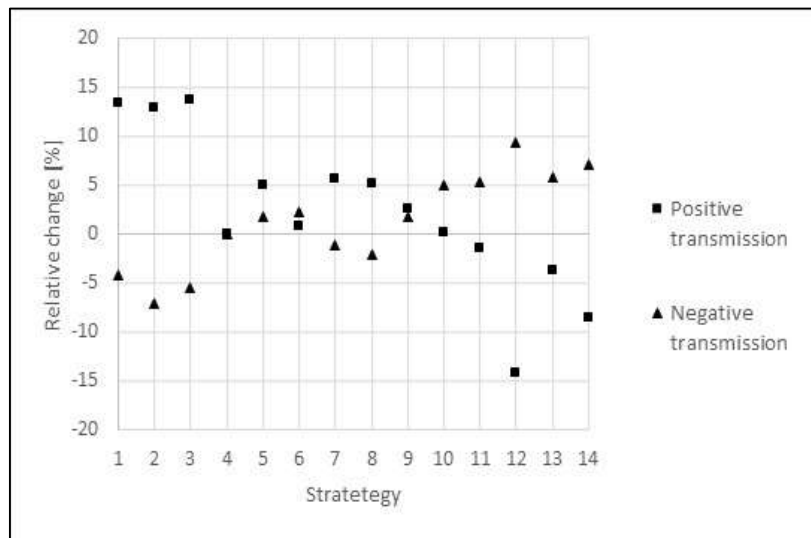
Figure 7-39 Relative change in transmission for different regulatory strategies compared to the base case

Figure 7-39 shows the relative change in the transmission for different regulatory strategies compared to the base-case (Strategy 4). No regulatory strategy leads to a negative relative change for both the positive and negative transmission. This means that none of the regulatory strategies will decrease all transmission. For Strategy 5, Strategy 6 and Strategy 9 both the positive and the negative transmission increases, while for the rest of the strategies one of the two increases while the other decreases.

There is a bigger potential of reducing the positive transmission through changes in the regulatory strategy than the negative transmission. If the main aim with the integration of solar collectors is to minimize the heat gain especially during the summer, strategy 12 is the best. Here the positive transmission is reduced with about 14 % compared to the base case. The negative transmission increases with about 9 %, but will still be lower than for the conventional wall.

7.5.7   Optimizing the tank set point temperature

Changing the tank set point temperature may heavily influence the collector performance. Even though low tank temperatures will require a re-heating tank to raise the temperature to a

level satisfactory for DHW, this introduces a possibility of increasing the collector performance and re-heat the second tank with a more effective energy source such as a heat pump. In the following investigations, only the tank set point temperature is modified. The other parameters are equal to the base case.
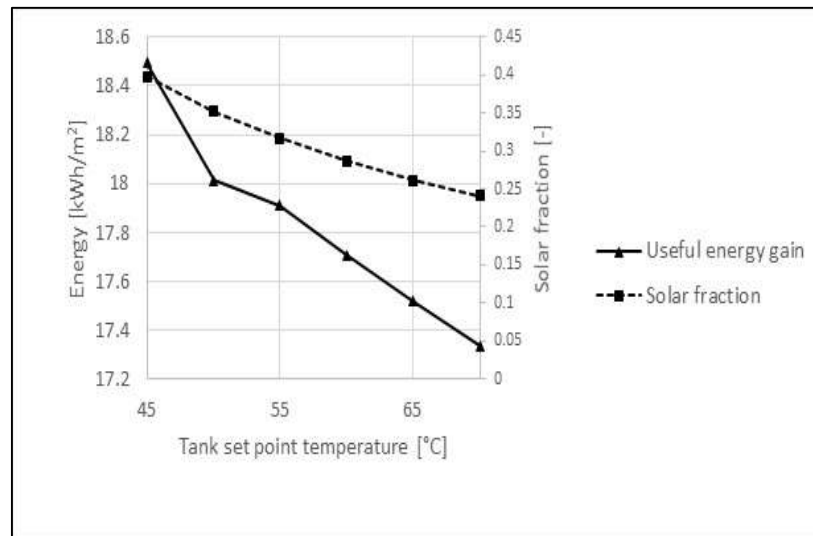
Solar fraction

Figure 7-40 Useful energy gain and solar fraction for different tank set point temperatures

The useful energy gain of the collector increases as the tank set point temperature decreases due to lower tank bottom temperatures and then higher collector efficiencies as seen in Figure 7-40. The auxiliary energy decreases as well. This leads to increased solar fractions. For low tank temperatures the systems needs an additional tank to re-heat the water to a satisfactory temperature for it to be used as domestic hot water. The economy of the system depend on the energy source of the reheating. If the reheating systems is electrical as well, the optimal design will be the situation where the solar collectors function the best. The big difference in the useful energy gain and the solar fraction for the lowest and highest tank set point temperature indicates that it may actually be beneficial to use two separate water tanks in solar collector systems, where only one tank is connected to the solar collector circuit and the tank temperature is kept as low as possible. This introduces higher investments costs, but it also simplifies the process of using a heat pump for covering the auxiliary heating load. The auxiliary energy related to heating a potential re-heating tank is not included in the results of Figure 7-40.

Operational time
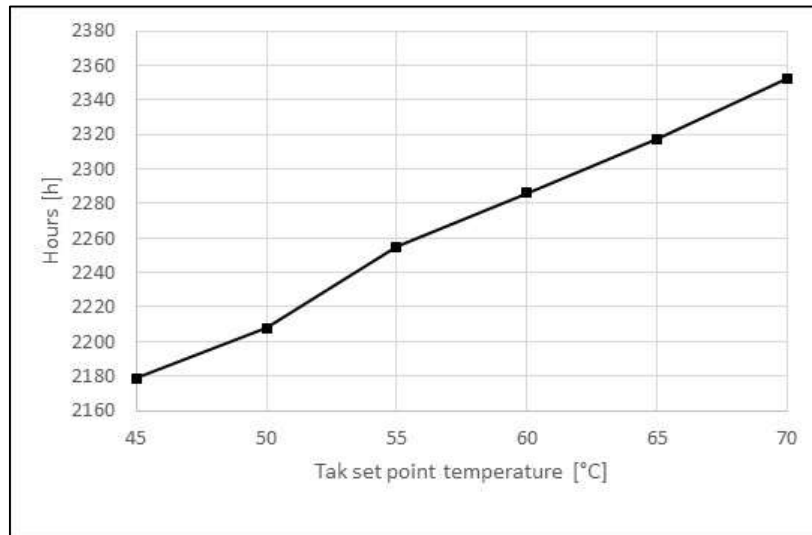
Figure 7-41 Operational time for different tank set point temperatures

When the tank set point temperature is low, the tank will earlier reach its set-point temperature, the stratification effects will be diminished and the operational time will be shorter. This explains the shape of the curve in Figure 7-41 Even though the solar fraction decreases as the tank temperature increases, the annual operational increases as well. Between tank temperatures of 45 and 70 degrees, the useful energy gain decreases with 5 % while the annual operational time increases with around 8 %. This means that for high tank temperatures the pumps are turned on for longer, but collects less energy. This indicates that also related to the operational time, the lowest tank set point temperature leads to the best system performance.

Transmission

16
14
12
10
8
6
4
2
0
-2
-4
-6
Relative change [%]
45
50
55
60
65
70
Tank set point temperature [°C]
Positive transmission
Negative transmission
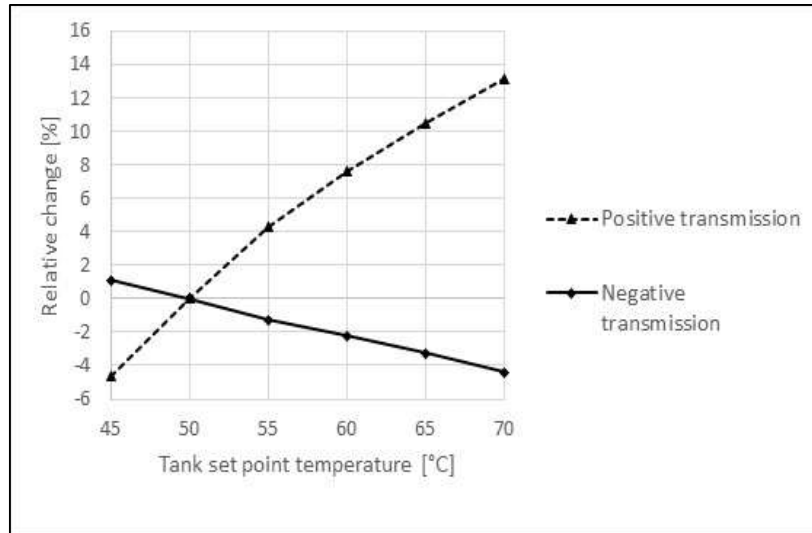
Figure 7-42 Relative change in annual transmission for different tank set point temperatures compared to the base case

As the tank set point temperature increases, the average absorber plate temperature increases accordingly. This increases the positive transmission, while the negative transmission decreases as seen in Figure 7-42.The positive transmission is more sensitive to the tank set point temperature and will increase with approximately 12 % as the set point temperature is raised from 50 to 70 degrees. The negative transmission is reduced by 4 % for the same temperature interval. Both of the curves are almost linear functions proportional to the change in the tank set point temperature.

7.5.8 Summary of effects of efficiency measures

Transmission
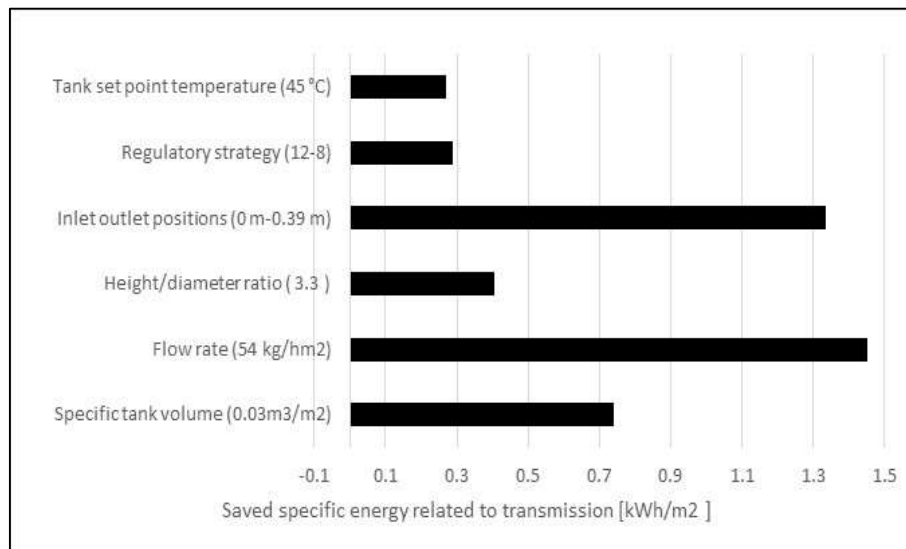
Figure 7-43 Potential of reducing transmission energy

The different optimization measures have different potentials of reducing the total transmission through the solar wall. Figure 7-43 summarizes the results of Chapter 7.5 and shows the maximum energy saving related to transmission for each of the efficiency measures. Changing the flow rate from 72 kg/hm^2 to 54 kg/hm^2 will give the highest energy savings of all the actions when translating the reduction in both the positive and negative transmission into saved energy for heating and cooling. In view of the transmission, all the parameters in the study can be modified to give energy savings compared to the base case. The measures with the smallest potential of reducing the transmission is the tank set point temperature and the regulatory strategy.

DHW system performance
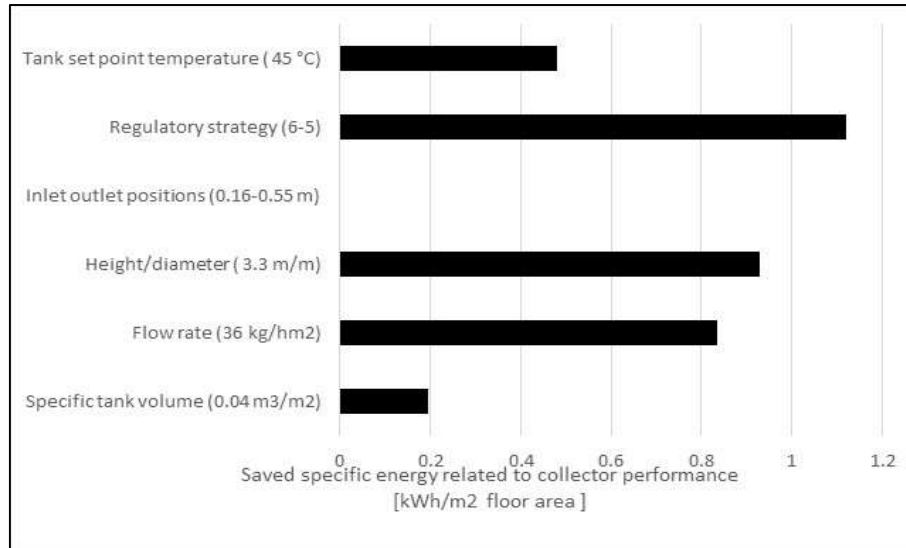
Figure 7-44 Potential of increasing collector performance

Figure 7-44 shows the potential of increasing the DHW system performance through the efficiency measures of Chapter 7.5. The results show that for properly designed system, with small parasitic effects, changing the regulatory strategy is the most promising measure to improve the system performance. The annual energy saving related to choosing the best regulatory strategy is 1.5 kWh/m^2 floor area compared to the base case. In the evaluation of the energy savings related to the set point temperature of the tank, it is assumed that a reheating tank is installed in series with the storage tank connected to the solar collector so the total energy input is equal for every case. For a proper comparison, this tank is heated by electricity. The energy savings related to changing the tank set point will then be the increased useful energy gain.

For all the measures except for the tank volume, the best situation for maximizing the system performance is the situation that gives the highest solar fraction. The tank volume that gives the highest useful energy gain also has the highest solar fraction, but it does not give the highest overall energy savings since the demanded auxiliary energy is high. The solar fraction alone does not reveal this; it only reflects the relationship between the useful energy gain and the auxiliary energy. The potential of increasing the system performance by modifying the heat exchanger placement in the tank is zero since the base case showed the best result.

DHW system performance and transmission
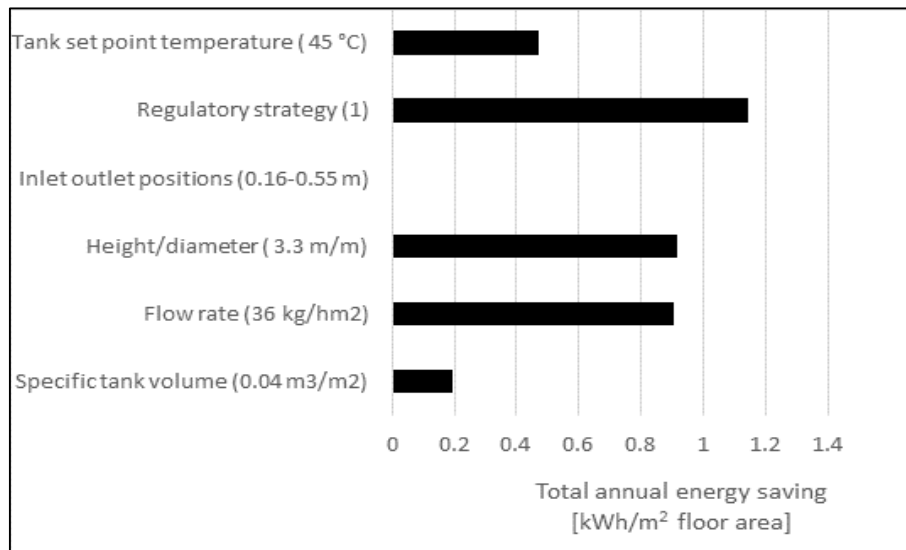
Figure 7-45 Potential of reducing total energy demand

Figure 7-45 shows the potential of reducing the total annual specific energy demand when accounting both the system performance and the transmission through 6.68 m^2 solar collectors. Since the energy savings related to the system performance are higher than the energy saving related to transmission, the optimal measures are the same as those in Figure 7-44. Changing the regulatory strategy will consequently give the highest total energy savings of 1.08 kWh/m^2. The optimal measure may reflect a situation where the transmission energy increases compared to the base case, but the overall energy demand is reduced. For the optimal measures, the positive transmission will increase when changing the tank volume, the regulatory strategy and the flow rate. The positive transmission will decrease for the optimal ratio between the height and the diameter and optimal tank set point temperature. Of the measures where the positive transmission increases, the flow rate is the most critical one. Here the positive transmission will increase with approximately 10 % as seen in Figure 7-27. For the other measures, the increase is only marginal. This aspect is important, especially for buildings without installed mechanical cooling and with large areas of integrated solar collectors.

8 Installation of heat pump

When installing a heat pump in series with the solar panels, the collector outlet fluid feeds the heat pump evaporator when the fluid temperature makes this profitable. This means that the system must be regulated differently than a normal system without the heat pump. By installing the heat pump, it is profitable to run the system also for lower solar collector outlet temperatures since the heat pump is more energy efficient than the auxiliary electric heater also for low evaporator temperatures. In the following investigations, the main pump is controlled according to the temperature in the water tank as seen in Appendix C. When the temperature in node 4 of the tank is lower than 50 degrees, the main circulation pump is started because heat input is needed to ensure high enough temperatures for DHW. The DHW outlet is in the top node, so by regulating the pump according to the temperature in node 4 it is certain that the DHW temperature is high enough at all times. If the temperature in node 2 of the tank also gets below 50 degrees, the heat pump or the solar collectors cannot deliver enough energy, and the auxiliary heater is also turned on. A flow diverter is installed after the solar collectors. The diverter guides the fluid flow through the heat pump if the collector outlet water temperature is within an acceptable range. If the water is hotter than this, it bypasses the heat pump and goes straight to the heat exchanger in the water tank. The TRNSYS system schematics of the combined solar collector heat pump system is given in Figure C-3 in Appendix C. The manufacturer data of the chosen heat pump is given in Appendix B. The heat pump is from the manufacturer Carrier, and is named the Aquazone 50PSW25-420 Water-to-Water Source Heat Pump with Puron Refrigerant (R410-A). This heat pump is chosen because it created to deliver a relatively small load, which suits the collector system. At the same time is it designed for relatively small flow rates at both the source and load side. This is also matches the system parameters.

8.1.1 Maximum evaporator inlet temperature of 10 °C

Figure 8-1 Monthly energy to water tank with a maximum evaporator inlet temperature of 10°C

Figure 8-1 shows the total energy delivered to the water tank with the use of a series installed heat pump with a maximum evaporator inlet temperature of 10 °C. The share describing the useful energy gain is the amount of energy that is collected by the solar collectors and bypasses the heat pump. The share describing the condenser heat is the total energy delivered by the heat pump. Some of this energy is actually delivered by the solar collectors, since the heat pump is installed in series with the collector panels. The heat pump is passive during five months of the year. The short heat pump operating time during these months are due to the low maximum evaporator inlet temperature. The collector outlet temperature is never lower than 10 degrees during these months at times when heat input is needed to the tank. The collector outlet temperature frequently drops below 10 °C during the winter months. This makes the collector outlet fluid enter the heat pump instead of going directly through the tank heat exchanger, and a share of the total delivered energy to the tank is therefore condenser heat. This happens most frequently during the colder months. A result of this is that the amount of auxiliary energy is bigger during the summer months compared to the coldest winter months where there is a substantial contribution from the heat pump. This could indicate that the regulatory strategy is not optimal.
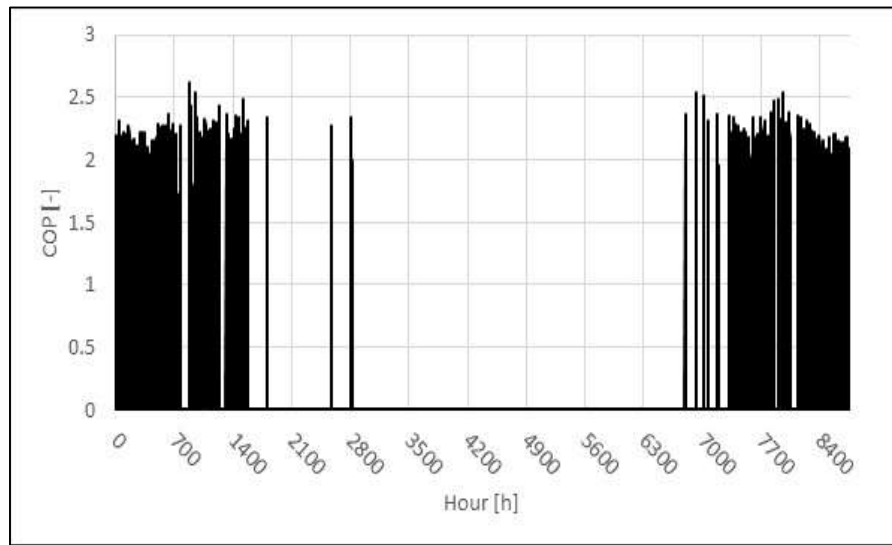
Figure 8-2 Annual heat pump COP with a maximum evaporator inlet temperature of 10°C

The annual average COP of the heat pump is 2.0. The COP is zero the months when the heat pump is not operational as seen in Figure 8-2. The rest of the year the COP fluctuates between 0 and 2.6. The higher COPs are obtained during the nigh time, which is when the collector outlet temperature drops below 10 °C. During some of the winter days the heat pump is not operational, and the COP will be 0. These fluctuations is what causes the coherent black areas in the Figure 8-2. When looking at a time span shorter than 8760 h, the COP visibly fluctuates between 0 and 2.6 throughout the day. Theoretically is it possible to obtain a COP far higher than 2.6 for solar assisted heat pumps. This depend on the heat pump characteristics.

Useful energy gain (kWh/m²)	Condenser heat (kWh/m²)	Auxiliary energy (kWh/m²)	Compressor energy (kWh/m²)	Circulation pump operating time (h)	Average COP
16.09	10.39	19.59	6.34	4035.67	2.0

Table 8-1 Annual energy budget with a maximum evaporator inlet temperature of 10°C

Compared to the base case, the annual useful energy gain with the use of the solar assisted heat pump is reduced by 12 % while the annual auxiliary energy decreases by 40 %. The heat pump introduces 6.34 kWh/m² floor area in compressor energy. Totally will the use of the heat pump with a 10 °C maximum evaporator inlet temperature give an annual energy saving

of 7.1 kWh/m^2 floor area, which constitutes to a 22 % energy reduction to DHW compared to the base case.

Positive transmission (kWh/m^2)	Negative transmission (kWh/m^2)
5.24	-13.76

Table 8-2 Annual transmission with a maximum evaporator inlet temperature of 10°C

Table 8-2 shows that there is a small reduction in the positive transmission and a substantial increase in the negative transmission with the use of the series installed heat pump compared to the base case. In the base case, the positive transmission was 5.9 kWh/m^2 while the negative transmission was -7.2 kWh/m^2. When translating increased negative transmission and decreased positive transmission into increased heating need and decreases cooling need, the overall energy saving with the use of this heat pump will be reduced by 0.25 kWh/m^2 floor area when accounting for transmission as well. This will lead to a total annual energy saving compared to the base case of 6.85 kWh/m^2 floor area or 21 %.

 There are a few disadvantages with the chosen system design. By regulating the operation of the circulation pump from the water tank temperature and not the water tank temperature in relation to the solar collector outlet temperature, one risk running the system also when the collector inlet water temperature is higher than the collector outlet temperature. This can especially happen during the winter months, meaning that this will rarely happen when the water bypasses the heat pump. When this happens during times when the water goes through the heat pump, the problem is only moderate. Even for low water temperatures, the COP of the heat pump is high enough to make the use of the heat pump profitable compared to auxiliary electric heating. This means that it is better to keep this regulatory strategy compared to turning the system off when this happens.

In the investigated case, this problem is small, but a few hours during the year, the fluid going through the heat exchanger is colder than the tank bottom temperature. This leads to the working fluid stealing about 0.6 kWh/m^2 annually. The entire aspect could be avoided by introducing a different regulatory strategy that detects when heat input is needed to the tank, and only lets fluid through the collectors when there is a temperature rise through them. When the radiation is too low, the water is sent through yet another bypass that diverts the water around the collectors, and straight to the heat pump. This will complicate the system further.

Another option is to install a dual source heat pump that uses ambient air as its heat source when there is not a temperature rise through the collectors.

8.1.2 Maximum evaporator inlet temperature of 15 °C

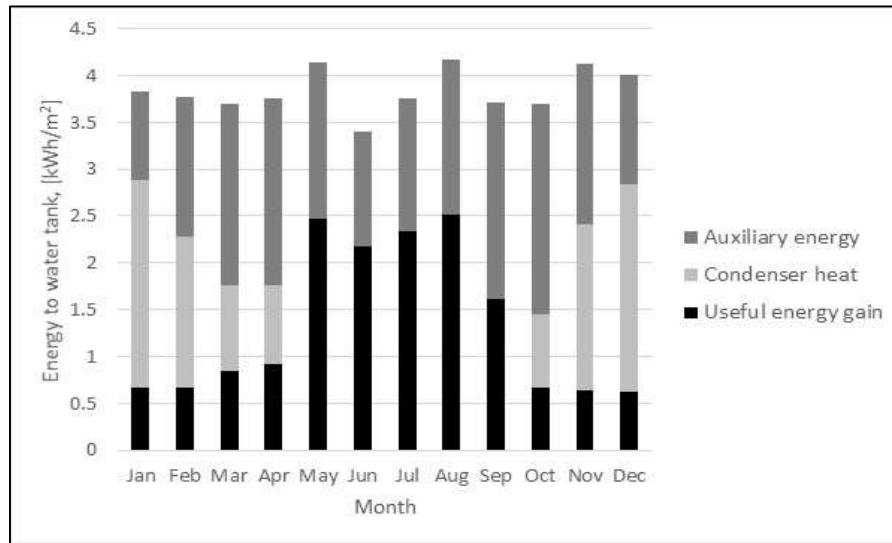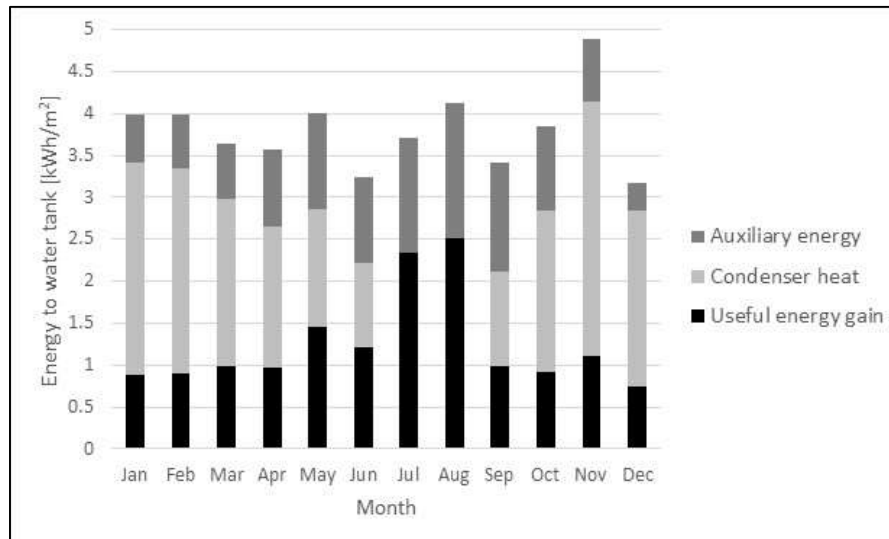*Figure 8-3 Monthly energy to water tank with a maximum evaporator inlet temperature of 15°C*

Figure 8-3 shows the energy delivered to the water tank with the use of a heat pump with a maximum evaporator inlet temperature of 15 °C. During July and August, the heat pump is not used, while the solar collectors and the auxiliary heater is operational. This means that the collector outlet temperature is never below 15 degrees these months. When increasing the maximum evaporator inlet temperature by 5 degrees, this gives that heat pump a 5 degrees bigger interval to operate. This leads to a longer system operating time compared to a maximum evaporator inlet temperature of 10 °C. Since the auxiliary heater is operational all months, it means that the solar collectors and the heat pump alone is not sufficient to cover the load. The useful energy gain during the winter months are smaller than for the base case, see Figure 7-10. This means that the heat pump system reheats water exiting the solar collector at times where the results from the base case system show that there is a potential of heat output from the solar collectors alone.
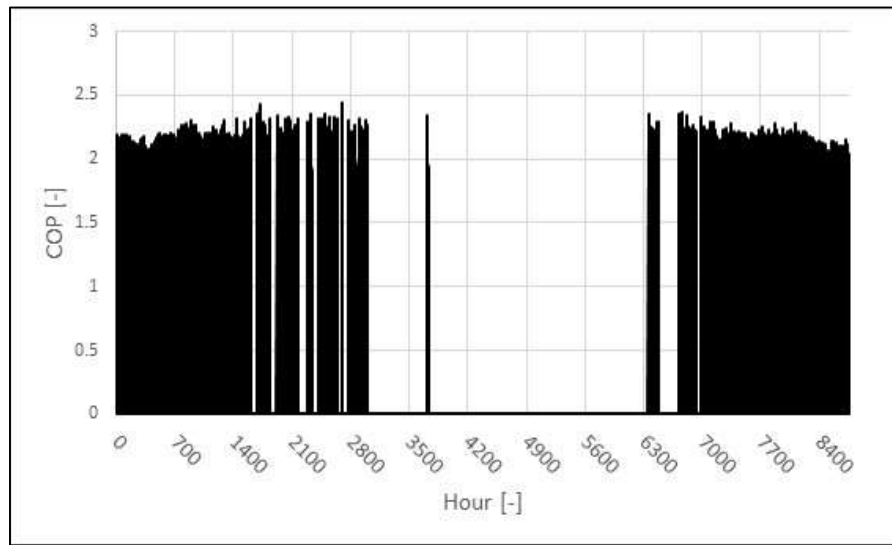
Figure 8-4 Annual heat pump COP with a maximum evaporator inlet temperature of 15°C

The COP of the heat pump fluctuates between 0 and 2-2.5 as the heat pump is turned on and off, see Figure 8-4. The COP is 0 during the summer months when the heat pump is passive and the average annual COP is also here 2.0.

Useful energy gain (kWh/m²)	Condenser heat (kWh/m²)	Auxiliary energy (kWh/m²)	Compressor energy (kWh/m²)	Circulation pump operating time (h)	Average COP
12.88	22.21	11.34	11.42	3222.19	2.0

Table 8-3 Annual energy budget with a maximum evaporator inlet temperature of 15°C

Compared to the base case, the useful energy gain is reduced by 27 % while the auxiliary energy to the electric heater is reduced by 65 % with the use of a heat pump with a maximum evaporator inlet temperature of 15 °C. At the same time is the energy used for the heat pump compressor 11.4 kWh/m² floor area. This means that the total auxiliary energy savings from using the heat pump is 10.25 kWh/m² floor area, which constitutes to a total annual energy saving of 31 % compared to the base case.

During the summer, the useful energy gain is higher with a 10 °C maximum evaporator inlet temperature, while the 15 °C maximum evaporator inlet temperature leads to the highest useful energy gain during the winter. The total annual useful energy gain and the circulation pump operating time is highest for the lower evaporator inlet temperature. Despite of this, the

total annual energy saving is higher for the 15 °C maximum evaporator inlet temperature. This means that the balance between the reduced electric auxiliary energy and the increased compressor energy is more favourable when the evaporator temperature is 15 °C compared to 10 °C.

Positive transmission (kWh/m²)	Negative transmission (kWh/m²)
5.09	-18.56

Table 8-4 Annual transmission with a maximum evaporator inlet temperature of 15°C

Compared to the 10 °C maximum evaporator inlet temperature and the base case, the positive transmission keeps decreasing while the negative transmission keeps increasing. When accounting for the transmission the total annual energy saving decreases by 0.44 kWh/m² when the transmission is included. This gives a total annual energy saving of 9.8 kWh/m² floor area, or 29.6 % compared to the base case.

8.1.3   Maximum evaporator inlet temperature of 20 ° C

Figure 8-5 Monthly energy to water tank with a maximum evaporator inlet temperature of 20°C

As the maximum evaporator inlet temperature is raised to 20 °C, the heat pump is operational throughout the entire year. This means that the collector outlet temperature drops below 20 degrees also during all of the summer months. The useful energy gain is lower than for the base case all months since the heat pump replaces the solar collectors at certain times during every month. The useful energy gain during the winter months are approximately the same for

a maximum evaporator inlet temperature of 15°C and 20 °C, This means that the heat pump collects about the same amount of energy, even though the temperature interval acceptable for the heat pump is increased with 5 degrees. In practice, this means that at times when the collector outlet temperature is below 20 degrees, it is actually also below 15 degrees. There is a contribution from the electric auxiliary heater also during the summer months. Figure 8-3 shows that the solar collectors has the potential of delivering more energy during these months. This will reduce the contribution from the heat pump, but there may exist a regulatory strategy that makes the system rum on only the solar collectors and the heat pump during these months. Finding the optimal strategy requires thorough investigations, since it will influence the situation for the rest of the months as well.
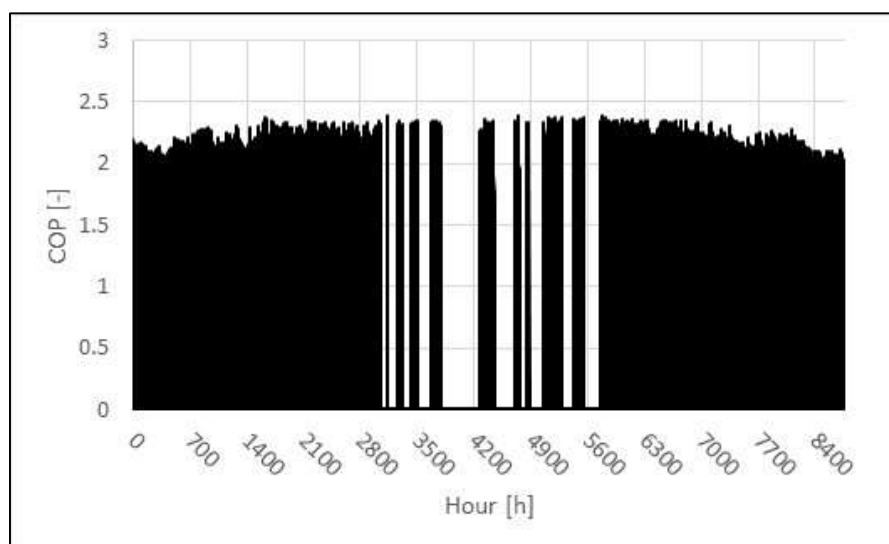
Figure 8-6 Annual heat pump COP with a maximum evaporator inlet temperature of 20°C

Also now the average COP is equal to the other cases. During the summer months, there are periods where the COP is zero, but this does not happen for an entire month coherently. This effect leads to the smaller monthly heat pump contributions for the summer months seen in Figure 8-5. This shows that the reduced heat pump contribution to the total energy load during the summer months compared to the remaining months are not induced by lower heat pump COP, but rather shorter heat pump operating times.

Useful energy gain (kWh/m²)	Condenser heat (kWh/m²)	Auxiliary energy (kWh/m²)	Compressor energy (kWh/m²)	Circulation pump operating time (h)	Average COP
12.58	26.36	7.76	16.74	2504.69	2.0

Table 8-5 Annual energy budget with a maximum evaporator inlet temperature of 20°C

The total useful energy gain decreases further as the maximum evaporator temperature increases from 15 °C to 20 °C, while the condenser heat increases. Compared to the base case the useful energy gain is reduced by 34 %. At the same time is the auxiliary energy reduced by 75 %, while 16.7 kWh/m² compressor energy is introduced. This leads to a total energy saving of 8.6 kWh/m², which constitutes to 26 % compared to the base case.

Positive transmission (kWh/m²)	Negative transmission (kWh/m²)
4.18	-19.22

Table 8-6 Annual transmission with a maximum evaporator inlet temperature of 20°C

Also now, the positive transmission decreases while the negative transmission increases further. When accounting for the transmission in the total annual energy saving it is reduced by 0.43 kWh/m² floor area annually. This gives a total energy saving of 8.17 kWh/m² floor area annually or 24.7 % compared to the base case.

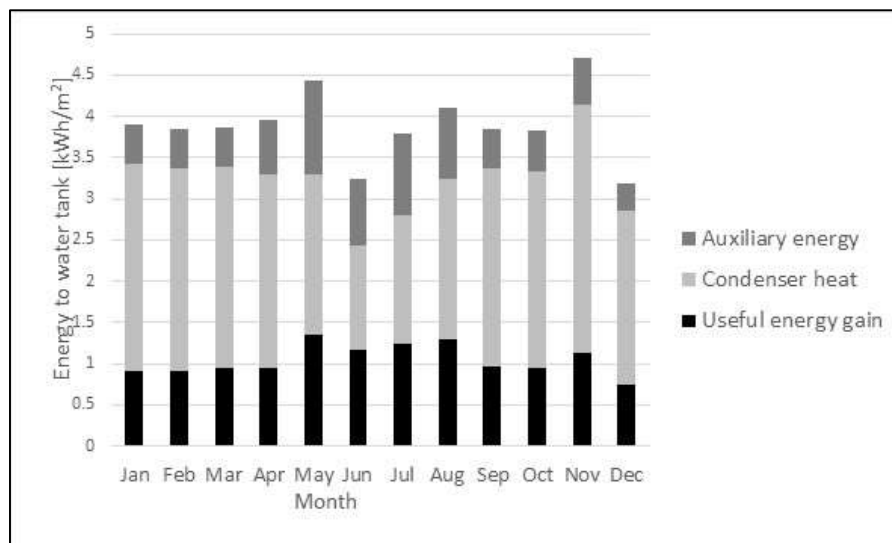### 8.1.4 Maximum evaporator inlet temperature of 25 °C
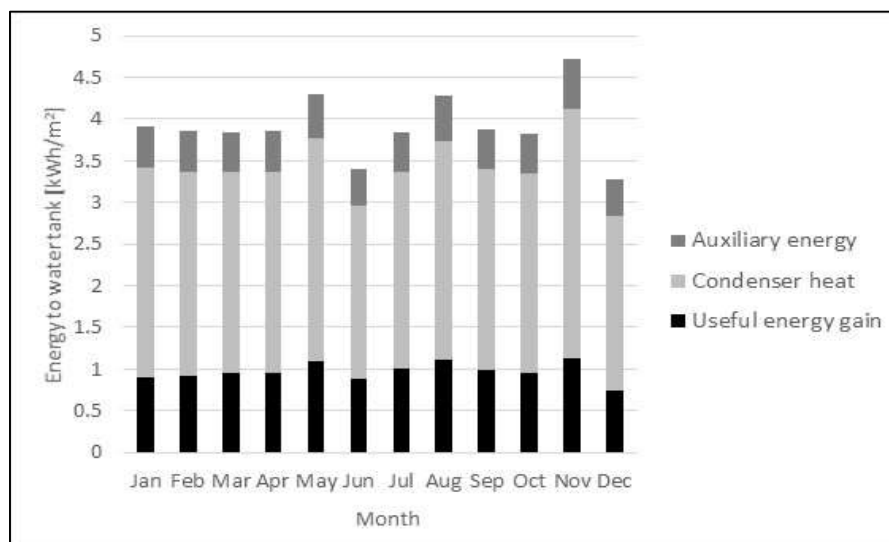
Figure 8-7 Monthly energy to water tank with a maximum evaporator inlet temperature of 25°C

As the maximum evaporator temperature is increased to 25 °C there is a substantial contribution from the heat pump throughout the year and monthly useful energy gain is almost constant. This means that the base case system collects a substantial its solar energy when the collector outlet temperature is below 25°C. See Figure 7-14 and Figure 7-10. Also now, there is an auxiliary contribution during the summer months. This contribution is even smaller than with a 20 °C maximum evaporator inlet temperature.
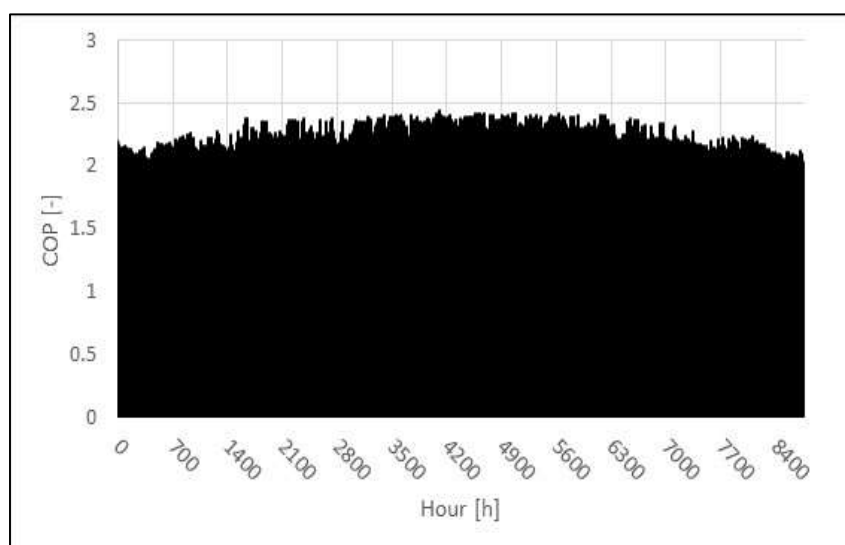
Figure 8-8 Annual heat pump COP with a maximum evaporator inlet temperature of 25°C

For the highest tested maximum evaporator inlet temperature the COP fluctuates rapidly between 0 and 2-2.5 throughout the entire year, see Figure 8-8. There are no longer stagnation periods where the heat pump is coherently passive. This leads to the most constant monthly heat pump contribution for all of the tested cases.

Useful energy gain (kWh/m²)	Condenser heat (kWh/m²)	Auxiliary energy (kWh/m²)	Compressor energy (kWh/m²)	Circulation pump operating time (h)	Average COP
11.65	29.42	5.91	20.58	1992.19	2.0

Table 8-7 Annual energy budget with a maximum evaporator inlet temperature of 25°C

Compared to the 20 °C maximum evaporator inlet temperature case, the increase in the condenser heat is bigger than the decrease in the useful energy gain. This means that this situation leads to stagnation periods when the tank is fully charged. Compared to the base

case, the useful energy gain is reduced by 36 %. The auxiliary energy is reduced by 82 % while there is a compressor energy consumption of 21 kWh/m² floor area. This leads to a total energy saving of 6 kWh/m², which constitutes to 18 % compared to the base case. This is substantially lower than for the 20 °C maximum evaporator inlet temperature, despite of the fact that the electrical auxiliary energy contribution is heavily reduced. This means that the balance between the lower useful energy gain and the increased compressor power is unfavourable.

Positive transmission (kWh/m²)	Negative transmission (kWh/m²)
1.26	-21.21

Table 8-8 Annual transmission with a maximum evaporator inlet temperature of 25°C

The positive transmission keeps decreasing and the negative transmission keeps increasing further as the maximum evaporator inlet temperature increases. When accounting for the transmission, the total annual energy saving is reduced by 0.39 kWh/m². This gives a total annual energy saving compared to the base case of 5.61 kWh/m² or 17 % compared to the base case.

9 Conclusion

The use of façade integrated solar collectors influence the thermal performance of the wall the collectors are installed in. The magnitude of this influence depends on the materials used in the wall and the meteorological environment. During a day in January in the Norwegian climate, the negative transmission is lower through solar walls compared to conventional walls. This applies both when the solar collectors are integrated in a lightweight wall consisting of 0.25 m insulation, and in a heavier wall with 0.2 m insulation and 0.2 m concrete. For a sunny and cloudy January day in Norway, the lightweight solar wall shows a reduced negative transmission of 81 % and 61 % respectively compared to the conventional lightweight wall. The heavy wall show a reduced transmission of 86 % and 66 % for the same days compared to the conventional heavy wall. For a sunny July day, the conventional walls show a positive transmission that is 86 % and 91 % lower than through the lightweight and heavy solar wall respectively. This may lead to overheating the building. If the system circulation pumps are turned off the entire day, the positive transmission will further increase. The insulation thickness at the base of the lightweigh solar wall can be reduced from 0.25 m to 0.15, and the solar wall will still perform better that the conventional lightweight wall. For the heavy solar wall, the insulation thickness can be reduced from 0.2 m to 0.05 m. This means that the energy saving during the winter day exceeds the potential increased cooling load the summer day even for smaller solar wall insulation thicknesses.

By installing 6.68 m^2 integrated solar collectors in the heavy wall on the south façade of a building in Oslo, the negative transmission is reduced by 38 kWh/m^2 through the area with the collectors. This equals a total annual energy saving for heating the building of 2.4 %. An annual positive transmission contribution of 5.9 kWh/m^2 is introduced as well. It is assumed that it can be removed through more solar shading, free cooling or opening windows. The collector system is designed according to recommendations from literature describing the optimal design of solar thermal systems. Efficiency measures on the collector system shows that lowering the flow rate from 72 kg/hm^2 to 54 kg/hm^2 leads to the biggest energy savings related to transmission throughout the year. This measure alone reduces the energy related to transmission with approximately 1.5 kWh/m^2 annually, compared to the initial system. When looking at the system performance, the most effective efficiency measure is changing the

regulatory strategy to increase the annual operating time of the solar collectors. This measure leads to an energy saving of 1.05 kWh/m^2 floor area annually compared to the initial system. This is also the measure that leads to the biggest total annual energy saving when accounting for both the transmission and the system performance. This regulatory strategy will lead to decreased transmission loads as well, giving a total annual energy saving of 1.08 kWh/m^2 floor area compared to the initial system. This indicates that special considerations must be made in the design of façade integrated solar collector systems, since they behave differently than conventional solar collector systems installed under the optimal slope and will require a different design to perform optimally..

Installing a heat pump in series with the solar collector panels introduces a potential of further improving the system performance. Changing the maximum evaporator inlet temperature influences the distribution of the energy supplied to the water tank from the collar collectors alone, the heat pump and the auxiliary heater in the tank. A maximum evaporator temperature of 15 °C showed the highest system performance. For this case, the energy amount collected by the solar panels alone was reduced by 27 %, while the auxiliary energy to the electric heater was reduced by 65 % compared to the same system without the heat pump. This lead to a total energy saving of 31 %. If transmission is accounted for as well, the total annual energy saving decreases marginally. With the use of the heat pump, the annual negative transmission increases by 11.36 kWh/m^2 while the positive transmission decreases by 0.81 kWh/m^2. This will consequently not lead to a bigger problem with overheating, but it reduces the total annually energy saving to 30 % compared to a collector system without a series installed heat pump.

10 Further work

Further studies on the field of façade integrated solar collectors should continue developing a total optimal system design, that overall maximises the system performance. This study has looked at the effect of single efficiency measures, while future studies should look at the implementation of several of these efficiency measures together, and find how to optimally combine them. This should give knowledge on the sensitivity of façade integrated solar systems, and which parameters that can be changed without influencing the system performance in a negative way. This will further contribute to the development of rules of thumb for the design of façade integrated solar collectors similar to those that exist for conventional externally mounted collectors under optimal slope. This work should include the aspect of economy, especially for efficiency measures that require new components. The optimal solar collector area should be a part of these investigations.

In view of solar assisted heat pumps, future investigations should look at both series installed heat pumps and parallel heat pumps. Indications from this study show that it is difficult to find an optimal regulatory strategy for series connected heat pumps. This should be further investigated by installing bypasses that prevents the system from running when there is not a temperature rise over the collectors. It could also be interesting to look at a system with a series installed dual source hear pump. This will require an even more complicated regulatory strategy, but could lead to enhanced system performance. The performance of the series installed heat pump system should be compared to the performance of a system with a parallel installed heat pump.

11 References

1.   Lavenergiprogrammet, *Prosjektering av passivhus.* 2013. 3rd.

2.   Li, R., Y.J. Dai, and R.Z. Wang, *Experimental and theoretical analysis on thermal performance of solar thermal curtain wall in building envelope.* Energy and Buildings, 2015. 87: p. 324-334.

3.   *Fornybar. Solenergiressurser i Norge*. 2007 [ONLINE] ; Available from: http://www.fornybar.no/solenergi/ressursgrunnlag#sol1.1.Accessed: 15.03.2015

4.   John A. Duffie, W.A.B., *Solar Engineering of Thermal Processes, 4th Edition*. 2013, Hoboken, New Jersey: John Wiley & Sons inc.

5.   *Pavlov,G.K., Oelsen,B.J., Seasonal ground solar thermal energy storag- review of systems and applications. ICIEE*

6.   *Haller, M.Y, Frank, E. On the potential of using heat from solar thermal collectors for heat pump evaporators, 2011. ISES Solar World Congress in Germany 2011*

7.   Banister, C.J., W.R. Wagar, and M.R. Collins, *Validation of a Single Tank, Multi-mode Solar-assisted Heat Pump TRNSYS Model.* Energy Procedia, 2014. 48: p. 499-504.

8.   Carbonell, D., et al., *Simulations of Combined Solar Thermal and Heat Pump Systems for Domestic Hot Water and Space Heating.* Energy Procedia, 2014. 48: p. 524-534.

9.   International Energy Agency, Solar Heating and Cooling Programme, *Country Report Norway,* 2014 [ONLINE] Available at: http://www.iea-shc.org/country-report-norway. Accessed: 07.07.2015

10.   International Energy Agency, Solar Heating and Cooling Programme, *Solar Heat Worldwde,* 2014 [ONLINE]. Available at: http://www.iea-shc.org/solar-heat-worldwide. Accessed 08.07.2015

11.   SINTEF Byggforsk, KanEnergi., *Mulighetsstudie:Ssolenergi i Norge.* 2011.

12.   Enova, *Tilskudd for solfangeranlegg* [ONLINE]. Available at: http://www.enova.no/finansiering/privat/enovatilskuddet-/solfanger/911/0/. Accessed 18.03.1015

13.   Florida Solar Energy Center,*For homes* [ONLINE] ; Available at: http://www.fsec.ucf.edu/en/consumer/solar_hot_water/homes/q_and_a/. Accessed 12.06.2015

14.   Basnet, A., *Master's Thesis in Sustainable Architecture; Architectural Integration of Photovoltaic and Solar Thermal Collector Systems into buildings.* 2012 Norwegian University of Science and Technology.

15. Flexiheat solfangere [ONLINE]. Available at: http://www.solvarming.no/Produkter/page15/page15.html, Accessed 01.04.2015

16. SolarTeknik, *Solar Tekniks solfangere er Effektive Året Rundt* [ONLINE]. Available at: http://no.solar-teknik.com/, Accessed 01.04.2015

17. Proctor.D, Czarnecki.J.T, *The effect of aging on a 22 year old solar water heater, 1985. Solar Energy vol.35. No 2. pp 175-180. Pergamont Press ltd.*

18. Fan.J, Chen.Z, Furbo.S, Perers.B, Karlsson.B., *Efficiency and lifetime of solar collectors for solar heating plants. Technical University of Denmark. Department of Civil Engineering.*

19. Kommunal og moderniseringsdepartementet, *Forskrift om tekniske krav til byggverk (Byggteknisk forskrift)*, 2010.

20. Theodore L. Bergman, F.P.I., *Fundamentals of Heat and Mass Transfer*. Vol. 7th. 2007: Wiley and Sons inc. New Jersey..

21. Whillier,A., S.G., *Effect of Material and Construc- tion Details on the Thermal Performance of Solar Water Heaters,* 1965. Solar Energy. Vol 1 pp 21-26. Elsevier

22. Probst, M.M.K., V.; Schueler, A.; de Chambrier,E.; Roecker, C., *Facade Integration of Solar Thermal Collectors: Present and Future*. Ecole Polytechnique Federale de Lausanne Lausanne, Switzerland.

23. Matuska, T. and B. Sourek, *Façade solar collectors.* Solar Energy, 2006. 80(11): p. 1443-1452.

24. E.M Sparrow, S.C.L., *Effect of adiabatic co-planar extension surfaces on wind related solar collector heat transfer coefficients.* ASME-Journal of Heat Transfer, 1981(103, 1981 Transactions): p. 268-271.

25. Stadler, I., *Facade integrated solar thermal collectors.* AEE- Arbeitsgemeinschaft Erneubare Energie: Gleisdorf, Austria.

26. Heywood, H., *Operating experience with solar heating.* JIHVE, 1971: p. 39(6):61–9.

27. Lunde, P.J., *Solar Thermal Engineering* 1st edition. 1980, New York, NY, USA: Wiley.

28. Chinnery,DNW., *Solar heating in South Africa.* CSIR-Research Report 248, 1981.

29. Löf, G.O.G, Tybout,R.A., *Cost of House Heating with Solar Energy.* Solar Energy, 1973. 14.

30. Garg, H.P., *Treatise on Solar Energy: Fundamentals of solar energy*. 1982 J. Wiley and sons, New York.

31. Tang, R. and T. Wu, *Optimal tilt-angles for solar collectors used in China.* Applied Energy, 2004. 79(3): p. 239-248.

32. Zijdemans, D., *Vannbaserte oppvarmings- og kjølesystemer*, 2014: Skarland Press AS.

33. *Barley,D., Winn,C.B., Optimal sizing of solar collectors by the method og relative areas, 1978. Solar Energy Vol.21. pp 279-289. Pergamont Press Ltd.*

34.   *Hausner.R, Fink.C, Stagnation behaviour of solar thermal systems, 2002. A Report of IEA SHC-Task 26. Arbeitsgemeinschaft Erneuerbare Energie, Austria*

35.   S.Harrison, C.A.C., *A review of strategies for the control of high temperature stagnation in solar collectors and systems.* 2012. SHC 2012. Energy Procedia 30 (2012) pp 793-804

36.   U.S. Department of Energy, *Heat Transfer Fluids for Solar Water Heaters* [ONLINE]. Available : http://energy.gov/energysaver/articles/heat-transfer-fluids-solar-water-heating-systems. Accessed 25.05.2015

37.   Hillerns, F., *The behaviour of heat transfer media in solar active thermal systes in view of the stagnation conditions*. 1999, IEA-SHC Task 26 Industy Workshop Borlange.

38.   Swep, *Solar heating* [ONLINE]. Available at: http://www.swep.net/Documents/BPHE%20technology/Solar_heating.pdf. Accessed 07.03.2015

39.   Engineering Toolbox, *Propylene Glycol based Heat-Transfer Fluids*. [ONLINE]. Available at: http://www.engineeringtoolbox.com/propylene-glycol-d_363.html. Accessed: 27.06.2015

40.   IEA Solar Heating and Cooling Programme, Annual report. *Feature article on Solar and Heat Pump Systems, 2014.*

41.   Apricus Solar Hot Water, *Solar hot water basics* [ONLINE]. Available at: http://www.apricus.com/html/solar_hot_water_basics.htm#.VQ-8e46UfT8). Accessed 10.03.2015

42.   Zelzouli, K., *Solar Thermal Systems Performances versus Flat Plate Solar Collectors Connected in Series.* Engineering, 2012. 04(12): p. 881-893.

43.   Furbo, S.S., LJ,. *Optimum solar collector fluid flow rates.* DTU Orbit, 1996. EuroSun´96. 10. Internationales Sonnenforu. Proceedings. DGS Sonnenenergie Verlags, MÜNCHEN: p. 189-193.

44.   Bakke, J.V., *Lecture notes from the course TEP14,* 2014. The Norwegian Uniersity of Science and Technology

45.   Andersen.I, *Planlegging av solvarmeanlegg for lavenergiboliger og passivhus. En introduksjon, 2008. SINTEF Byggforsk Prosjektrapport 22*

46.   Amerongen. G, Lee.J.V, Suter. JM,   *Report- Legionella and solar water heaters*, 2013

47.   Çomaklı, K., et al., *The relation of collector and storage tank size in solar heating systems.* Energy Conversion and Management, 2012. 63: p. 112-117.

48.   Shariah.A.M, Lôf.G.O.G, *The optimization of tank-volume to collector area for a thermosyphon solar water heater, 1995. Renewable Energy, Vol.7, No.. pp. 289-300. Elsevier Science Ltd. Pergamon.*

49.   Nationen. *Vi bruker 200 liter vann hver dag*. 2003 [ONLINE]; Available at: http://www.nationen.no/tunmedia/vi-bruker-200-liter-vann-hver-dag/. Accessed 03.06.2015

50.   Trier.D, *Solar district heating guidelines, Solar collectors, 2012. Solar District Heating, Fact Sheet 7.1.*

51.   Chen, Z., et al., *Efficiencies of Flat Plate Solar Collectors at Different Flow Rates.* Energy Procedia, 2012. 30: p. 65-72.

52.   Nilsson, G., *Conversation with Gunnar Nilsson from Solhaug AS.* 2015.

53.   Dr. Bens Solar Hot Water Systems, Optimal Design in *Solar Hot Water Systems- How Does Size Alter Performance?* [ONLINE] Available at: http://www.solarhotwater-systems.com/optimal-design-in-solar-hot-water-systems-how-does-size-alter-performance/. Accessed 20.05.2015

54.   Polysun Online, *Polysun simulation tool*. [ONLINE] Available at: http://www.polysunonline.com/PsoPublic/app/home/access.Accessed 24.07.2015

55.   Equa. *IDA Indoor Climate and Energy*. 2013; [ONLINE] Available from: http://www.equa.se/en/ida-ice. Accessed 24.07.2015

56.   *TRNSYS 17, Manual Volume 1 Getting Started*

57.   Matuska, T.M., J. ; Zmrhal, V., *Design tool KOLEKTOR 2.2 for virtual prototyping of solar flat-plate collectors*. Czech Technical University, Faculty of Mecanical Engieering, Department of Environmental Engineering: Prague, Czech Republic.

58.   Gupta, S.K., *Numerical Methods for Engineers 1 st edition.* 1995.New Age Interationsl (P) Limited, Publishers.

59.   W.Swinbank, *Long Wave Radiation From Clear Skies.* Royal Meteorological Society, 1963. 89: p. 339-348.

60.   X.Berger, D.B., F.Garnier, *About the Equivalent Radiative Temperature for Clear Skies.* Solar Energy, 1984. 32: p. 275-733.

61.   *NS 6946, Bygningsmetoder og Elementer- Varmemotstand og Varmegjennomgang Beregningsmetode.* Norsk Standard, 2007.

62.   *TRNSYS 17, Manual Volume 5, The Multizone building*

63.   *TRNSYS 17, Manual Volume 4 , Mathematical reference.*

64.   T.Afjei, M.W., *Compressor heat pump including frost and cycle losses- Model description and implementating into TRNSYS.* 1997.

65.   International Solar Energy Society, *1999 ISES Solar World Congress Proceedings.* 1999.

66.   Dokka.T.H, Wiberg.A.H, Georges.L, Mellegård.S, Time.B, Haase.M, Maltha.M, Lien A.G., A Zero emission consept analysis of a single family house, 2013. ZEB Project report 9-2013. SINTEF Academic Press.

67.   Norsk Standard, *NS 3031:2014 Beregning av bygningers energiytelse - Metode og data.* 2014.

68.   Knight.I,Manning.M, Swinton.M, Ribbernik.H, European and Canadian non-HVAC Electric and DHW Load Profiles for Use in Simulating the Performance of Residential Cogeneration Systems, 2007. IEA/ECBCS Annex 42 Subtask A.

69.   Engineering Toolbox, Pressure loss in copper pipes [ONLINE]. Available at: http://www.engineeringtoolbox.com/pressure-loss-copper-pipes-d_930.html. Accesses 01.06.2015

70.   Engineering Toolbox, *Darcy Weisbach Equation* [ONLINE] Available at: http://www.engineeringtoolbox.com/darcy-weisbach-equation-d_646.html. Accessed.01.06.2015

71.   Engineering Toolbox ,*Colebrook equation* [ONLINE]. Available from: http://www.engineeringtoolbox.com/colebrook-equation-d_1031.html. Accesses 01.06.2015

72.   Engineering Toolbox, *Roughness & Surface Coefficients of Ventilation Ducts* [ONLINE]. Available from: http://www.engineeringtoolbox.com/surface-roughness-ventilation-ducts-d_209.html. Accesses 01.06.2015

Thermal performance of façade integrated solar collector systems used in Norwegian climate

Marte W. Nilsson

ABSTRACT: The use of façade integrated solar collectors activates the building envelope in the collection of thermal energy. This paper looks at the performance of façade integrated solar collectors in the Norwegian climate. The study shows that both heavy and lightweight solar walls leads to lower negative transmission during winter days compared to conventional walls. They also lead to higher positive transmission during summer days. Heavy walls are more suited for collector integration since the positive transmission is limited, and the reduction in the negative transmission is high compared to conventional walls. By comparing the solar wall performance a sunny summer day and a cloudy winter day, a lightweight solar wall can have an insulation thickness of 0.15 m and still perform better than the conventional wall with 0.25 m insulation. A heavy solar wall can have an insulation thickness of 0.05 m and still perform better than the conventional heavy wall with 0.2 m insulation and 0.2 m concrete. The transmission through the wall is sensitive to the collector system parameters. Changing the collector flow rate had the highest effect on the transmission and lead to an energy saving of 1.5 kWhm^{-2} annually. The biggest energy saving related to collector performance was obtained by changing the regulatory strategy of the system. This saved 1.05 kWhm^{-2} floor area annually. The use of a series connected heat pump further improved system performance with a potential energy saving of 30 %.

1 Introduction

As stricter demands are set to the thermal performance of building envelopes through the implementation of passive houses and zero emission buildings, domestic hot water represents a relatively bigger part of the energy consumption of the building. Solar energy can be utilized as a useful energy source almost everywhere on the planet and it is highly suited for domestic hot water purposes in particular. The use of solar thermal energy systems is a wildly used technology especially in central Europe and in Asia. Extensive research have been conducted on the thermal performance of solar collector systems, while only a few studies have looked at the consequences of integrating the collector into the façade of the building. It is evident that the integration of the solar collectors may influence the indoor environment of the building. In addition will the integration influence the performance of the collector, as it set restrictions that impedes optimal installation. R.Li et al. [1] investigated the transmission through a façade integrated solar curtain wall and found that the solar wall contributes to heating the wall and the building during the winter. The cooling load during the summer increased, but the façade integrated solar walls were superior to the conventional walls. Matuska and Sourek [2] found that façade solar collectors should have an area increased by approximately 30 % to achieve a 60 % solar fraction compared to a solar collector installed with an optimal slope. The same study revealed that vertical installation of the solar collectors leads to reduced heat transfer coefficients due to natural convection between the absorber and the cover, wind induced heat transfer and the back and frame heat loss coefficients. The latter is further documented through the research of EM. Sparrow et al. [3] where it is found that the local heat transfer coefficient of a plate exposed to an airflow is bigger around the edges compared to the center. Matuska and Sourek [4] further found that façade solar collectors could achieve comparable solar fractions as roof collectors only for oversized systems in relation to the DHW load. The interior temperature was raised by 2 K with a middleweight envelope construction, but the temperature raise was decreasing with sufficient insulation. T.T Chow et al. [5]show the potential of integrated hybrid solar systems combining integrated solar collectors and photovoltaic panels. The results show increased thermal and electrical efficiencies as well as reduced thermal loads of the building. Even though studies show promising result as to the integration of solar collectors, externally mounted collectors are more used. K. Farkas et al.[6]conducted a survey revealing the reasons why the use of façade collectors is moderate. The aim for the survey was to develop

guidelines and recommendations to accelerate the use of building integrated solar systems.

A façade integrated solar collector wall installed in the solar house in the Green Energy Laboratory in Shanghai is the basis for this work. A thermal model created at Shanghai Jiao Tong University describes the thermal performance of the wall. This model is used to investigate the thermal performance of the wall installed in Norwegian climate through simulations in TRNSYS.

1.1 The solar collector panels

The façade integrated solar curtain wall consist of a conventional wall element where the external weather barrier is replaced with a solar collector. There is no thermal separation between the wall element and the solar collector, meaning that the insulation is a part of both the collector and the wall. This innovative configuration does not only activate the building envelope in the utilization of renewable energy, but it also simplifies the implementation of solar energy in buildings of today. The solar collectors can be used to collect energy for space heating, absorption cooling and domestic hot water. This makes the use of façade integrated solar collectors especially interesting in high-rise buildings with high thermal demands. Here the roof areas are small compared to the wall areas, and façade integrating the collectors will solve the problem with space for the equipment, and makes it easier to introduce solar collectors in an aesthetical acceptable way. At the same time will the solar collectors influence the thermal performance of the wall element. Designed correctly, it introduces the potential of increasing the amount of passive heat to the building. This will reduce the heating demand of the building especially during the winter months. These aspects mean that there are several advantages with integrating the collectors into the wall. However, it is important to realize that the integration also may lead to an increased cooling need during the summer. At the same will the integration inhibit the installation of the collectors. The collector performance are influenced by the tilt angle of the collector panel and the vertical installation will lead to decreased collector performance compared to the optimal slope. This means that thorough investigations are necessary to design a system that will reduce the energy consumption throughout the year. The following investigations are based on a solar wall installed on the south façade on a building in Oslo, Norway. The wall consist of four modules of flat plate collectors installed in parallel. The structural parameters of each of the collector panels are given in Table 1 and Table 3.

Collector with (m)	0.885
Collector length (m)	1.905
Collector area (m)	1.69
Glass cover thickness (m)	0.003
Air gap depth (m)	0.018
Absorber plate thickness (m)	0.003
Tube outside diameter (m)	0.010
Tube inside diameter (m)	0.009
Tube length (m)	1.795
Tube separation (m)	0.115

TABLE 1 Collector structural parameters

1.2 System

The solar collectors are connected to a heat distribution system as seen in Figure 1. The circulation pump is controlled according to the temperature difference between the bottom of the water tank and the outlet of the solar collector. The pump is turned on when the temperature difference exceeds eight degrees and off for a difference lower than five degrees. The total solar collector area is 6.68 m^2, and the installed storage tank is a stratified water tank with a volume of 450 l. Immersed in the tank is an auxiliary electric heater. The tank parameters are given in Table 2.

Tank volume	0.450
Tank height	1.4
Tank diameter	0.64
Heat exchanger inlet height	0.78
Heat exchanger outlet height	0.166
Auxiliary heater height	1.08
Thermostat height	1.01

TABLE 2 Tank parameters

1.3 Performance indicators

The dynamic model describing the thermal performance of the façade integrated solar collectors and the wall they are installed in is created at Shanghai Jiao Tong University [1]. The performance of the system are evaluated through the following performance indicators.

1.3.1 Useful energy gain

The useful energy gain of the collector is the amount of energy that is transferred from the collector panel to the water in the pipes. This is found through an energy balance between the transformation of incident solar energy to useful energy in
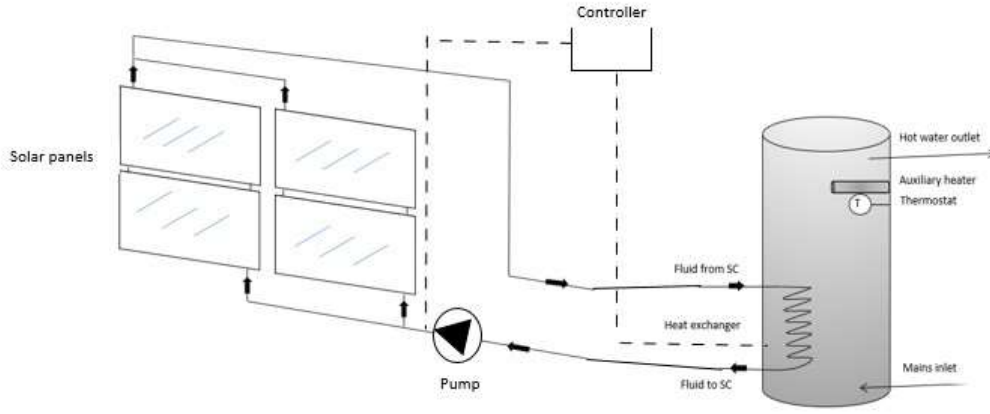
FIGURE 1 Collector system

Material	Density (kg/m³)	Thermal capacity (J/kg·k)	Thermal Conductivity (W/m·K)	Absorptivity (-)	Emissivity (-)
Glass cover	2600	790	1.1	0.01	0.84
Absorb plate	2700	880	237	0.95	0.18
Tube	8900	390	401	—	—
Insulation	37	1670	0.025	—	0.9

TABLE 3 Properties of solar collector module

the collector system and the thermal and optical losses, see Eq.1.

$$q_u = A_c \left(S - U_L(T_{pm} - T_a) \right)$$
$$= WF'(S - U_L(T_f - T_a)) \qquad (1)$$

A_C is the collector area, S is solar radiation, U_L is the overall all heat transfer coefficient, T_{pm}, and T_a is the mean absorber plate temperature and the ambient temperature respectively. W is the fin length, F' is the collector efficiency factor, S is the absorbed solar energy and U_L is the collector heat loss coefficient. T_f is the fluid temperature and T_a is the ambient air temperature. The second relation is used in the dynamic model since the mean absorber temperature is hard to evaluate. The following equations rewrite Eq.1 [7].

The energy balance of the fluid flowing a length Δy in the pipe is

$$\left(\frac{\dot{m}}{n}\right) C_p T_{f|y} - \left(\frac{\dot{m}}{n}\right) C_p T_{f|y+\Delta y} + \Delta y q_u' = 0 \qquad (2)$$

Dividing by Δy and finding the limit as Δy approaches zero gives Eq. 3, where n is the number of tubes.

$$\dot{m}C_p \frac{dT_f}{dy} - nWF'(S - U_L(T_f - T_a)) = 0 \qquad (3)$$

By assuming that U_L is a linear function of T_f-T_a Eq.4 is developed, which gives the outlet temperature of the fluid. U_{fo} and U_{fi} is the outlet and inlet fluid temperature.

$$\frac{T_{fo} - T_a - {}^S/_{U_L}}{T_{fi} - T_a - {}^S/_{U_L}} = \exp(-\frac{U_L A_c F'}{\dot{m}C_p}) \qquad (4)$$

From this, Eq. 1 can be rewritten to Eq. 5.

$$q_u' = WF'(S - \frac{U_L(T_{fi}+T_{fo})}{2} + \left(h_{r,p-ins} + h_{c,p-ins}\right)T_{ins} + \left(h_{r,p-c} + h_{c,p-c}\right)T_c) \qquad (5)$$

h are the heat transfer coefficients and the subscripts r and c before the comma stands for convection and radiation while p, ins, and c after the comma stands for plate, insulation and cover.

1.3.2 Transmission

The integrated solar collectors influence the indoor environment through positive and negative transmission. The transmission is calculated from the temperature difference between the inner surface temperature of the wall and the room temperature

as seen in Eq.6.

$$q_i = h_w(t_{w-i} - t_i) \qquad (6)$$

h_w is the total heat transfer coefficient between the wall and the indoor air, t_{w-i} is the inner wall temperature and t_i is the indoor air temperature.

1.4 Energy balances

The dynamic model consist of energy balances for each layer of the solar collector. The temperature of each layer is found through these balances, which are solved through the finite difference method. The temperatures are used find the collector and wall performance through the useful energy gain and the transmission loads.

1.4.1 Glass cover

The energy balance of the glass cover is given in Eq. 7

$$\delta_c C_c \frac{dt_c}{d\tau} = I(\alpha_c) - (h_{c,c-a} + h_{r,c-a})(t_a - t_c) -$$
$$(h_{c,c-p} + h_{r,c-p})(t_p - t_c) \qquad (7)$$

δ_c, ρ_c, C_c and α_c are the thickness, the density, the specific heat and the absorbance of the glass cover, respectively. I is the total solar radiation on the collector. t_c, t_a and t_p are the cover temperature, the ambient temperature and the absorber plate temperature, respectively. $h_{c,c-a}$ and $h_{r,c-a}$ are convection heat transfer coefficient and radiation heat transfer coefficient between the cover and the air. $h_{c,c-p}$ and $h_{r,c-p}$ are convection heat transfer coefficient and radiation heat transfer coefficient between the cover and the plate.

1.4.2 Absorber plate
The energy balance of the absorber plate is given in Eq. 8.

$$\rho_p \delta_p C_p \frac{dt_p}{d\tau} = I(\tau_c \alpha_c) - (h_{c,p-c} +$$
$$h_{r,p-c})(t_p - t_c) - (h_{c,p-ins} + h_{r,p-ins})(t_p - t_{ins}) +$$
$$\delta_p \lambda_p \frac{d^2 t_p}{dz^2} \qquad (8)$$

Boundary conditions necessary to solve this second order differential equation are given by the symmetry at the centerline between two pipes, and the energy balance at the base, see Eq. 9-10.

$$\frac{dt_p}{dz}\Big|_{z=0} = 0 \qquad (9)$$

$$\frac{dt_p}{dz}\Big|_{z=\frac{W_0 - D_0}{2}} = h_{p-f}(t_f - t_p) \qquad (10)$$

τ is the transmittance of the cover. t_{ins} is the insulation layer temperature. $h_{c,p-ins}$ and $h_{r,p-ins}$ are convection heat transfer coefficient and radiation heat transfer coefficient between the plate and insulation. The subsctipt p stands for plate. W_0 is the distance between the tubes, D_0 is the internal diameter of the tubes and t_f is the fluid temperature. h_{p-f} is the heat transfer coefficient between the plate and the tube. The temperature gradient in the z- direction describes the temperature profile between the pipes.

1.4.3 Insulation
The energy balance of the insulation is given in Eq.11.

$$\frac{\partial t_{ins}}{\partial \tau} = \frac{\lambda_{ins}}{\rho_{ins} C_{ins}} \frac{\partial^2 t_{ins}}{\partial x^2} \qquad (11)$$

The boundary conditions necessary to solve this equation are the energy balance on the outside and inside of the insulation layer, see Eq. 12-13.

$$-\lambda_{ins}(\frac{\partial t_{ins}}{\partial x})_{x=0} = (h_{c,col-i} + h_{r,col-i})$$
$$(t_{ins} - t_i) \qquad (12)$$
$$-\lambda_{ins}(\frac{\partial t_{ins}}{\partial x})_{x=delta} = (h_{c,p-i} + h_{r,p-i})$$
$$(t_{ins} - t_p) \qquad (13)$$

t_{ins} and t_i are the insulation temperature and the room temperature, respectively. $h_{c,col-i}$ and $h_{r,col-i}$ are convection heat transfer coefficient and radiation heat transfer coefficient between the collector and the room, respectively.

1.4.4 Fin efficiency

The sheet material in the absorber is a good conductor. It is thus assumed that the temperature drop trough the plate is negligible. This assumption allows for treating the regions between the tubes as common fins that can be solved as a normal fin problem illustrated in Eq.14

$$S\Delta z - U_L \Delta z(T - T_a) + \left(-k\delta \frac{dT}{dz}\right)_z -$$
$$\left(-k\delta \frac{dT}{dz}\right)_{z+\Delta z} = 0 \qquad (14)$$

Through discretization by the finite difference method, this equation creates an expression for the

value Ta-S/U_L used to find the fluid outlet temperature and later the useful energy gain of the collector.

1.4.5 Energy balance through flow direction of tubes

The pump is switched on according to how the regulation system is controlled. When the pump is on, the heat transferred from the absorber plate is brought away by the water in the tube to the tank. The mathematical description is given in Eq. 15-16.

Pump operation mode

$$\left(\frac{D_i}{2}\right)^2 \rho_f p_f C \frac{dt_f}{d\tau} = D_e h_{p-f}(t_p-t_f) -$$
$$\left(\frac{D_i}{2}\right)^2 v_f \rho_f C p_f \frac{dt_f}{dy} \quad (15)$$

Pump off- mode

$$\left(\frac{D_i}{2}\right)^2 \rho_f p_f C \frac{dt_f}{d\tau} = D_o h_{p-f}(t_p-t_f) \quad (16)$$

2 Results and discussion

2.1 Method

The following results are obtained from simulations in TRNSYS. The dynamic model of the solar curtain wall is implemented as a separate component in the TRNSYS environment. The other components are from the TRNSYS standard library and are the type 60 water tank, the type 3b pump and the type 2 differential controllers. The concept building is modelled in the Type 56 multi-zone building, and the heat pump is the type 401 TRNSYS heat pump. Every simulation has a time step of 0.001 h, which is small enough to ensure accurate results.

2.2 Instantaneous transmission for different walls

A detailed study was carried out to find indications of the influence of the meteorological situation on the thermal performance of the integrated solar collectors. Two conventional walls consisting of
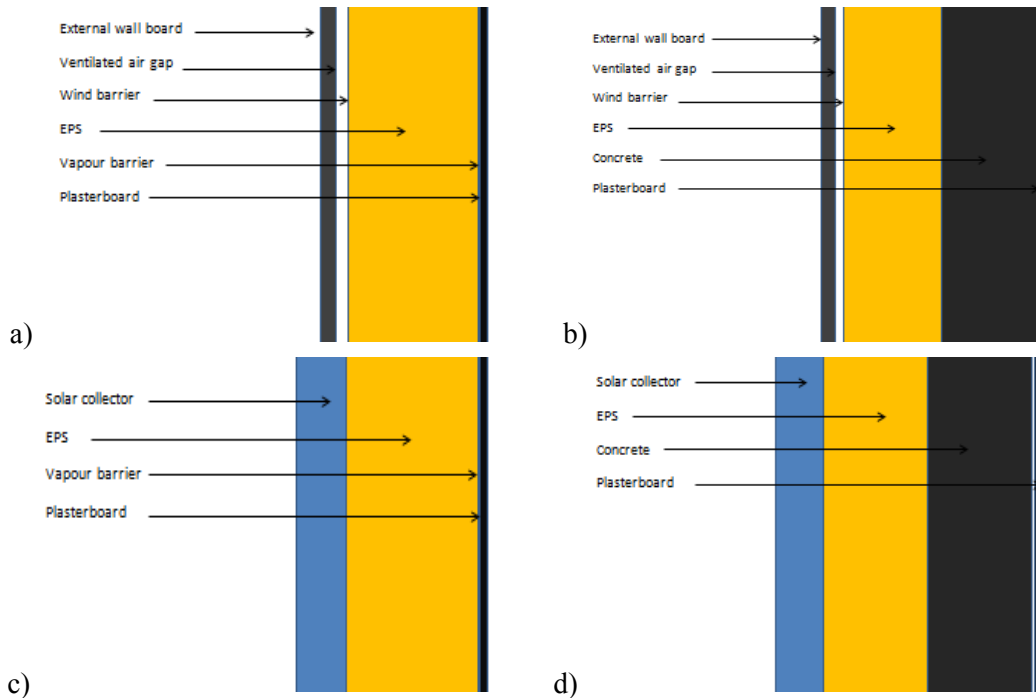

FIGURE 2 Conventional walls a) Wall A b) Wall B Solar walls c) Wall C d) Wall D

	Thermal conductivity (Wm⁻¹K⁻¹)	Thermal capacity (kJ Kg⁻¹ K⁻¹)	Density (kg/m⁻³)
Plasterboard	0.16	0.84	950
Concrete	2.1	0.8	2400
EPS	0.038	1.45	30

TABLE 3 Structural wall parameters

0.25 m timber framed insulation (Wall A) and 0.20 m insulation and 0.20 m concrete (Wall B), and the same walls with an integrated solar collector (Wall C and Wall D), see Figure 2. Both of the conventional walls have a U- value of approximately 0.17 kWhm^{-2}. To reveal the situation under the most extreme weather conditions, the walls were tested for one cloudy winter day in January, and one sunny summer day in July. Positive transmission reflects transmission to the building and negative transmission is transmission from the building. From Figure 3 it can be seen that both of the solar walls lead to positive transmission on the summer day, while this contribution is marginal for the conventional walls. The winter day, the solar walls lead to a smaller negative transmission compared to the conventional walls. The lighter walls (Wall A and Wall C) has both the highest positive and negative transmission the two days. Compared to Wall A, The negative transmission is reduced by 61 % the cloudy winter day through Wall C. Wall D shows a reduction of 66 % compared to Wall B. The sunny summer day, Wall C and Wall D introduce a positive transmission 86 % and 91 % higher than the conventional walls as seen in Table 4. The lighter walls react rapidly to temperature and radiation changes. Not only will the light solar wall lead to higher total transmission, it also imposes a much higher transmission load the summer day.

2.3 Potential of reducing the insulation thickness
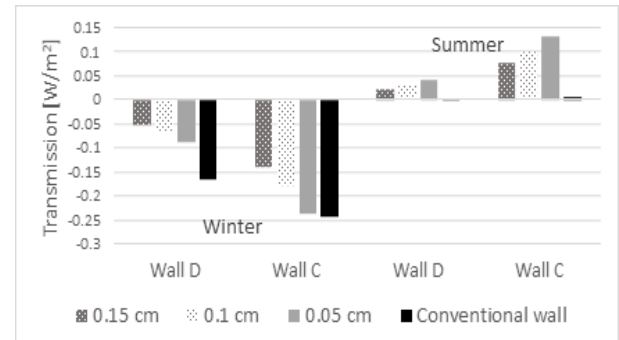
FIGURE 4 Potential of reducing insulation thickness

The influence of the solar collectors on the thermal performance of the walls allows for the configuration of the solar walls to be changed while still obtaining the same thermal performance as the conventional wall. For Wall type C the winter day, a solar curtain wall insulated with 0.05 m of insulation (the light grey pole) will have a marginally lower transmission compared to a conventional wall insulated with 0.2 m of the same insulation (the black pole), as seen in Figure 4. For Wall D, an insulation thickness of 0.05 m mounted behind a
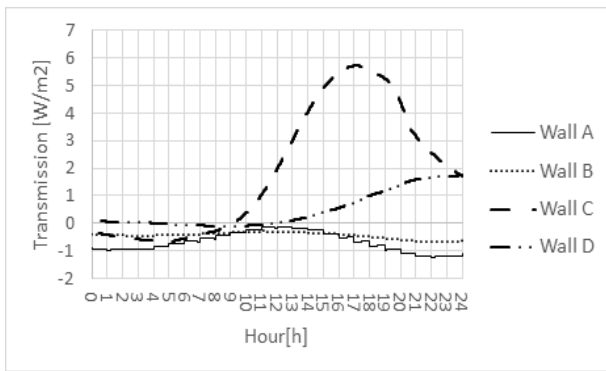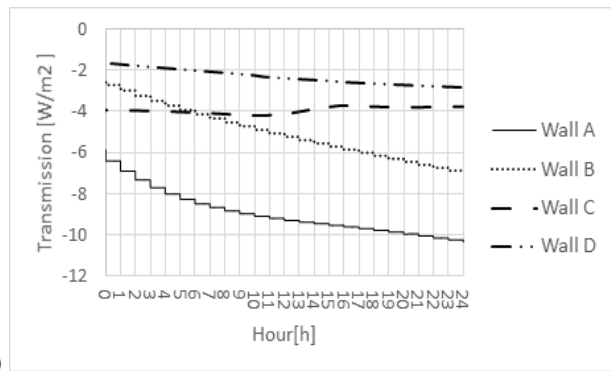
FIGURE 3 Instantaneous transmission load through 24 hours for
a) sunny summer day b) cloudy winter day.

	Wall A		Wall B		Wall C		Wall D	
Transmission (kWhm^{-2}) Positive (+) negative (-)	+	-	+	-	+	-	+	-
Sunny summer day	0.007	-0.012	0.001	-0.008	0.058	0.000	0.034	0.000
Cloudy winter day	0.000	-0.244	0.000	-0.164	0.000	-0.094	0.000	-0.056

TABLE 4 Daily transmission

0.2 m slab of concrete will have approximately 50 % lower transmission during the investigated winter day compared to the same concrete slab insulated with 0.2 m insulation. None of the conventional walls introduce mentionable positive transmission during the winter. By reducing the insulation thickness in Wall D to 5 cm, the saved energy related to negative transmission during the winter day still exceeds the extra positive transmission the summer day compared to Wall B. For Wall C, the insulation thickness can only be reduced to 15 cm, or else the potential increased cooling need during the summer day will exceed the decreased heating need during the winter day.

2.4 Annual performance

Extensive investigations were performed to reveal the influence of the solar walls on a building envelope throughout an entire year in Norwegian climate. A concept building with a heated floor area of 160 m^2 were tested. The walls of the building are equal to Wall B. On the south wall of this building, 6.68 m^2 solar collectors are integrated, constituting to Wall D. The collectors contribute to the DHW need. The building has an annual space heating need of 66 $kWhm^{-2}$ and no mechanical cooling. System parameters of the solar collector system are given in Table 5. Parasitic effects such as energy for running the main pump is neglected due to the small energy consumption. The pipes are sufficiently big to ensure small pressure losses. Figure 5 shows the transmission through wall B and Wall D throughout the year when installed on the south wall in Oslo climate. Compared to the conventional wall, the solar wall has a reduced negative transmission and an increased positive

transmission throughout the year. The negative transmission decreases from 45.22 $kWhm^{-2}$ to 7.2 $kWhm^{-2}$ when the conventional wall is integrated with a solar collector, see Table 6. This decrease in the negative transmission leads to a reduction in the overall space heating need of the concept building of 2.4 % annually.

The collectors deliver approximately 18 $kWhm^{-2}$ floor area to the DHW tank. This constitutes to 36 % of the total DHW energy consumption. The electric auxiliary heater delivers the rest.

Total solar collector area (m^2)	6.68
Daily DHW load (l/day)	300
System mass flow rate ($kgh^{-1}m^{-2}$)	72
Regulatory strategy (dT on- dT off)	8-5
Tank volume (m^3)	0.450
Tank set point temperature (°C)	50
Tank height (m)	1.4
Tank height vs. diameter ratio (-)	2.14
Heat exchanger (HX) height (m)	0.39
Heat exchanger inlet height (m)	0.55

TABLE 5 Parameters for initial system

	Positive transmission (kWh/m^2)	Negative transmission (kWh/m^2)	Specific useful energy gain (kWh/m2)
Wall B	0	45.22	-
Wall D	5.9	7.2	18.2

TABLE 6 Transmission and useful energy gain for collector wall
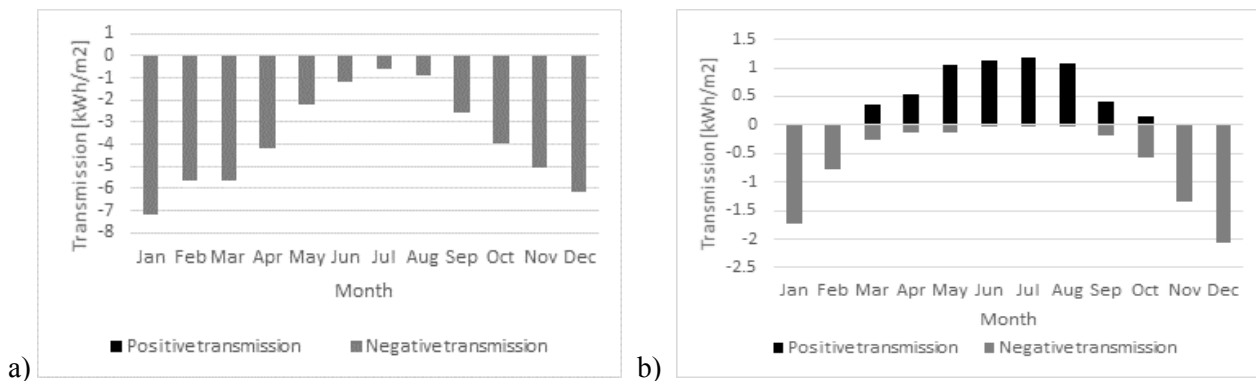

a)

b)

FIGURE 5 Monthly transmission through a) Wall B b) Wall D

2.5 Potential of increasing system performance

Figure 6 shows the potential of changing the initial system design seen in Table 5 to achieve a higher system performance. Of the efficiency measures investigated, changing the flow rate has the highest potential of reducing the energy related to transmission, see Figure 6 a). By reducing the flow rate to 54 $kgh^{-1}m^{-2}$ the energy consumption to counteract the transmission is reduced by 1.45 $kWhm^{-2}$ compared to the initial system design. Changing the tank set point temperature and the regulatory strategy will have the smallest impact on the transmission with only 0.3 $kWhm^{-2}$ as the best scenario. Figure 6 b) shows the potential of changing the initial system design to improve the collector performance. The most effective measure is changing the regulatory strategy to increase the operational time of the collectors throughout the year. By doing this, the energy saving compared to the initial system design is 1.5 $kWhm^{-2}$ floor area.
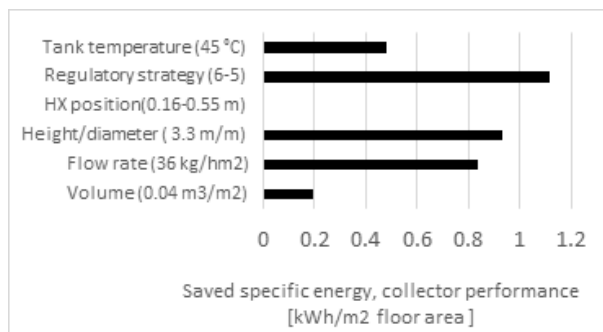
a)
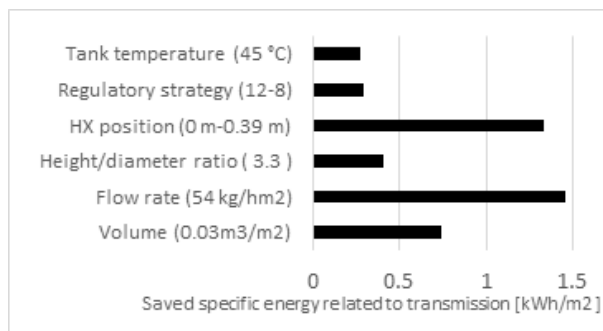
b)

FIGURE 6 Saved specific energy after efficiency measure a) transmission b) collector performance

2.6 Series installed heat pump

The system performance can be further increased by installing a heat pump in series with the solar collector. The solar collector then feeds the heat pump evaporator with heated water. A bypass is installed allowing the water to pass the heat pump and go straight to the tank heat exchanger when the collector outlet temperature is high enough. The system runs whenever there is a heating need in the tank. The auxiliary heater is only operational when the solar collector and heat pump cannot cover the load. The annual heat pump operational time depends on the maximum evaporator inlet temperature. Figure 7 shows the monthly energy contribution from the solar collector alone, the heat pump and the auxiliary heater for different maximum evaporator inlet temperatures. It can be seen that smaller maximum evaporator inlet temperatures lead to lower heat pump contribution. For the lowest temperatures, the heat pump is not operational during the summer months. This means that the collector outlet temperature exceeds the maximum allowed evaporator inlet temperature at all times. Here the auxiliary heater and the solar collector cover the entire load. The fact that there is a substantial auxiliary heating contribution during the summer months indicates that a bigger solar collector area can be installed. The useful energy gain from the collectors decreases as the heat pump operational time increases, see Table 7. During months where the collector outlet temperature frequently drops below the maximum evaporator inlet temperature, the heat pump replaces the collector. In reality, the collectors deliver heat also when the heat pump is operational since they preheat the water entering the heat pump. The biggest energy saving is achieved with a maximum evaporator inlet temperature of 15°C. This reduces the useful energy gain directly from the collectors by 27 % while the auxiliary energy from the immersed electric heater is reduced by 65 %. Combined does this lead to an annual energy saving of 31 %. As the maximum evaporator temperature increases, the negative transmission increases while the positive transmission decreases, see Table 7. The main reason for this is the decreased system operating time. This reflects a situation more similar to the conventional wall since the collectors only have a small influence on the transmission when the pump is turned off. When accounting for transmission as well, the total annual energy saving is reduced from 31 % to 30 % since the negative transmission increases.
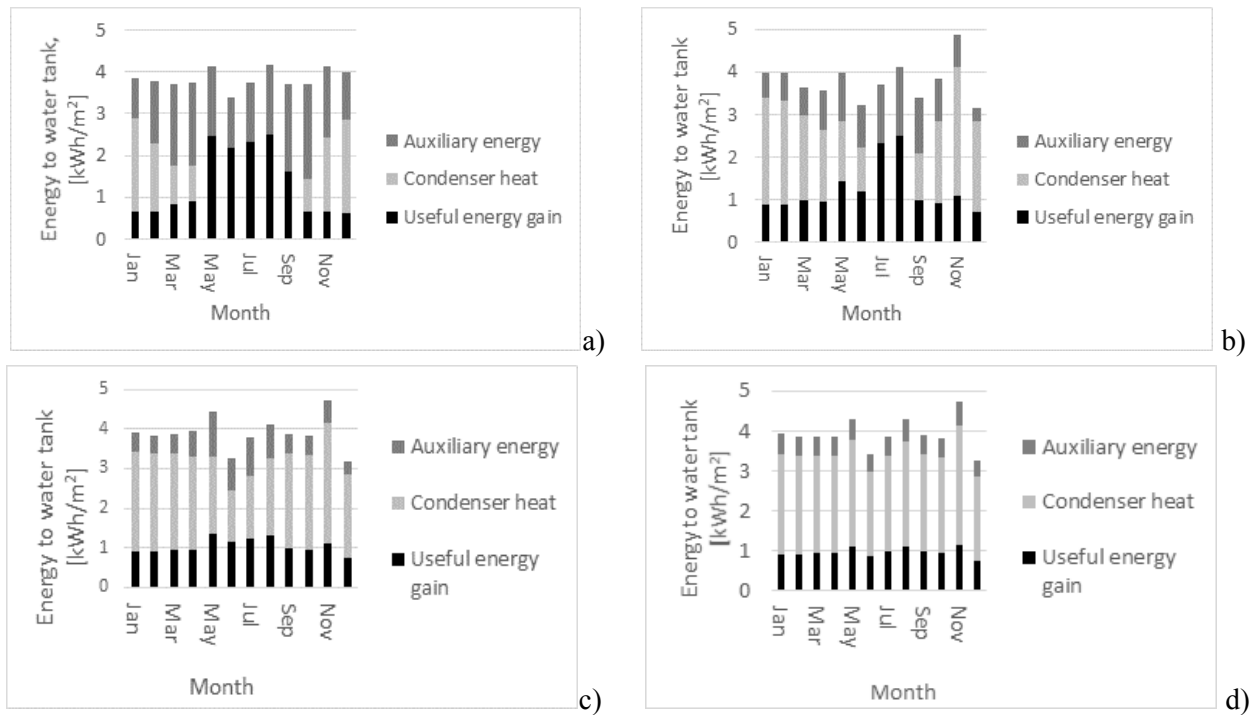
FIGURE 7 Energy contribution from heat pump, solar collector and auxiliary heater for maximum evaporator inlet temperature of a) 10°C b) 15°C c) 20°C d) 25°C

Temperature	Useful energy gain (kWhm⁻²)	Condenser heat (kWhm⁻²)	Auxiliary energy (kWhm⁻²)	Compressor energy (kWhm⁻²)	Main pump operating time (h)	Average COP (-)	Positive transmission (kWhm⁻²)	Negative transmission (kWhm⁻²)
10	16.09	10.39	19.59	6.34	4035.67	2.0	5.24	-13.76
15	12.88	22.21	11.34	11.42	3222.19	2.0	5.09	-18.56
20	12.58	26.36	7.76	16.74	2504.69	2.0	4.18	-19.22
25	11.65	29.42	5.91	20.58	1992.19	2.0	1.26	-21.21

TABLE 7 System performance for different maximum evaporator inlet temperature

3   Conclusion

Façade integrated solar collectors improve the thermal performance of the building envelope when installed on existing walls with a U- value of 0.17 Wm⁻²K⁻¹. Heavier walls perform better than lighter walls as the positive transmission is lower for these walls. For a concept building with 6.68 m² façade integrated solar collectors installed on the south wall, the reduced annual negative transmission is 84 % compared to the conventional wall. This constitutes to a 2.4 % reduction of the total space heating need.   The use of façade integrated solar collectors allows for the wall element behind the collector   to be installed with less insulation and still perform equal to a conventional wall. For a heavy solar wall, an insulation thickness of 0.05 m mounted om a 0.2 m slab of concrete will perform better than a conventional wall with 0.2 m insulation on the same concrete slab. For a light solar wall with insulation only, an insulation thickness of 0.15 m behind the collector will perform better than a conventional insulated wall with 0.25 m insulation.

Changing the system design influenced both the transmission through the wall and the collector performance. The transmission is most sensitive to the system flow rate. Lowering the flow rate from 72 to 54 kgh⁻¹m⁻² can lead to an energy saving related to transmission of 11.2 %. The tested system has few parasitic effects. To improve the annual collector performance, a regulatory strategy that maximizes the collector operating time will lead to the highest useful energy gain, and lowest auxiliary energy demand. Changing the regulatory strategy from 8-5 to 6-5 leads to an energy saving of 8.2 % annually. Further collector performance improvements can be achieved with the use of a series connected water source heat pump. With a maximum evaporator inlet temperature of 15°C, there is an annual energy saving of 30 % compared to the system without the heat pump.

References

1.   Li, R., Y.J. Dai, and R.Z. Wang, Experimental and theoretical analysis on thermal performance of solar thermal curtain wall in building envelope. Energy and Buildings, 2015. **87**: p. 324-334.

2.   Matuska, T. and B. Sourek, Façade solar collectors. Solar Energy, 2006. **80**(11): p. 1443-1452.

3.   E.M Sparrow, S.C.L., Effect of adiabatic coplanar extension surfaces on wind related solar collector heat transfer coefficients. ASME-Journal of Heat Transfer, 1981(103, 1981 Transactions): p. 268-271.

4.   Matuska, T. and B. Sourek, Solar systems with facade integrated collectors. Czech Technical University in Prague, Dept. of Environmental Engineering: Prague, Czech Republic.

5.   Chow, T.T., W. He, and J. Ji, An experimental study of façade-integrated photovoltaic/water-heating system. Applied Thermal Engineering, 2007. **27**(1): p. 37-45.

6.   Farkas, K. and M. Horvat, T.41.A.1 Building integration of Solar Thermal and Photovoltaics: barriers, needs and strategies, in IEA SHC Task 41 Solar Energy and Architecture. 2012.

7.   John A. Duffie, W.A.B., Solar Engineering of Thermal Processes, 4th Edition 4th ed. 2013, Hoboken, New Jersey: John Wiley & Sons inc.

Appendix A- Dynamic model of the solar thermal curtain wall

The dynamic model of the solar curtain wall is built on the following equations. The author has obtained the equations from documentation sent from the creator of the model, Ms Rui Li and from a thorough analysis of the FORTAN code.

The model makes the following simplifications:

1. Heat flow through the cover is one dimensional
2. There is one dimensional heat flow through back insulation
3. The temperature gradient in the direction of flow and between the tubes can be treated independently
4. Properties are independent of temperature

The heat transfer coefficients are given in Table A-1.

Energy balance of the glass cover

$$\rho_c \delta_c C_c \frac{dt_c}{d\tau} = I(\alpha_c) - (h_{c,c-a} + h_{r,c-a}(t_a - t_c) - (h_{c,c-p} + h_{r,c-p})(t_p - t_c) \qquad (A.1)$$

δ_c, ρ_c, C_c and α_c are the thickness, the density, the specific heat and the absorbance of the glass cover, respectively. I is the total solar radiation on the collector. t_c, t_a and t_p are the cover temperature, the ambient temperature and the absorber plate temperature, respectively. $h_{c,c-a}$ and $h_{r,c-a}$ are convection heat transfer coefficient and radiation heat transfer coefficient between the cover and the air. $h_{c,c-p}$ and $h_{r,c-p}$ are convection heat transfer coefficient and radiation heat transfer coefficient between the cover and the plate, and the subscripts φ and γ can be replaced by p and c, respectively in Table A-1.

The effect of evaporation of potential moist on the collectors have been neglected, thus assuming dry conditions.

Energy balance of the absorber plate

$$\rho_p \delta_p C_p \frac{dt_p}{d\tau} = I(\tau_c \alpha_c) - (h_{c,p-c} + h_{r,p-c})(t_p - t_c) - (h_{c,p-ins} + h_{r,p-ins})(t_p - t_{ins}) + \delta_p \lambda_p \frac{d^2 t_p}{dz^2} \quad (A.2)$$

δ_p, ρ_p, C_p, α_p and λ_p are the thickness, the density, the specific heat and the absorbance and the thermal conductivity of the plate respectively. τ is the transmittance of the cover. t_{ins} is the insulation layer temperature. $h_{c,p-ins}$ and $h_{r,p-ins}$ are convection heat transfer coefficient and radiation heat transfer coefficient between the plate and insulation and the subscripts φ and γ can be replaced by p and *ins*,respectively for the heat transfer coefficient in the following table. h_{p-f} is the heat transfer coefficient between the plate and the tube.

The two boundary conditions necessary to solve this second-order differential equation are given by symmetry at the centreline and the energy balance at the base, which is presented as Equations A.3 and A.4

$$\frac{dt_p}{dz}\big|_{z=0} = 0 \tag{A.3}$$

$$\frac{dt_p}{dz}\big|_{z=\frac{W_0 - D_0}{2}} = h_{p-f}(t_f - t_p) \tag{A.4}$$

The temperature gradient in the z- direction describes the temperature difference between the pipes.

Fin efficiency

The sheet material in the absorber is a good conductor. From this, one can assume that the temperature drop trough the plate is negligible. This assumption allows for treating the regions between the tubes as common fins that can be solved as a normal fin problem. The energy balance of the fin section is given in Equation A.5.

$$S\Delta z - U_L \Delta z(T - T_a) + \left(-k\delta \frac{dT}{dz}\right)_z - \left(-k\delta \frac{dT}{dz}\right)_{z+\Delta z} = 0 \tag{A.5}$$

Through discretization, Equation A.5 is used to create an expression for the term $T_a - S/U_L$ used in the equation for the fluid outlet temperature (Equation A.11) and later the useful energy gain of the collector (Equation A.12).

Energy balance trough flow direction of the tubes

The pump is switched on according to how the regulation system is controlled. When the pump is on, the heat transferred from the absorber plate is brought away by the water in the tube to the tank. The mathematical description is given through Equation A.6 where D_i and D_o is the internal and external pipe diameter. When the pump is off, the energy balance is given by Equation A.7.

Pump operation mode

$$\left(\frac{D_i}{2}\right)^2 \rho_f p_f C \frac{dt_f}{d\tau} = D_e h_{p-f}(t_p - t_f) - \left(\frac{D_i}{2}\right)^2 v_f \rho_f C p_f \frac{dt_f}{dy} \tag{A.6}$$

Pump off mode

$$\left(\frac{D_i}{2}\right)^2 \rho_f p_f C \frac{dt_f}{d\tau} = D_o h_{p-f}(t_p - t_f) \tag{A.7}$$

When the pump is operating, the temperature gradient is in the y- direction, which describes the temperature change of the fluid between the inlet and the outlet of the solar collector.

The useful energy gain

The useful energy gain per unit flow length of pipe is given from Equation A.8, where W is the fin length, F' is the collector efficiency factor, S is the absorbed solar energy U_L is the collector heat loss coefficient, T_f is the fluid temperature and T_a is the ambient air temperature.

$$q'_u = WF'(S - U_L(T_f - T_a)) \tag{A.8}$$

This version of the equation describing the useful energy gain is used in the FORTAN code. Further revisions must be made to find the heat loss coefficient and the fluid temperature. This process is described through Equation A.9-A.11.

The energy balance of the fluid flowing a length Δy in the tube is given in Equation A.9

$$\left(\frac{\dot{m}}{n}\right)C_p T_{fly} - \left(\frac{\dot{m}}{n}\right)C_p T_{fly+\Delta y} + \Delta y q_u' = 0 \qquad (A.9)$$

Dividing by Δy and finding the limit as Δy approaches zero gives Equation A.10.

$$\dot{m}C_p \frac{dT_f}{dy} - nWF'\left(S - U_L(T_f - T_a)\right) = 0 \qquad (A.10)$$

By assuming that U_L is a linear function of T_f-T_a, Equation A.11 gives the outlet temperature of the fluid

$$\frac{T_{fo} - T_a - S/U_L}{T_{fi} - T_a - S/U_L} = \exp\left(-\frac{U_L A_c F'}{\dot{m}C_p}\right) \qquad (A.11)$$

From this, Equation A.8 can be rewritten to Equation A.12.

$$q_u' = WF'(S - \frac{U_L(T_{fi}+T_{fo})}{2} + \left(h_{r,p-ins} + h_{c,p-ins}\right)T_{ins} + \left(h_{r,p-c} + h_{c,p-c}\right)T_c) \qquad (A.12)$$

Energy balance of insulation

Assuming constant properties and one-dimensional heat transfer through the insulation, the governing equation becomes Equation A.13. The boundary conditions at the outside and inside of the insulation can be expressed as Equations A.14 and A.15.

$$\frac{\partial t_{ins}}{\partial \tau} = \frac{\lambda_{ins}}{\rho_{ins} C_{ins}} \frac{\partial^2 t_{ins}}{\partial x^2} \qquad (A.13)$$

$$-\lambda_{ins}\left(\frac{\partial t_{ins}}{\partial x}\right)_{x=0} = (h_{c,col-i} + h_{r,col-i})(t_{ins} - t_i) \qquad (A.14)$$

$$-\lambda_{ins}\left(\frac{\partial t_{ins}}{\partial x}\right)_{x=delta} = (h_{c,p-i} + h_{r,p-i})(t_{ins} - t_p) \qquad (A.15)$$

δ_{ins}, λ_{ins}, C_{ins} and ρ_{ins} are the thickness, the thermal conductivity, the specific heat and density of insulation layer, respectively. t_{ins}, and t_i are the insulation temperature and the room temperature, respectively. $h_{c,col-i}$ and $h_{r,col-i}$ are convection heat transfer coefficient and radiation heat transfer coefficient between the collector and the room, respectively. These equations describe the variation of temperature with time and position. The equation is a partial differential equation, which solution often include infinitive series and transcendental equations. The equation can be solved through several different methods, such as separation of variables, Laplace transformation and the finite difference method. The finite difference method is chosen for this study.

No.	Item	Equation or value	
1	Convection to ambient	$h_{c,c-a} = 5.7 + 3.8v$	
2	Radiation to ambient	$h_{r,c-a} = \varepsilon_c \sigma \dfrac{(t_c^4 - t_{sky}^4)}{t_c - t_a}$	$t_{sky} = 0.0552(t_a)^{1.5}$
3	Convection to interior	$h_{c,\varphi-\gamma} = \dfrac{Nu_\delta \lambda_{air}}{\delta_{\varphi\gamma}}$	
		$Nu_\delta = 0.197(Gr_\delta \Pr)^{\frac{1}{4}}(\dfrac{\delta_{\varphi\gamma}}{L})^{\frac{1}{9}}$	$8600 < Gr_\delta < 2.9 \times 10^5$
		$Nu_\delta = 0.073(Gr_\delta \Pr)^{\frac{1}{3}}(\dfrac{\delta_{\varphi\gamma}}{L})^{\frac{1}{9}}$	$2.9 \times 10^5 < Gr_\delta < 1.6 \times 10^7$
4	Radiation to interior	$h_{r,\varphi-\gamma} = \sigma \dfrac{(t_\varphi^2 + t_\gamma^2)(t_\varphi + t_\gamma)}{\dfrac{1}{\varepsilon_\varphi} + \dfrac{1}{\varepsilon_\gamma} - 1}$	
5	Convection in tubes	$h_{p-f} = \dfrac{Nu_D \lambda_f}{D_i}$	$Nu_D = 0.023 \mathrm{Re}_D^{0.8} \Pr_f^{0.4}$
6	Convection to indoor	$h_{c,col-i} = \dfrac{Nu_H \lambda_{air}}{H}$	
		$Nu_H = 0.59(Gr \Pr)^{\frac{1}{4}}$	$10^4 < Gr < 3 \times 10^9$
		$Nu_H = 0.0292(Gr \Pr)^{0.39}$	$3 \times 10^9 < Gr_\delta < 2 \times 10^{10}$
		$Nu_H = 0.10(Gr \Pr)^{0.11}$	$Gr > 2 \times 10^{10}$
7	Radiation to indoor	$h_{r,col-i} = \sigma \dfrac{(t_{ins}^2 + t_i^2)(t_{ins} + t_i)}{\dfrac{1}{\varepsilon_{col}} + \dfrac{1}{\varepsilon_i} - 1}$	

Table A-1 Heat transfer coefficients

Appendix B- Heat pump characteristics

The heat pump under investigation is a Carrier Aquazone 50PSW25-420 Water-to-Water Source Heat Pump with Puron Refrigerant (R410-A) heat pump. Its characteristics is given in the following.

Condenser inlet temperature (°C)	Evaporator inlet temperature(°C)	Condenser output (kW)	Compressor power (kW)
24.70	-6.67	2.09	0.71
30.20	-6.67	2.00	0.78
35.72	-6.67	1.90	0.84
41.20	-6.67	1.80	0.90
46.80	-6.67	1.70	0.97
25.11	-1.11	3.20	0.75
30.60	-1.11	3.10	0.81
36.11	-1.11	3.09	0.88
41.67	-1.11	3.07	0.95
47.20	-1.11	3.04	1.02
25.60	4.44	2.80	0.78
31.11	4.44	2.70	0.85
36.60	4.44	2.50	0.92
42.11	4.44	2.40	0.99
47.60	4.44	2.30	1.06
26.11	10.00	3.20	0.81
31.60	10.00	3.30	0.88
36.70	10.00	2.90	0.96
42.20	10.00	2.80	1.03
47.30	10.00	2.70	1.11
26.70	15.55	3.60	0.85
32.20	15.55	3.50	0.92
37.70	15.55	3.30	1.00
43.20	15.55	3.20	1.08
48.70	15.55	3.10	1.16
27.30	21.11	4.10	0.88
32.80	21.11	3.90	0.96
38.30	21.11	3.80	1.04
43.80	21.11	3.60	1.12
49.20	21.11	3.50	1.21
28.00	26.66	4.50	0.92
33.40	26.66	4.40	1.00
38.90	26.66	4.20	1.08
44.40	26.66	4.10	1.17
49.80	26.66	3.90	1.26

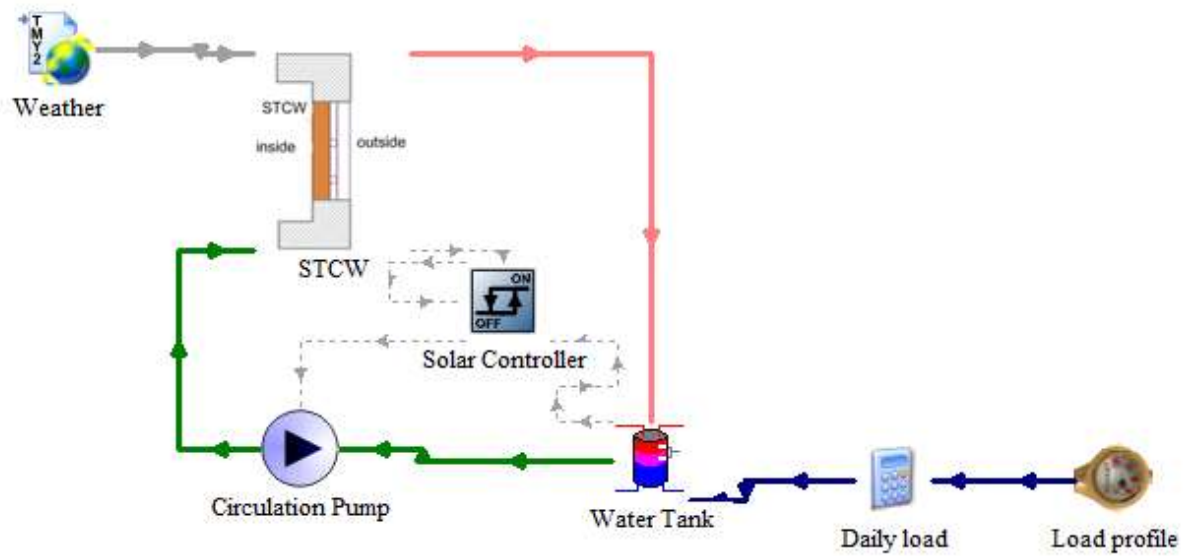# Appendix C – TRNSYS model schematics

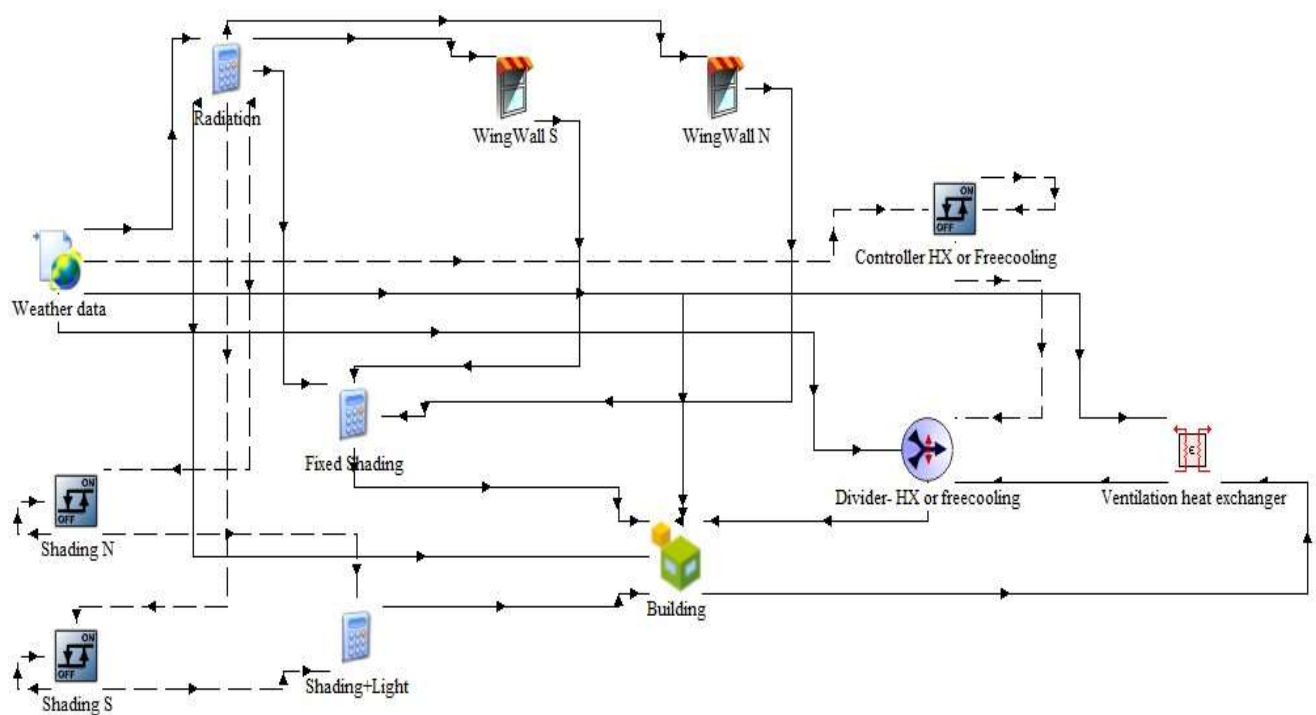*Figure C-1 TRNSYS model schematics of solar wall system*

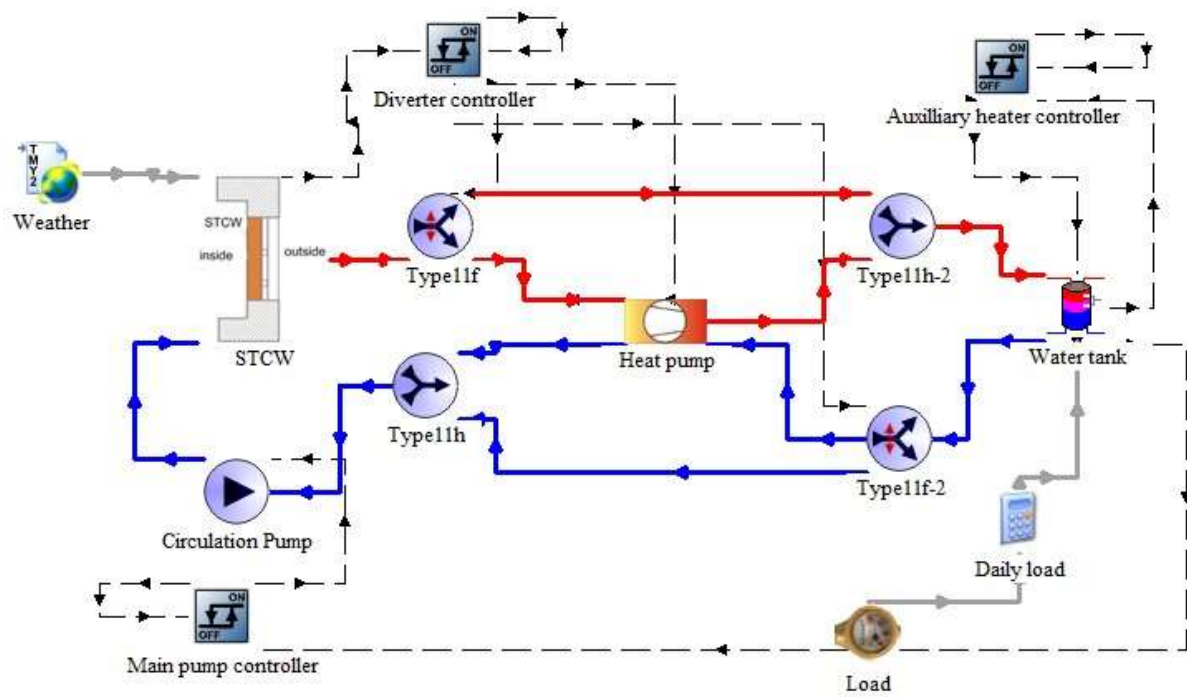*Figure C-2 TRNSYS model schematics of conventional wall and concept building system*

Figure C-3 TRNSYS model schematics of combined heat pump and solar wall system